

AD-A055 753

MATERIALS SCIENCES CORP BLUE BELL PA  
EFFECTS OF ENVIRONMENT, AND DAMPING AND COUPLING PROPERTIES OF --ETC(U)  
JAN 78 S N CHATTERJEE, S V KULKARNI

F/G 11/4

F44620-76-C-0080

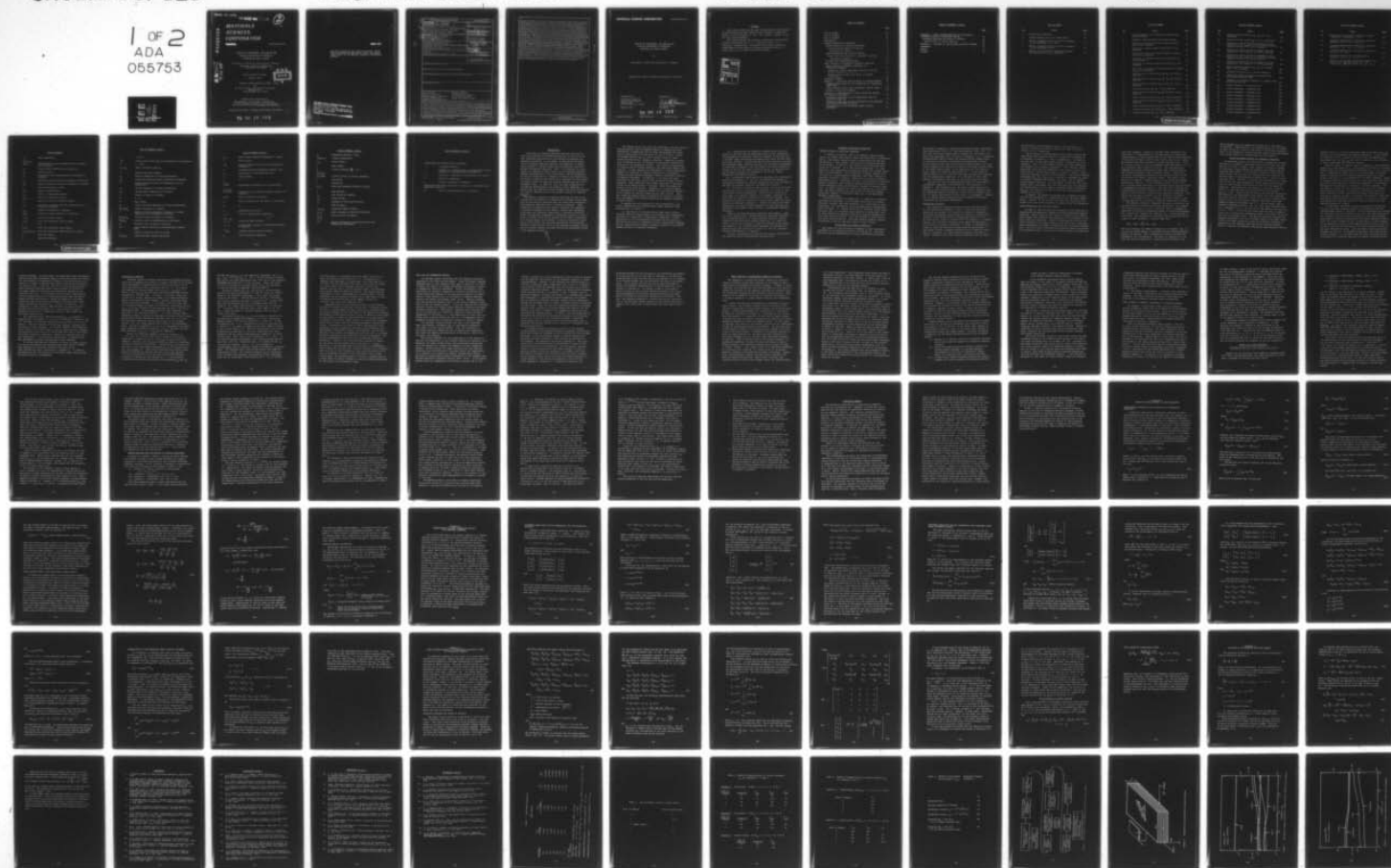
UNCLASSIFIED

MSC/TFR/802/1151

AFOSR-TR-78-1066

NL

1 OF 2  
ADA  
055753



FOR FURTHER TRAN

2  
SC

# MATERIALS SCIENCES CORPORATION

MSC/TFR/802/1151

EFFECTS OF ENVIRONMENT, AND DAMPING AND  
COUPLING PROPERTIES OF COMPOSITE  
LAMINATES ON PANEL FLUTTER

Sailendra N. Chatterjee and Satish V. Kulkarni  
MATERIALS SCIENCES CORPORATION  
Blue Bell, PA 19422

Final Scientific Report  
January 1978

Prepared under F44620-76-C-0080  
for

Air Force Office of Scientific Research  
Building 410  
Bolling AFB, D.C. 20332

## Conditions of Reproduction

Reproduction, translation, publication,  
use and disposal in whole or in part by or  
for the United States Government is permitted.

Approved for public release; distribution unlimited.

78 06 19 132

AD A 055753

AD No. 1  
FILE COPY

DDC  
JUN 22 1978  
E



2

ABSTRACT 78-1068

FOR FURTHER TRAN

MATERIALS  
SCIENCES  
CORPORATION

327220AQA

QUALIFIED REQUESTORS MAY OBTAIN ADDITIONAL COPIES  
FROM THE DEFENSE DOCUMENTATION CENTER, ALL OTHERS  
SHOULD APPLY TO THE NATIONAL TECHNICAL INFORMATION  
SERVICE.

DDC  
JUN 22 1978  
PROG 17  
E

327220AQA  
JUN 22 1978  
PROG 17  
E

AIR FORCE OFFICE OF SCIENTIFIC RESEARCH (AFSC)  
NOTICE OF TRANSMITTAL TO DDC  
This technical report has been reviewed and is  
approved for public release IAW AFR 190-12 (7b).  
Distribution is unlimited.  
A. D. BLOSE  
Technical Information Officer

REPORT DOCUMENTATION PAGE		READ INSTRUCTIONS BEFORE COMPLETING FORM
1. REPORT NUMBER <b>AFOSR-TR-78-1066</b>	2. GOVT ACCESSION NO.	3. RECIPIENT'S CATALOG NUMBER <b>9</b>
4. TITLE (and Subtitle) <b>EFFECTS OF ENVIRONMENT, AND DAMPING AND COUPLING PROPERTIES OF COMPOSITE LAMINATES ON PANEL FLUTTER.</b>	5. TYPE OF REPORT & PERIOD COVERED <b>FINAL rept.</b> <b>1 Mar 76 - 30 Nov 77</b>	6. PERFORMING ORG. REPORT NUMBER <b>MSC/TFR/802/1151</b>
7. AUTHOR(s) <b>SAILENDRA N CHATTERJEE</b> <b>SATISH V KULKARNI</b>	8. CONTRACT OR GRANT NUMBER(s) <b>F44620-76-C-0080</b>	
9. PERFORMING ORGANIZATION NAME AND ADDRESS <b>MATERIALS SCIENCES CORP</b> <b>BLUE BELL OFFICE CAMPUS, MERION TOWLE HOUSE</b> <b>BLUE BELL, PA 19422</b>	10. PROGRAM ELEMENT, PROJECT, TASK AREA & WORK UNIT NUMBERS <b>16 2307B1 17 B1</b> <b>61102F</b>	
11. CONTROLLING OFFICE NAME AND ADDRESS <b>AIR FORCE OFFICE OF SCIENTIFIC RESEARCH/NA</b> <b>BLDG 410</b> <b>BOLLING AIR FORCE BASE, D C 20332</b>	12. REPORT DATE <b>Jan 1978</b>	
14. MONITORING AGENCY NAME & ADDRESS (if different from Controlling Office)	13. NUMBER OF PAGES <b>138</b> <b>12 135p.</b>	
	15. SECURITY CLASS. (of this report)  <b>UNCLASSIFIED</b>	
15a. DECLASSIFICATION/DOWNGRADING SCHEDULE		
16. DISTRIBUTION STATEMENT (of this Report)  <b>Approved for public release; distribution unlimited.</b>		
17. DISTRIBUTION STATEMENT (of the abstract entered in Block 20, if different from Report)		
18. SUPPLEMENTARY NOTES		
19. KEY WORDS (Continue on reverse side if necessary and identify by block number) <b>Panel flutter</b> <b>Complex modulus</b> <b>Dynamic stability</b> <b>Environmental factors</b> <b>Graphite/epoxy composites</b> <b>Structural damping</b> <b>Shear deformations</b> <b>Shear correction factor</b> <b>Dynamic viscoelasticity</b>		
20. ABSTRACT (Continue on reverse side if necessary and identify by block number) <b>The problem of panel flutter of epoxy matrix composite laminates is investigated in this report. Emphasis is placed upon incorporating into the analysis an appropriate constitutive relation for the composite laminate. This requires consideration of coupling effects between extension and bending, and bending and twisting. It also requires consideration of shear deformation effects as a function of laminate construction and stacking sequence, and frequency dependent dynamic viscoelastic behavior of composite laminates. In addition, an approach for the determination of the effects of moisture and temperature on the laminate constitutive equations is outlined. Finally, the panel flutter of</b>		

symmetric laminates in cylindrical bending is investigated in order to assess the effects of the composite material parameters such as laminate construction, shear deformation, and damping upon the critical flutter parameter. The correspondence principle for vibrations of viscoelastic composites is utilized for the determination of lamina/laminate complex properties from the constituent complex properties. An analytical/numerical procedure (based on the thickness-shear mode cut-off frequency matching technique) to obtain the shear correction factors associated with the transverse shear stiffnesses is developed. In addition, a method is also formulated for evaluating the transverse shear coupling term. The shear correction factors for a limited number of composite laminates are presented. The results demonstrate the usefulness of the approach and indicate some general trends which will be of value in the design of composite laminate panels. The investigation of panel flutter characteristics of symmetric laminates indicates that both shear deformation and damping have significant effects. In general, introduction of little structural damping lowers the flutter load considerable from the case when there is no damping. Further increases in damping cause the flutter load to increase. These observations are in agreement with the well-known results of destabilizing effect of damping in non-conservative elastic systems. Contrary to the effect of structural damping, aerodynamic damping stabilizes the system. Compressive prestress has a destabilizing effect. Bending-extension coupling due to nonsymmetric temperature and moisture distribution in a symmetric laminate does not have any degrading influence on the critical flutter parameter. Effects of moisture and temperature gradient, studied by the use of master curves and a shift hypothesis of epoxy matrix show that these environmental factors could significantly influence the flutter characteristics of laminates.

UNCLASSIFIED

SECURITY CLASSIFICATION OF THIS PAGE (When Data Entered)



**EFFECTS OF ENVIRONMENT, AND DAMPING AND  
COUPLING PROPERTIES OF COMPOSITE  
LAMINATES ON PANEL FLUTTER**

By

Sailendra N. Chatterjee and Satish V. Kulkarni

Approved for public release; distribution unlimited.

Prepared for:

Air Force Office of  
Scientific Research  
Building 410  
Bolling AFB, D.C. 20332

January 1978

Approved by:



B. Walter Rosen  
President

**78 06 19 132**



# FOREWORD

This report summarizes the work accomplished by The Materials Sciences Corporation under AFOSR Contract F44620-76-C-0080 from March 1, 1976 to November 30, 1977. Mr. William J. Walker is the Air Force Program Manager.

The Program Manager and Principal Investigator for Materials Sciences Corporation are Dr. S. V. Kulkarni and Dr. S. N. Chatterjee, respectively. The authors would like to gratefully acknowledge the many helpful discussions they had with Dr. Z. Hashin and Dr. B. W. Rosen during this program.

ACCESSION for	
DTIC	Write Section <input checked="" type="checkbox"/>
DDC	Diff Section <input type="checkbox"/>
UNANNOUNCED	<input type="checkbox"/>
JUSTIFICATION	<input type="checkbox"/>
BY	
DISTRIBUTION/AVAILABILITY CODES	
Dist.	AVAIL. and/or SPECIAL
A	

# TABLE OF CONTENTS

	<u>Page</u>
LIST OF TABLES . . . . .	ix
LIST OF FIGURES . . . . .	xi
LIST OF SYMBOLS . . . . .	xv
INTRODUCTION . . . . .	1
LAMINATE CONSTITUTIVE RELATIONS . . . . .	4
DAMPING EFFECTS IN COMPOSITE LAMINATES . . . . .	4
Lamina/Laminate Complex Properties. . . . .	4
Discussion of Results . . . . .	5
SHEAR-DEFORMATION AND COUPLING EFFECTS . . . . .	6
Shear Correction Factors for Composite Laminates . . . . .	8
Discussion of Results . . . . .	11
MOISTURE AND TEMPERATURE EFFECTS . . . . .	14
PANEL FLUTTER OF VISCOELASTIC COMPOSITE LAMINATES . . . . .	17
PANEL FLUTTER OF SYMMETRIC LAMINATES IN CYLINDRICAL BENDING . . . . .	21
Results for (0/90) Laminates Obtained by the Use of the Criterion $\Delta_R = \Delta_I = 0$ . . . . .	22
Results Obtained from Calculation of Complex Eigenvalues . . . . .	25
CONCLUDING REMARKS . . . . .	32
APPENDIX A - EFFECTIVE COMPLEX MODULI OF LAMINA/LAMINATE. . . . .	35
CORRESPONDENCE PRINCIPLE FOR VIBRATIONS OF VISCOELASTIC COMPOSITES . . . . .	35
LAMINA COMPLEX MODULI FROM CONSTITUENT COMPLEX MODULI . . . . .	38
LAMINATE COMPLEX STIFFNESSES . . . . .	41
APPENDIX B - DETERMINATION OF SHEAR CORRECTION FACTORS FOR COMPOSITE LAMINATES. . . . .	42
THICKNESS SHEAR MODE CUT-OFF FREQUENCIES FROM THE ELASTICITY SOLUTION . . . . .	43
THICKNESS SHEAR MODE CUT-OFF FREQUENCIES FROM LAMINATED PLATE SHEAR DEFORMATION THEORY. . . . .	47
DETERMINATION OF THE TRANSVERSE SHEAR COUPLING STIFFNESS . . . . .	53

TABLE OF CONTENTS (contd.)

	<u>Page</u>
APPENDIX C - PANEL FLUTTER ANALYSIS OF VISCOELASTIC LAMINATED PLATES IN CYLINDRICAL BENDING. . . . .	56
GOVERNING EQUATIONS AND METHOD OF ANALYSIS . . . . .	56
Panel Flutter of [0/90] Laminate. . . . .	62
APPENDIX D - SOLUTION OF THE MOISTURE DIFFUSION PROBLEM .	64
REFERENCES . . . . .	67
TABLES. . . . .	71
FIGURES . . . . .	76

LIST OF TABLES

<u>No.</u>	<u>Title</u>	<u>Page</u>
1	Constituent Properties	71
2	Various Damping Levels for Epoxy Matrix	72
3	Effect of Damping Levels on Flutter Parameter $\bar{\lambda}_{cr}$ for Laminates 1, 2, and 3	73
4	Effect of Damping Levels on Flutter Parameter $\bar{\lambda}_{cr}$ for Laminates 4 and 5	74
5	Effects of Environment, Aerodynamic Damping and Prestress on $\bar{\lambda}_{cr}$ for Laminate 6	75



# LIST OF FIGURES

<u>No.</u>	<u>Title</u>	<u>Page</u>
1	Various Modules in the Composite Laminate Panel Flutter Problem	76
2	Composite Lamina/Laminate Coordinate Systems	77
3	Variation of Lamina and Matrix Complex Young's Moduli with Frequency	78
4	Variation of Lamina Complex Shear Moduli with Frequency	79
5	Variation of Lamina and Matrix Complex Poisson's Ratios with Frequency	80
6	Variation of Laminate Extensional Stiffness $\tilde{A}_{11}$ with Frequency	81
7	Variation of Laminate Bending Stiffness $\tilde{D}_{11}$ with Frequency	82
8	Variation of Laminate Transverse Shear Stiffnesses $\tilde{A}_{44,55}$ with Frequency	83
9	Shear Correction Factors $k_{44}$ and $k_{55}$ for $[0/90]_s$ Laminate	84
10	Shear Correction Factors $k'_{44}$ and $k'_{55}$ for $[0/90]_s$ Laminate	85
11	Shear Correction Factors $k'_{44}$ and $k'_{55}$ for $[\pm 15^\circ]_s$ Laminate	86
12	Correction Factor $k''_{45}$ for $[\pm 15^\circ]_s$ Laminate	87
13	Shear Correction Factors $k''_{44}$ and $k'_{55}$ for $[\pm 30^\circ]_s$ Laminate	88
14	Shear Correction Factor $k''_{45}$ for $[\pm 30^\circ]_s$ Laminate	89
15	Shear Correction Factors $k'_{44}$ and $k'_{55}$ for $[\pm 40^\circ]_s$ Laminate	90
16	Shear Correction Factor $k''_{45}$ for $[\pm 40^\circ]_s$ Laminate	91
17	Correction Factor $k'_{55}$ and $k'_{44}$ for $[\pm 45]_s$ Laminate	92
18	Correction Factor $k''_{45}$ for $[\pm 45]_s$ Laminate	93

# LIST OF FIGURES (contd.)

<u>No.</u>	<u>Title</u>	<u>Page</u>
19	Shear Correction Factors $k'_{55}$ , $k'_{44}$ for $[\pm\theta]_s$ Laminates	94
20	Shear Correction Factor $k''_{45}$ for $[\pm\theta]_s$ Laminates	95
21	Variation of Shear Correction Factors with the Fraction of $\pm 45^\circ$ Layers in a $[0/\pm 45/90]_s$ Laminate (Equal Fractions of $0^\circ$ and $90^\circ$ Layers)	96
22	Variation of Shear Correction Factors with the Fraction of $\pm 45^\circ$ Layers in a $[0/\pm 45]_s$ Laminate	97
23	Variation of Shear Correction Factors with the Fraction of $\pm 45^\circ$ Layers in a $[\pm 45/0/90]_s$ Laminate (Equal Fractions of $0^\circ$ and $90^\circ$ Layers)	98
24	Variation of Shear Correction Factors with the Fraction of $\pm 45^\circ$ Layers in a $[\pm 45/0]_s$ Laminate	99
25	Shear Correction Factors $k'_{55}$ , $k'_{44}$ for Antisymmetric $[\pm\theta]$ Laminates	100
26	Moisture Distribution in a Coated Composite	101
27	Coordinate System of Composite Laminate Panel with Airflow and Prestress	102
28	Schematic of Structural Response vs. Dynamic Pressure (from ref. 38)	103
29	Flutter Parameter - Frequency Plot	104
30	Flutter Parameter - Frequency Plot	105
31	Flutter Parameter - Frequency Plot	106
32	Flutter Parameter - Frequency Plot	107
33	Flutter Parameter - Frequency Plot	108
34	Flutter Parameter - Frequency Plot	109
35	Flutter Parameter - Frequency Plot	110
36	Flutter Parameter - Frequency Plot	111
37	Flutter Parameter - Frequency Plot	112

# LIST OF FIGURES (contd.)

<u>No.</u>	<u>Title</u>	<u>Page</u>
38	Master Curve for Dynamic Properties of Epoxy - Reference Temperature = 70°F	113
39	Frequency Spectrum for [0/90/0/90] <sub>s</sub> Cross-Ply Laminate 4, a/h = 60, h = .06 in.	114
40	Frequency Spectrum for [0/90/0/90] <sub>s</sub> Cross-Ply Laminate 5, a/h = 10, h = 0.06 in.	115
41	Frequency Spectrum for [±45/0 <sub>2</sub> /90] <sub>s</sub> Laminate 6, a/h = 40, h = .06 in.	116
42	Frequency Spectrum for [+45/-45/0 <sub>2</sub> /90] <sub>s</sub> Laminate 7, a/h = 10, h = .06 in.	117
43	Effect of Environment, Aerodynamic Damping and Prestress on Amplitude Ratio vs. $\bar{\lambda}$ for [±45/0 <sub>2</sub> /90] <sub>s</sub> Laminate 6, a/h = 40, h = .06 in.	118

# LIST OF SYMBOLS

$a, b$	panel dimensions,
$a_n, b_n, c_n,$ $d_n, e_n$	coefficients in series expressions for displacement variables,
$A_n$	column vector containing $a_n, b_n, c_n, d_n, e_n$ ,
$A_R$	amplitude ratio,
$A_{ij}$	extensional and transverse shear stiffnesses of laminate,
$A'_{ij}$	modified transverse shear stiffnesses of laminate,
$B_{ij}$	bending-extension coupling stiffnesses of laminate,
$c$	free stream speed of sound,
$C, C_i$	moisture concentration
$C_{ij}$	moduli in contracted notation,
$C_{ijkl}$	elastic or relaxation moduli,
$d_n$	mesh size infinite difference scheme
$D_0$	real part of complex bending stiffness $\tilde{D}_{11}$ at a reference frequency,
$D_{ij}$	bending stiffnesses of laminate,
$D_{ijkl}^*$	effective complex moduli of a composite,
$e C_{ijkl}^*$	effective elastic moduli,
$E_A, E_T$	axial and transverse Young's moduli,
$f$	$\pi/\lambda\omega$ ,
$G_A, G_T$	axial and transverse shear moduli,
$G_{12}, G_{23} (=G_{13})$	axial and transverse shear moduli of a layer,
$h$	layer thickness,
$H$	laminate thickness,



# LIST OF SYMBOLS (contd.)

$i$	$(-1)^{1/2},$
$I, \bar{I}$	rotary inertia term and its nondimensional counterpart,
$I'$	$I - R^2/P,$
$k_{ij}, k'_{ij}$	shear correction factors,
$K$	plane strain bulk modulus,
$K_n$	matrices appearing in flutter determinant,
$K_{ij}$	corrected transverse shear stiffnesses of laminate,
$\bar{K}$	global stiffness matrix for determining cut-off frequencies,
$L_n$	vectors appearing in flutter determinant,
$L_{ij}$	average shear compliance of laminate,
$m$	number of layers in laminate,
$m'$	$m + 1,$
$M$	Mach number,
$M_n$	inertia matrices appearing in flutter determinant,
$M_x, M_y, M_{xy}$	moment resultants in laminate,
$N$	number of terms retained in truncation of series expressions of displacement variables,
$N_x, N_y, N_{xy}$	in-plane stress resultants in laminate,
$N_{xx}^0, \bar{N}_{xx}$	prestress and its nondimensional counterpart,
$p$	variable used in Laplace transforms,
$P, \bar{P}$	axial inertia term and its nondimensional counterpart,
$q$	dynamic pressure of the air stream,
$Q_x, Q_y, Q_j$	transverse shear stress resultants,

# LIST OF SYMBOLS (contd.)

$Q_{ij}$	plane stress reduced stiffnesses of a layer,
$r$	ratio $G_{23}/G_{12}$ ,
$R, \bar{R}$	coupling inertia term and its nondimensional counterpart,
$S$	nondimensionalized aerodynamic damping term,
$S_{ij}$	compliances in contracted notation,
$t$	time variable,
$t'$	$t - \tau$ ,
$u, v, w,$ $U, V, W$	displacement variables in $x, y, z$ directions,
$u^0, v^0, w^0$ $U^0, V^0, W^0$	displacements of reference surface (center) of laminate,
$x, y, z$	global cartesian coordinates,
$z_i$	local coordinate for $i$ th layer in $z$ direction,
$\alpha_n$	$n\pi$ ,
$\bar{\beta}$	compressibility factor,
$\gamma_{1,2}$	roots of characteristic equation,
$\gamma_{xz}, \gamma_{yz},$ $\gamma_4, \gamma_5$	transverse shear strains,
$\Gamma_4, \Gamma_5$	average shear strains (in contracted notation) in laminate,
$\Gamma^*_{ijkl}$	transform domain effective moduli,
$\delta_i$	finite difference operators

# LIST OF SYMBOLS (contd.)

$\Delta_n$	expression defined in text,
$\Delta(\Delta_R + i\Delta_I)$	flutter determinant,
$\epsilon_{ij}$	strain tensor,
$\lambda$	wave length,
$\bar{\lambda}$	flutter parameter $\frac{2q}{\beta D_0} \cos \Lambda$ ,
$\bar{\lambda}_{cr}, \bar{\lambda}_{cri}$	
$\bar{\lambda}_{cr}(\text{weak})$	critical values of flutter parameter,
$\Lambda$	flow angle,
$\mu$	diffusivity
$\nu_A, \nu_T$	axial and transverse Poisson's ratios,
$\rho$	mass density,
$\rho_a$	free stream air density,
$\sigma_{ij}$	stress tensor,
$\sigma_i$	stresses in contracted notation,
$\tau$	time variable,
$\tau_{xz}, \tau_{yz}$	transverse shear stresses,
$\tau_4, \tau_5$	shear stresses in contracted notation,
$\psi_x, \psi_y$	plate rotation variables,
$\bar{\psi}_x, \bar{\psi}_y$	
$\omega, \bar{\omega}$	complex frequency of vibration and its non-dimensional counterpart.



LIST OF SYMBOLS (contd.)

Superscripts and symbols over a quantity:

- $\sim$  a complex quantity,
- $-$  average of a quantity over a representative volume element or a nondimensionalized quantity,
- $+,-$  values of a quantity at the surfaces of a region,
- $*$  effective properties,
- $\wedge$  Laplace transform of a quantity.

Subscripts other than those used in tensor (or contracted) and summation notations:


- $R,I$  real and imaginary parts of a quantity.



## INTRODUCTION

Utilization of advanced composites has been motivated by their high strength and stiffness properties, as well as by the cost advantages associated with the fabrication processes for composite structures. As the number of applications increases and as the design expertise improves, the capability to assess their response to various loading and environmental conditions becomes increasingly important. Thus, it is necessary to investigate the influence of such factors as the frequency-dependent damping characteristics of the constituents, and the degradation of material properties as a function of moisture and temperature. The effect of material anisotropy can be important for the problem of flexure, where the shear and flexural deformations may be of a comparable order. In addition, since the shear properties and the damping characteristics are primarily matrix dependent, it appears that the combined effects of damping and shear deformations will play an important role in the dynamic response of composite materials.

The dynamic response of composite materials has been investigated with the objective of assessing the influence of the geometry and the material variables upon the vibrational frequencies and dispersion characteristics in composite laminates. These studies are an essential first step in assessing the response of a structure subjected to more complex transient and aerodynamic loads which are frequently experienced in aerospace structures. A direct and important consequence of aerodynamic loading on structures is flutter, which can be defined as the dynamic instability of an elastic body in an airstream. A form of oscillatory instability which differs from the more conventional lifting surface flutter is panel flutter, which is the interaction between the missile or aircraft surface skin panel motions and aerodynamic forces in the supersonic regime.



The effects which arise from the viscoelastic and the resulting damping behavior and the combined effects of damping and shear deformation in composites have not been investigated very extensively, particularly from the point of view of flutter. Hence, the problem studied here is that of panel flutter of fiber-reinforced epoxy matrix composite laminates. Emphasis is placed upon incorporating into the analysis an appropriate constitutive relation for the composite laminate. This requires consideration of coupling effects between extension and bending, and bending and twisting. It also requires the consideration of shear deformation effects as a function of laminate construction and stacking sequence and the frequency-dependent dynamic viscoelastic behavior of composite laminates. In addition, it is known that edge restraints of the panel tend to limit strongly the panel flutter amplitude. This limitation often causes the modes of structural failure to be those peculiar to fatigue, rather than explosive fracture of the skin surface. Therefore, it is also necessary to investigate the interaction between the environmental degradation of composite laminate properties and panel flutter. Thus, this study can appropriately be termed as the effects of environment, and damping and coupling properties of composite laminates on panel flutter.

In keeping with the objectives of this investigation, the effort consisted of the following tasks (these tasks are shown schematically in figure 1):

(i) Derivation of fiber-reinforced epoxy matrix lamina/laminate effective complex moduli by utilizing the correspondence principle for vibrations of viscoelastic composites. A brief description of the correspondence principle and the analytical derivations are given in Appendix A, while a discussion of damping and the lamina/laminate complex properties appears in the section "Damping Effects in Composite Laminates."

(ii) Determination of composite laminate shear correction factors by matching the thickness-shear mode cut-off frequencies (corresponding to infinitely large wave lengths) as obtained from a "refined" shear deformation laminated plate theory and the exact elasticity solution. An approach has also been evolved to estimate the transverse shear coupling stiffness. The analytical methodology is described in Appendix B and the coupling and shear-deformation effects as well as the shear-correction factors as obtained from the matching technique are discussed in the section "Shear-Deformation and Coupling Effects."

(iii) Preliminary investigation for extending the constitutive relations developed in (i) and (ii) to consider the effects of moisture and temperature, salient features of which are outlined in the section entitled "Moisture and Temperature Effects."

(iv) Analysis of composite laminate panel flutter by utilizing the laminate constitutive relations developed in (i) and (ii) and linear piston theory aerodynamics. Since the main objective of this study is to evaluate effects of environment, attention is restricted to response of laminates in cylindrical bending. The governing differential equations are derived and a method for their solution is outlined in Appendix C. Effects of damping and shear-deformation on critical flutter parameter for some laminates are evaluated in the section "Panel Flutter of Viscoelastic Composite Laminates."

Based on the above-mentioned analytical developments, predictive tools (specifically, computer programs) have been developed for the determination of (i) lamina/laminate effective complex properties from constituent complex properties, (ii) shear correction factors as a function of laminate construction and stacking sequence, (iii) critical flutter parameter for viscoelastic laminates using the results of (i) and (ii), and (iv) transient moisture distribution in a laminate.

Finally, conclusions are drawn from the results thus obtained and areas for future investigations are identified.



## LAMINATE CONSTITUTIVE RELATIONS

### DAMPING EFFECTS IN COMPOSITE LAMINATES

A vibrating structure, such as a composite laminate panel, has at any instant some kinetic energy and some strain (or potential) energy. The kinetic energy storage is associated with the mass and velocity at that instant, and the strain energy storage with the stiffness. In addition, the structure also dissipates some energy as it deforms. It is this energy dissipation - or, more precisely, this conversion of mechanical energy into thermal energy - that is called damping. Unlike mass and stiffness, damping does not refer to a unique physical phenomenon, and hence, damping is much more difficult to define. There are a multitude of damping mechanisms such as: interface friction, fluid viscosity, turbulence, acoustic radiation, eddy currents, magnetic hysteresis, and mechanical hysteresis (also called internal friction or material damping). In order to analyze or predict the damping of a given structure, one should ideally take into account all possible damping mechanisms; however, in practical cases, one or two mechanisms generally predominate.

The primary effects of damping are (i) reduction of vibration amplitudes at resonances, with attendant reductions in stresses, structural fatigue, and sound radiation; (ii) rapid decay of free vibrations; (iii) attenuation of structureborne waves propagating along the panel, i.e. reduced conduction of vibratory energy along the panel; and (iv) increased sound isolation (transmission loss). All these effects are generally beneficial from the standpoint of noise and vibration control. Since the problem of airflow over a thin panel involves both the noise and vibration aspects, damping is expected to have an important effect on panel flutter.

### Lamina/Laminate Complex Properties

The reason for the occurrence of damping in fiber-reinforced composites is the dissipative nature of epoxy matrix. The fiber and matrix may be characterized as linear viscoelastic materials.



The problem of damping in composite materials has been investigated both analytically (refs. 1-3) and experimentally (refs. 4-6). If the fiber and matrix complex moduli (storage and loss moduli) are known from experiments as a function of frequency, it is a relatively straightforward task to obtain the lamina/laminate complex moduli by utilizing the dynamic viscoelastic correspondence principle. This principle states that "the effective complex moduli of a viscoelastic composite are obtained by replacing the phase elastic moduli by the phase complex moduli in the expressions for the effective elastic moduli of identical phase geometry." If the effective elastic moduli are of a form such that they are explicitly obtained from the constituent properties, as in references 7 and 8, the dynamic correspondence principle is particularly simple to apply.

The logic for the correspondence principle for vibrations of viscoelastic composites is reconstructed from reference 1 in Appendix A. The expressions for the lamina complex moduli as a function of phase complex moduli (from the elastic composite cylinder assemblage model of references 7 and 8) and the laminate (see fig. 2) complex stiffnesses are also given in the Appendix. Results for the lamina/laminate complex properties obtained from these expressions are discussed subsequently.

#### Discussion of Results

The constituent properties used to obtain the results given in this section are tabulated in table 1. Note that the fiber properties are assumed to be elastic and frequency independent. The frequency-dependent Young's moduli of epoxy are obtained from reference 2 and extrapolated for frequencies greater than  $10^3$ . The loss factor is seen to increase with the frequency. In general, however, the loss factor frequency curve passes through peak(s) and trough(s) at certain frequencies. A change in temperature is likely to alter the location of these peaks and peak values. A good amount of data on damping characteristics of metals is available in literature. For epoxy matrices, however, such data is scarce. Poisson's ratios for various frequencies given in table 1

are calculated on the assumption that the matrix material is elastic in dilation and the bulk modulus is  $.3824 \times 10^6$  psi, a constant for all frequencies.

The variation of Graphite/epoxy lamina complex Young's and shear moduli and Poisson's ratio as a function of frequency is illustrated in figures 3, 4, and 5, respectively. In figure 3, the real part of the lamina axial modulus is insensitive to the frequency. This is to be expected because the fiber properties are assumed to be frequency independent. The transverse lamina properties (both real and imaginary), the imaginary part of the axial modulus, and the shear moduli in figure 4, however, follow the matrix property variation with frequency. The complex laminate stiffnesses  $\tilde{A}_{11}$ ,  $\tilde{D}_{11}$ ,  $\tilde{A}_{44,45}$  as a function of frequency are shown in figures 6 through 8 for  $[0/90]_S$ ,  $[0_2/\pm 45]_S$ , and  $[0/\pm 45/90]_S$  Graphite/epoxy laminates. For the complex extensional ( $\tilde{A}_{11}$ ) and bending ( $\tilde{D}_{11}$ ) stiffnesses, only the imaginary parts are functions of frequency while for the complex transverse shear stiffnesses ( $\tilde{A}_{44,55}$ ), the variation of both the real and imaginary parts is governed by the matrix.

In summary, the complex stiffnesses for a composite lamina/laminate are obtainable in a simple manner from the phase complex moduli. However, at the present time, data are lacking for the properties of the fiber and matrix at higher values of frequencies.

#### SHEAR-DEFORMATION AND COUPLING EFFECTS

A number of theories have been developed in the literature to characterize the mechanical response of fiber-reinforced composite laminates. These range from the classical laminated plate theory which employs the Kirchhoff-Love hypothesis to the solutions of the exact elasticity equations. Since in composites the ratio of the Young's modulus to the shear modulus can be very large, transverse shear deformations in plates of such materials can be quite significant. For this reason, laminated plate theories based on Kirchhoff-Love hypotheses (refs. 9-10) are not always adequate for predicting

structural response. Failure to consider shear deformation may lead either to overestimates of the frequencies of vibration or underestimates of static deflections for the smaller plate dimension to the plate thickness ratios of less than or equal to 10. Shear deformations have been considered in plate theories (refs. 11-16) in a manner similar to that in Timoshenko-type beam theory (ref. 17) by introducing shear correction factors. The laminated plate response can also be predicted by higher order theories such as the elasticity theory or the "continuum" theory. Solutions to the static and dynamic problems have been obtained (refs. 18-20) by utilizing the "exact" elasticity theory. The scope of this analysis is, however, limited because of the lengthy and tedious computations involved. In the "continuum theory" (refs. 21-22) for a layered medium consisting of alternating plane parallel layers of homogeneous isotropic materials, the local layer rotations are assumed distinct and the transition from the pair of alternating layers to the continuum is achieved by a smoothing operation. This theory has also been referred to as the "effective stiffness" theory. The drawback of the "effective stiffness" theory is that its applicability to "real-world" composite laminates is limited.

The coupling effects in composite laminates arise out of the extension-bending and bending-twisting stiffnesses. For example, the stiffness  $B_{ij}$  ( $i, j = 1, 2, 6$ ) in equation (B17) in Appendix B represents the coupling phenomenon between stretching and bending. For a symmetrical layup of the laminate,  $B_{ij} = 0$  and coupling is eliminated. For unsymmetrical laminates with alternating  $+0^\circ/-0^\circ$  layers of equal thickness, it can be shown that

$$(B_{16} , B_{26}) = \frac{-h^2}{m} (C_{16} , C_{26}). \quad (1)$$

Thus by increasing the number of layers  $m$  in a laminate (fig. 2),  $B_{16}$  and  $B_{26}$  become smaller in magnitude and the bending extension coupling is reduced. This is because the laminate becomes more homogeneous with increasing  $m$ . The effect of coupling is to reduce the natural frequency of a laminate and the degree of the



effect depends upon the number and orientation of the layers in the laminate. Implications of the coupling effect will be evident on panel flutter by virtue of the change in the natural frequency. Also, in the presence of uniform in-plane loads (prestressed panels), the coupling effect will assume particular significance.

#### Shear Correction Factors for Composite Laminates

As mentioned earlier, the need for the consideration of shear deformation in composite laminates arises from the fact that the material is "soft" in shear. Also, because the modes of interest for the panel flutter problem are primarily the flexural and the thickness shear modes, it is logical to consider a theory which would include only the pertinent deformations and eliminate the unwanted modes or deformations associated with it such as the extensional modes. Besides, it has also been demonstrated in reference 20 that the shear deformation theory shows good correlation with the exact elasticity-solution for the first few modes of vibration. Associated with this theory is the shear correction factor,  $k$ , occurring with the transverse shear stiffnesses  $A_{ij}$  ( $i, j = 4, 5$ ). These correction factors are obtained by matching the results of the approximate plate theory with those obtained from more accurate solutions, either for the static (energy formulation; ref. 11) or the dynamic problem (thickness-shear mode frequency matching technique; ref. 12). For the static case of isotropic homogeneous plates (ref. 11), this shear correction factor is obtained to be  $k = 5/6$ , while for the dynamic case (ref. 12), it is  $k = \pi^2/12$ . It is also well known that the shear correction factor for an orthotropic homogeneous plate is the same ( $=\pi^2/12$ ) as that for an isotropic plate. The approach generally followed for composite laminates is to use a constant value of the shear coefficient of the shear correction factor for different laminates irrespective of the laminate construction and stacking sequence. There is, however, considerable uncertainty associated with using a



constant value of  $k$  for all transverse shear stiffnesses ( $A_{44}$ ,  $A_{45}$  and  $A_{55}$ ) for all laminates and stacking sequences. It was noted in reference 20 that  $k$  should be different for the deformations associated with  $\gamma_{yz}$  and  $\gamma_{xz}$  and that it should be also a function of fiber orientation and stacking sequence.

Referring again to equation (B17) in Appendix B, the extension-bending ( $B_{ij}$ ) and bending ( $D_{ij}$ ) stiffnesses are functions of stacking sequence while the transverse shear stiffnesses ( $A_{ij}; i, j=4, 5$ ) are not. Thus, a constitutive theory should be developed which is accurate enough to consider all the stacking sequence effects but simple enough to be used in a form suitable for structural dynamics. Hence, an approach has to be formulated by which the transverse shear stiffness coefficients which are ordinarily independent of the stacking sequence can be obtained as a function of stacking sequence. The only manner in which this can be achieved by utilizing a simple shear deformation theory is to develop a procedure to obtain the shear correction factors associated with these stiffnesses as a function of stacking sequence and laminate construction. While this problem has been considered in references 3, 15, and 16, a systematic approach to study the effects of laminate construction and stacking sequence is lacking.

In this study, the shear correction factors are obtained by utilizing the exact elasticity theory and considering only the thickness-shear modes of vibration. Cut-off frequencies are obtained for infinitely long wave lengths in the limit and these frequencies are compared with the cut-off frequencies for the same thickness shear mode of vibrations obtained from the shear deformation theory. Since the cut-off frequencies will theoretically not match because of the approximate nature of the shear deformation theory, they are forced to match by the inclusion of the shear correction factor in the shear deformation theory. Since the exact elasticity solution accounts not only for the laminate construction, but also for the stacking sequence, it is evident that the shear correction factors so obtained will indeed be functions of laminate construction and

stacking sequence. In this regard, two approximate shear deformation theories have been considered; namely, the one which does not account for the matching of interlaminar stresses at the interfaces by considering a constant transverse shear strain through the thickness of the laminate (refs. 13 and 14), and the one which considers piecewise continuous transverse shear strains through the laminate in an average fashion by matching the interlaminar stresses at the interface (ref. 23). It is observed that the shear correction factors as obtained from each of these approximate shear deformation theories differ significantly, though the products of the shear corrections factors and the corresponding transverse shear stiffnesses (defined by the matrix  $K_{ij}$ ,  $i, j=4, 5$ ) are identical. It is interesting to note, however, that the shear correction factors obtained from the latter theory for a large number of layers approach the value for a homogeneous material, while those from the former theory do not.

The transverse shear coupling stiffness  $A_{45}$ , as obtained in equation (B17) in Appendix B, is zero for orthotropic, symmetric, and  $[\pm\theta]$  laminates ( $\pm\theta$  laminates having equal percentages of  $+\theta$  and  $-\theta$  layers). Thus the coupling stiffness  $K_{45}$  ( $k_{45}A_{45}$  or  $k'_{45}A'_{45}$ ) also vanishes for these laminates. In reality, however, the transverse shear force  $Q_x$  will induce both  $\gamma_{xz}$  and  $\gamma_{yz}$  shear strains, although the magnitude of the latter will be smaller than that of the former. The actual coupling is expected to reduce for laminates which are more homogeneous. In the present investigation, an approach has been developed to assess the magnitude of this coupling.

The analytical/numerical procedure to obtain the shear correction factors by matching the thickness-shear mode cut-off frequencies obtained from the exact elasticity solution and the shear-deformation theory is described in Appendix B. In addition, the method for the evaluation of the transverse shear coupling term has been outlined in the Appendix.

### Discussion of Results

The shear correction factors obtained by the methods described above and in Appendix B are shown in figures 9 through 24 for various mid-plane symmetric laminates with the fiber direction of the  $0^\circ$  layer coinciding with the x direction (see fig. 2). The results are reported for various values of the ratio  $r = G_{23}/G_{12}$  ( $r < 1$ ) where  $G_{12}$  and  $G_{23}$  ( $=G_{13}$ ) are the axial and transverse shear modulus, respectively, of each layer. In figure 9, the shear correction factors for a  $[0/90]_s$  laminate are based on the shear-deformation theory of reference 14 which assumes a constant transverse shear strain across the thickness. It is evident from the figure that for increasing number of layers, the correction factors  $k_{44}$  and  $k_{55}$  ( $k_{45} = 0$  for this laminate) do not approach the value  $\pi^2/12$  for a homogeneous plate. This phenomenon has also been observed in reference 16 for the static solution. If a more "refined" shear deformation theory is used which considers a constant value of inter-laminar shear stress through the thickness (ref. 23), it is seen that the shear correction factors  $k'_{44}$  and  $k'_{55}$  for the  $[0/90]_s$  laminate (fig. 10) indeed approach the value for the homogeneous plate. As noted in Appendix B, it is of no consequence as to which shear correction factors are used ( $k_{ij}$  or  $k'_{ij}$ ), provided that the shear stiffness  $K_{ij}$  ( $k_{ij}A_{ij}$  or  $k'_{ij}A'_{ij}$ ) are identical.

Results for mid-plane symmetric angle-ply laminates ( $\pm\theta$ ,  $\theta = 15^\circ, 30^\circ, 40^\circ$ , and  $45^\circ$ ) are given in figures 11-18 and are summarized in figures 19 and 20. Since  $A'_{45}$  is equal to zero for symmetric laminates, the correction factor  $k_{45}$  cannot be calculated and does not have any significance. A quantity  $k''_{45}$  is defined with the help of which the coupling stiffness  $K_{45}$  can be calculated as  $K_{45} = k''_{45} (K_{44}K_{55})^{1/2}$ . These results show that the coupling shear correction factors  $k''_{45}$  approach zero and  $k'_{55}$  and  $k'_{44}$  approach  $\pi^2/12$  with increasing  $m$ , as in the case of cross-ply laminates. It should be pointed out that results for  $r > 1$  can be easily obtained from the results given here by interchanging  $k'_{44}$  and  $k'_{55}$ .



for the case  $G_{23}/G_{12} = 1/r$  and leaving  $k_{45}''$  unchanged. For  $r = 1$ ,  $k_{44}' = k_{55}' = \pi^2/12$  and  $k_{45}'' = 0$ . For  $m > 8$ , the correction factors  $k_{44}'$ ,  $k_{55}'$  do not differ appreciably from  $\pi^2/12$  for all the laminates considered provided that  $r$  is not too small. Hence, the value of  $\pi^2/12$  can be used in the plate theory if  $A_{ij}'$  are obtained in a manner as outlined in Appendix B and reference 23.

Correction factors  $k_{44}'$ ,  $k_{55}'$ , and  $k_{45}''$  for a  $[0/+45/-45/90]_s$  laminate with equal percentages of  $0^\circ$  and  $90^\circ$  layers are shown in figure 21 for different percentages of  $\pm 45^\circ$  layers and various values of the ratio  $r$ . Similar plots for  $[0/\pm 45]_s$ ,  $[\pm 45/0/90]_s$ , and  $(\pm 45/0)_s$  laminates are given in figures 22-24. Figures 21-24 show that the coupling term  $k_{45}''$  is extremely small when the volume of  $\pm 45^\circ$  layers (equal volume of  $+45$  and  $-45$ ) is less than 0.5. In general, for laminates with a large number of  $0^\circ$ ,  $90^\circ$ , and  $\pm\theta$  layers arranged in a periodic fashion, the term  $k_{45}'$  is likely to be small.

Correction factors  $k_{44}'$ ,  $k_{55}'$  for antisymmetric laminates constructed with a sequential arrangement of  $+\theta$  and  $-\theta$  layers are plotted against  $\theta$  for various values of  $r$  in figure 25. It may be noted that for  $r = .2$ , a discontinuity exists in the plots for a value of  $\theta = \theta_0$ , where  $\theta_0$  depends on the total number of layers  $m$ , but is very close to  $12^\circ$ . Near the discontinuity, the cut-off frequencies corresponding to the first u-dominated mode (antisymmetric) and the second v-dominated mode (symmetric) are close to each other. Also, they do not coalesce at  $\theta = \theta_0$ . For  $\theta < \theta_0$ , the larger frequency corresponds to the u-dominated mode and the lower one is for the v-dominated mode. As  $\theta$  passes through  $\theta_0$ , the roles are reversed. Near  $\theta = \theta_0$ , the antisymmetric u-displacement field is strongly coupled with symmetric v displacements. The laminated plate theory cannot predict any symmetric displacement fields. The correction factors  $k_{55}'$  are calculated so as to predict the frequency corresponding to the u-dominated mode, but the usefulness of such factors near  $\theta = \theta_0$  is limited.



The discontinuity is pronounced when the number of layers  $m$  is small and cannot be identified for  $m = 8$ . Fortunately, for commonly used laminates,  $m$  is large and  $r$  is of the order of 0.5 or higher, and the laminated plate theory can be used to predict the plate response with reasonable accuracy in such cases. However, when  $G_{23}$  and  $G_{12}$  are of different order, the laminated plate theory should be used with caution. The coupling between antisymmetric  $u$  and  $v$  displacements is extremely small in these laminates, and the coupling stiffness can be taken equal to zero. It should be pointed out that as the number of layers is increased,  $k'_{55}$ ,  $k'_{44}$  quickly approach  $\pi^2/12$ .

Laminated plates can be constructed with various stacking sequences of layers of different orientations. Correction factors for only a limited number of such laminates are presented here. The results demonstrate the usefulness of the approach and indicate some general trends which will be of value in design of such plates. In this regard, it should be mentioned that for the application considered in this study (panel flutter of viscoelastic laminates), shear moduli of each layer are frequency-dependent complex quantities. To determine the effects of shear deformation of such laminates, one may consider the problem of wave propagation in a heterogeneous viscoelastic medium. Alternatively, one can take recourse to the dynamic correspondence principle (ref. 1) provided analytical expressions for correction factors are available. The solution presented here does not yield closed-form analytical expressions. However, for a given stacking sequence of layers, the correction factors depend only on the ratio  $r = G_{23}/G_{12}$ . Therefore, if the imaginary part of this ratio in a viscoelastic case is small and the real part is fairly constant over a frequency range near the cut-off frequencies, the values given here can be used as reasonable estimates in the viscoelastic case as well. In particular, the limiting value of  $\pi^2/12$  for a laminate made of a large number of layers arranged in a periodic fashion holds both for the elastic and viscoelastic cases.

## MOISTURE AND TEMPERATURE EFFECTS

An important aspect associated with the laminate constitutive equations is the effect of environment. Since the dynamic response characteristics of the composite panel must be known for its entire lifetime, the effects of changing environment and material wearout or degradation should be considered. Recent developments in the application of polymeric composites to aircraft structures have revealed significant changes in the mechanical properties and dimensions of these materials due to the effects of combined absorbed moisture and thermal environment (refs. 24-29). Material degradation will primarily manifest itself in the form of property (stiffness as well as strength) losses. It has been observed that absorbed moisture coupled with thermal spikes adversely influences the matrix controlled properties. Additionally, absorbed water molecules may act as a plasticizer and, therefore, reduce the glass transition temperature of the matrix, i.e., the temperature at which there is a strong loss of matrix modulus and with it, a corresponding loss of composite strength and a significant increase in material damping.

For the panel flutter problem, the loss in the transverse shear and flexural stiffnesses due to interlaminar degradation will affect critical flutter speeds. Also, the alteration in the glass transition temperature due to humidity and temperature will alter the damping characteristics of the matrix (refs. 29-31) and hence, the laminate.

The analysis approach for the determination of the effects of moisture and temperature on the laminate constitutive equations is to determine the lamina diffusivities from constituent diffusivities using the conductivity analogy and composite cylinder assemblage results. Having obtained the lamina diffusivities (and these diffusivities could be functions of moisture content and temperature), it is possible to calculate the laminate through-the-thickness transient or steady state moisture distribution in the laminate from the one-dimensional diffusion equation (refs. 32-33). If the lamina diffusivities are independent of the moisture content and if the

problem is solved for a given temperature, which is constant throughout the laminate, the solution of the diffusion equation is rather straightforward. However, if one considers the diffusivities as a function of moisture and/or temperature and if there is a temperature gradient across the laminate then the solution has to be obtained by numerical methods. The reason for obtaining the transient state moisture content in a laminate is that a laminate which is mid-plane symmetric initially may behave in an unsymmetrical fashion when subjected to a nonuniform moisture/temperature environment. This is because of different moisture contents and/or temperature through the thickness and as a result, different material properties for each layer. Thus, not only the flexural properties are changed because of the inclusion of moisture/temperature effects, but the laminate also tends to behave in an unsymmetric fashion and thus increasing the coupling effect. Of course, since the properties of the lamina are functions of the moisture content and the moisture content is a function of the thickness coordinate, appropriate shift factors will be utilized from existing experimental data to determine the laminate properties as a function of temperature and moisture distribution.

A computer program for numerical solution of the moisture diffusion equation with temperature/moisture dependent diffusivities which vary across the thickness as well as change with time has been developed. A finite difference scheme in space coordinate and a predictor corrector technique in time variable are employed for this purpose. The approach is outlined in Appendix D. Sharp discontinuity in diffusivities due to the presence of layers of different materials is also considered. For this purpose, moisture content in the two materials at the common boundary, as well as moisture transfer across the interface, are assumed to be equal. The approach discussed here (details of which are given in Appendix D) has been used to solve the moisture diffusion problem in a coated composite. The results are compared in figure 26 with those obtained in reference 32. It should be noted that the



difference between the two solutions is not significant and appears to be entirely due to the fact that in reference 32 the moisture concentrations in the two materials at an interface are not assumed to be the same whereas they are considered the same in the present study. The procedure outlined here can be easily modified to account for different concentrations in the two materials as considered in reference 32. No attempt is made in this study to obtain solution of the nonlinear diffusion problem in the case of moisture-dependent diffusivities because data describing dependence of diffusivity on moisture concentration are scarce. However, the approach presented is a general one and can yield solution of the nonlinear problem without any more effort than what is needed in the linear case as appropriate input data become available.



### PANEL FLUTTER OF VISCOELASTIC COMPOSITE LAMINATES

The capability to assess the dynamic response of composite materials becomes increasingly important as the number of their applications in aerospace structures increases. A number of investigations, as noted earlier, have been performed in this regard to assess the influence of the geometric and material variables upon the vibrational frequencies and dispersion characteristics. These studies are an essential first step in assessing the response of a structure subjected to a more complex transient and aerodynamic load.

A direct and important consequence of aerodynamic loading is panel flutter. The problem of panel flutter (as distinct from the more conventional lifting surface flutter) can be stated quite simply. A fluid stream passes over the surface of a thin plate (or shell) as illustrated in figure 27. The objective is to determine the stability or instability of the fluid structural system. In particular, one is seeking to establish the stability or flutter boundaries separating stable and unstable motion. If the system is unstable, the nature of the unstable solution can be investigated further by considering nonlinear oscillations. On the other hand, if the system is stable, the structure merely responds to fluctuations in the fluid stream. A schematic of structural response is given in figure 28 (from ref. 38) where the plate deflection to the plate thickness ratio is plotted versus the dynamic pressure of the flow. Below a certain value of the dynamic pressure, the predominant phenomenon is that of noise, while above a certain dynamic pressure, the amplitudes increase significantly and that is termed flutter. Also, panel flutter is a supersonic phenomenon. As is obvious from figure 28 for larger values of the dynamic pressure, geometric nonlinearities influence the problem. Physically, the nonlinearity results from the tension induced in the plate by bending deformations. This tension increases with increasing plate deflection and thereby limits the unstable motion

to a finite amplitude. This limitation often causes the modes of structural failure to be those peculiar to fatigue rather than explosive fracture of the skin surface. A linear model (like the one considered here) which does not include the effects of in-plane deformations of the plate would of course predict infinite deflections at the critical dynamic pressure.

Considerable work has been done in the problem of panel flutter over the past two decades (see, for example, refs. 34-38). Most analyses can be placed in one of four categories based on the structural and aerodynamic theories considered: (i) linear structural theory; quasi-steady aerodynamic theory; (ii) linear structural theory; inviscid, potential aerodynamic theory; (iii) nonlinear structural theory; quasi-steady aerodynamic theory; and finally (iv) nonlinear structural theory; inviscid, potential aerodynamic theory. As one would expect, the significant body of the literature is in the first category because it is the simplest. Unfortunately, this analysis has two major weaknesses: (i) it does not account for structural nonlinearities; hence it can only determine the flutter boundary and can give no information about the flutter oscillation itself; and (ii) the use of quasi-steady aerodynamics neglects the three-dimensionality and unsteadiness or memory of the flow. Hence it cannot be used for Mach number close to 1. However, it is known that panel flutter occurs in the vicinity of  $M \gtrsim 1$ . Since it is not the intent of the present effort to investigate the effect of geometric nonlinearities as well as the appropriateness of the various aerodynamic theories, only the linear structural theory and the quasi-steady aerodynamic theory of the first category would be utilized for the analysis. Specifically, the linear piston theory aerodynamics (ref. 39) which includes aerodynamic damping will be used in the proposed investigation. This theory proposes that the aerodynamic loading on the panel is proportional to the instantaneous slope of the panel (which also suggests that panel flutter is a nonconservative stability problem).

The critical dynamic pressure will be a function of the composite laminate panel constitutive relations (which consider dynamic viscoelastic behavior of the laminate as well as the bending-extension and bending-twisting coupling). Other factors which affect the critical pressure are the flow angle, and also the presence of in-plane compressive forces (prestress). In the presence of coupling in laminates, the in-plane forces will assume particular significance because their destabilizing effect will increase. The panel geometry (plate aspect ratio) and boundary conditions will also have noticeable influence on the flutter parameter. However, in the present study, the primary objective is to assess the influence of some of the unique characteristics of composite laminates on panel flutter. These characteristics are damping, coupling, and shear deformation and environmental effects. Effects of these characteristics will be investigated in detail and the importance of other analysis variables will be studied in a cursory fashion.

Damping effects can be considered for the problem of panel flutter by the inclusion of aerodynamic and structural damping (for example, refs. 40 and 41). In the former case, damping is proportional to velocity, while in the latter case, damping is incorporated through the complex moduli. Inclusion of damping is important for the present problem because of the following reasons:

- (i) Damping is an inherent property of composite laminates and as such cannot be ignored for structural dynamics problems.
- (ii) Though the velocity dependent damping increases the flutter dynamic pressure, it has been observed that damping in the form of viscoelastic complex moduli can frequently have a destabilizing effect.
- (iii) A theory which neglects damping predicts zero dynamic pressure for flutter whenever the mid-plane load has



caused two panel vibration frequencies to coalesce (zero dynamic pressure flutter points).

If one considers aerodynamic and structural damping where the effect of the latter is included by modifying both the membrane and bending terms with a linear damping coefficient, the same anomolous behavior as in (iii) is predicted. In reference 41 it was suggested that structural damping should modify only those terms in the equations associated with bending. Such a procedure removes the physically untenable effects which render the flutter parameter insensitive at the transition point to the panel aspect ratio and boundary condition. With reference to the complex properties of composite laminates, such a procedure for considering only flexural damping only cannot be always true because of the possibility of extension-bending coupling.

The flutter of sandwich and orthotropic panels has also been the subject of numerous investigations (for example, refs. 42-44). However, it is only recently that some effort has been directed towards the flutter analysis of composite laminate plates. The behavior of composite laminates is different from orthotropic panels (which, incidentally, are a special case of a general composite laminate) because of the coupling effects. Results in references 45 and 46 indicate that the ply orientations (and, hence, coupling) and the anisotropy ratios strongly influence the dynamic instability.

The effect of shear flexibility and rotary inertia has been considered primarily for sandwich panels because of the finite core shear stiffness (see, for example, ref. 43). Inclusion of both shear flexibility and rotary inertia, while still affecting the flexural motion, admits two additional degrees of freedom. They are termed as the thickness shear and thickness twist modes. In general, both these motions produce transverse deflections and thus influence the aerodynamic loading. It was observed in reference 43 that these two modes markedly change the frequency

coalescence behavior and failure to account for them can lead to significant overestimates of flutter dynamic pressure values. Once again, for composite laminates, the "soft" shear moduli increase the importance of shear deformation. Additionally, both the shear deformation and material damping are matrix dominated. Hence their combined effect can affect panel flutter significantly.

In the present investigation, a "refined" shear deformation theory is utilized to characterize the composite laminate panel response. The shear correction factors in this theory are obtained for the specific laminate under consideration.

#### PANEL FLUTTER OF SYMMETRIC LAMINATES IN CYLINDRICAL BENDING

The emphasis in the present study is on the composite material parameters rather than on the geometric and aerodynamic aspects of the panel flutter problem. Hence the logical choice for the panel geometry is the one corresponding to a cylindrical bending deformation (infinitely long in the  $y$  direction) with simply supported edges. The procedure for flutter analysis of such panels is outlined in Appendix C.

Given the frequency-dependent complex moduli of the constituents (fiber and matrix) at different temperatures and for various moisture concentrations, the lamina properties can be computed by the use of methods outlined in Appendix A giving due consideration to the actual temperature and moisture distribution in the laminate. Complex moduli of each lamina for various frequencies are calculated for the actual temperature and moisture content at the lamina location by the use of linear interpolation. One can then obtain the laminate properties and shear correction factors based on the procedure outlined in Appendices A and B. Formulation of the flutter determinant for a general laminated plate by the use of the Galerkin procedure is discussed in Appendix C. In general, it is necessary to evaluate eigenvalues of a matrix of size  $5N \times 5N$ , where  $N$  is the number

of terms retained in each of the infinite series expressions chosen for the five displacement variables. A technique for reducing the size of the matrix by omitting some of the modes which are unimportant is also discussed in the Appendix. Since the laminate properties are dependent on frequency, the eigenvalues must be determined by the use of trial and error procedure. At first the eigenvalues for  $\bar{\lambda} = 0$  corresponding to each N are determined. Attention is then restricted to frequencies less than or equal to the highest flexural frequency. This frequency range is then divided into several parts. Average properties in each part are then used to determine the points at which imaginary parts of eigenvalues change sign as  $\bar{\lambda}$  is gradually increased. Properties at these points (corresponding to the real part of  $\omega$ ) are then used to recalculate the eigenvalue and the flutter parameter. This procedure is repeated to achieve the desired accuracy. Convergence of any trial and error procedure is strongly dependent on the starting point as well as the increments by which the parameter to be determined is changed. The procedure used here has the same limitation and, therefore, in certain cases, it had to be repeated to obtain the results sought.

An alternate approach to determine the flutter parameter for (0/90) laminates is also presented in Appendix C. In this approach, the problem is reduced to the calculation of the determinant of a matrix of size N x N for a range of values of  $\bar{\lambda}$  and real part of  $\omega$ . Denoting the real and imaginary parts of these determinants as  $\Delta_R$  and  $\Delta_I$ , the value of  $\bar{\lambda}_{cr}$  can be obtained from the condition  $\Delta_R = \Delta_I = 0$ . In the initial stages of this work, this approach was used to obtain the required value of  $\bar{\lambda}_{cr}$  and the results obtained are presented in the next subsection.

#### Results for (0/90) Laminates

Obtained by the Use of the Criterion  $\Delta_R = \Delta_I = 0$

Results for the following three symmetric laminates, each 0.06" thick, are presented here (the fiber direction in the 0° layer is assumed to coincide with the x axis):



- (i) Laminate 1, Boron/epoxy,  $[0/90]_s$ , span  $a = 0.6"$ ,  
 $a/H = 10$
- (ii) Laminate 2, Boron/epoxy,  $[0/90]_{2s}$ , span  $a = 0.6"$ ,  
 $a/H = 10$
- (iii) Laminate 3, Graphite (T300/epoxy)  $[0/90]_{2s}$ ,  
span  $a = 3.6"$ ,  $a/H = 60$

All the layers in the laminates are of equal thickness. Properties of the fibers and the matrix are listed in table 1. Both boron and graphite fibers are assumed to be elastic with the same properties for all frequencies. The epoxy matrix is elastic under hydrostatic stress with bulk modulus  $K = 0.3824 \times 10^6$  psi for all frequencies. Variation of Young's modulus  $E$  with frequency in the range  $5 \leq \text{Re}(\omega) \leq 3 \times 10^3$  is taken from reference 2. Because of the low value of  $a/H$  ratio for the first two laminates, properties at higher frequencies are required in the flutter analysis. They are obtained (see table 1) by linear extrapolation from the data in reference 2. The value of the shear correction factor  $k_{55}$  is chosen to be 0.8. Since the shear moduli  $G_{23}$  and  $G_{12}$  of each of the layers are of the same order, this choice is adequate. For each of the laminates, several levels of damping have been considered. The imaginary parts of  $E$  and  $\nu$  of the epoxy matrix in table 1 for all frequencies are multiplied by a factor depending on the level of damping (as listed in table 2) and the real parts are left unaltered.

The  $\bar{\lambda}$ - $\text{Re}(\bar{\omega})$  curves on which the real and imaginary parts of the determinants are zero are plotted in figures 29 through 37. for the three laminates under consideration. Note that  $\bar{\omega}^2 = \bar{P} \omega^2$ , where  $\bar{P}$  is defined in equation (C3) of Appendix C. Calculations for Graphite/epoxy laminates with constructions similar to laminates 1 and 2 and Boron/epoxy laminates with the construction of laminate 3 have also been made. Because of similar trends in the results, a discussion pertaining to these additional laminates has been omitted here. For the same reason, results for Graphite/epoxy and Boron/epoxy laminates of  $[0/90]_s$  construction and length 3.6" (same as that of laminate 3) are not presented.

For the first two laminates ( $a/H = 10$ ), shear deformations have significant effect on the modes of flutter as seen in figures 29-35. On the other hand, for laminate 3 ( $a/H = 60$ ) and flutter occurs by coalescence of the first two modes which are predominantly flexural in nature (figs. 36 and 37). In the first two laminates, the  $\bar{\lambda}$ - $\text{Re}(\bar{\omega})$  plots (figs. 30 - 32, 34 and 35) show three points of kinetic instability. Two of these points are clearly due to coalescence of two consecutive modes of flexural vibration. Table 3 lists the parameters  $\bar{\lambda}_{\text{cr1}}$  (coalescence of fourth and fifth mode) and  $\bar{\lambda}_{\text{cr2}}$  (coalescence of second and third mode) for kinetic instability for various levels of damping. The first flexural mode does not appear to coalesce with other modes in the range of  $\bar{\lambda}$  and  $\text{Re}(\bar{\omega})$  considered, but it appears that there is a point ( $\bar{\lambda}_{\text{cr3}}$ ) at which unstable motion is possible when damping is present. However, as  $\bar{\lambda}$  is increased further, one finds another point of cross-over; i.e. the motion tends to become stable again (see fig. 32). This point of cross-over occurs at a value of  $\lambda$  which is high as compared to  $\bar{\lambda}_{\text{cr3}}$  in the figure. The value of  $\lambda_{\text{cr3}}$  is very low and this instability does not occur when there is no damping.

Similar results, obtained by the use of the method, outlined in Appendix C, for calculating real and imaginary parts of  $\omega$  are presented later. These results indicate that as  $\bar{\lambda}$  is increased beyond  $\bar{\lambda}_{\text{cr3}}$ ,  $\omega_I$ , the imaginary part of  $\omega$  changes signs, indicating that the motion becomes unstable. However, the  $\omega_I$  does not increase rapidly as  $\bar{\lambda}$  is increased, which means that the instability is not of a very severe nature.

For laminate 3, the frequency at which flutter appears to occur is between the first two frequencies of flexural motion and the effects of sheer deformation do not seem to have any significant influence on flutter characteristics (see figures 36, 37). When damping is present, the critical flutter parameter is significantly lowered (see table 3). However, as  $\bar{\lambda}$  is increased beyond  $\bar{\lambda}_{\text{cr}}$ , the curves  $\bar{\lambda} = f(\omega_R)$  for  $\Delta_R = 0$  and  $\Delta_I = 0$  approach each other again,

indicating that the instability becomes less severe as  $\bar{\lambda}$  is increased. Beyond  $\bar{\lambda} = 215$  the two curves separate out again, indicating an onset of severe flutter. These characteristics are clearly demonstrated in the results presented in the next section. It should be pointed out here that possible existence of a weak first mode flutter in low supersonic, transonic range in other theoretical predictions and experimental results similar to those observed here is discussed in reference 38.

The results given in this section show that introduction of little damping lowers the flutter load considerably from the case when there is no damping. Further increase in damping causes the flutter load to increase again as observed in laminates 1 and 2. However, the increase is not very significant. These observations are in agreement with well-known results of destabilizing effect of damping in nonconservative elastic systems (see, for example, refs. 40, 47). The destabilizing effects observed here as well as the severity of instability corresponding to  $\bar{\lambda}_{cr3}$  found in laminates 1 and 2 and  $\bar{\lambda}_{cr}$  in laminate 3 have been investigated further by employing techniques described in Appendix C for determining real and imaginary parts of  $\bar{\omega}$ . These results are presented in the next sub-section.

#### Results Obtained from Calculation of Complex Eigenvalues

To study environmental, damping, coupling and shear deformation effects on strong as well as weak instabilities, complex eigenvalues  $\omega$  have been calculated for the following T300/epoxy symmetric laminates. The  $0^\circ$  direction is assumed to coincide with the x-axis and thickness of the laminates is equal to .06".

- (i) Laminate 4,  $(0/90)_{2s}$  laminate is reconsidered,  
 $a/h = 60, a = 3.6"$
- (ii) Laminate 5,  $(0/90)_{2s}, a/h = 10, a = 0.6"$
- (iii) Laminate 6,  $(\pm 45/0_2/90)_s, a/h = 40, a = 2.4"$
- (iv) Laminate 7,  $(\pm 45/0_2/90)_s, a/h = 10, a = 0.6"$

T300 fiber properties used for these calculations are the same as those listed in table 1. Input epoxy matrix properties



are plotted against frequency in figure 38. To calculate matrix properties at different temperature and moisture concentrations, use is made of the well known shift hypothesis (references 48, 49). Assumed shift factors are also shown in the same figure. For frequencies in the range  $10 - 10^3$  Hertz in situ storage modulus and loss tangents are assumed to be the same as those given in reference 2. For low frequencies, these values are assumed to behave in a manner similar to those of an epoxy resin, as reported in reference 48 (with due consideration to shifts). The bulk modulus of the matrix is assumed to be  $0.488 \times 10^6$  psi (from ref. 2) which is real and constant for all temperature and moisture content. It should be pointed out that this value is different from the one listed in table 1, used to obtain the results in one previous subsection, and for this reason quantitative results presented here may differ a little from those discussed earlier. Fiber properties are assumed to be real and independent of temperature and moisture content. Experimental data on constituent properties at various frequencies, temperature and moisture content are scarce, and therefore, the approach which is discussed above and appears to be a consistent one, has been used to estimate the input data. The results obtained are discussed and conclusions are drawn with due consideration to the calculated laminate properties and, therefore, effects of other types of input properties can be estimated if the corresponding laminate properties are known.

Real and imaginary parts of  $\tilde{\omega} = \omega \cdot \sqrt{\rho a^4 / D_0}$  for various values of  $\bar{\lambda} = 2a^3 q / (\beta D_0)$  are plotted in figures 39-42 for the laminates 4-7, respectively. The values of critical flutter parameter are also listed in these figures. The solid lines represent the solutions for the reference state, i.e. the laminate is at room temperature (70°F.) and is dry. The dotted lines are for a prescribed moisture and temperature gradient as shown in figure 39. The temperatures on top and bottom surfaces are 250° and 70°F respectively. Moisture concentration in the matrix materials

on these surfaces are 2.57% and zero. Five terms of the series representation ( $N = 5$ ) were retained in all the calculations. A total of twenty modes to include the effect of four displacement variables,  $W$ ,  $\psi_x + W$ ,  $x$ ,  $\psi_y$  and  $U_0$ , were considered in laminate 7, where bending-extension coupling effects due to unsymmetric moisture, temperature distribution should have the largest influence. No destabilizing effect was noticed. Extensional stiffnesses appear to be extremely high to have any influence on flutter characteristics. Therefore, fifteen modes were retained for laminate 6 and ten were retained for laminates 4 and 5, where there is no coupling between the shear deformations  $\psi_x + W$ ,  $x$  and  $\psi_y$ .

Observations and comments made in the previous subsection also hold for the results presented in figures 39-42. Figure 40 clearly shows that the imaginary part of  $\omega$  increases slowly and then decreases again as  $\bar{\lambda}$  is increased beyond  $\bar{\lambda}_{cr3}$ . Instabilities at  $\lambda = \lambda_{cr1}$  and  $\lambda_{cr2}$  are much more severe. Shear deformation has a tremendous influence on the critical flutter parameter. By arbitrarily increasing the shear stiffness (increasing the shear correction factor by 1000 times), the critical flutter parameter for laminate 5 is increased from 48 to 117 (see fig. 40) and severe flutter then occurs by coalescence of modes 1 and 2.

For laminate 4, where shear deformation effects are negligible,  $\bar{\lambda}_{cr}$  is significantly lowered by introduction of damping. Also, the imaginary parts of  $\bar{\omega}$  change sharply from positive to negative at  $\lambda_{cr}$ , but severity of flutter does not increase until  $\bar{\lambda}$  is increased by quite a good amount beyond  $\bar{\lambda}_{cr}$ . This characteristic has been pointed out in the previous subsection.

In laminate 7, the weak instability sets in at very low value of  $\bar{\lambda}$  as in the case of laminate 5. However, as  $\bar{\lambda}$  is increased significantly,  $\bar{\omega}_1$  corresponding to mode 1 changes sign again from negative to positive, but  $\bar{\omega}_2$  corresponding to mode 2

becomes negative and yields a severe instability. On the other hand, it appears that inclusion of moisture-temperature effects causes  $\bar{\omega}_I$  corresponding to mode 1 to increase in magnitude causing a strong flutter instability. Near these points of severe instability, strong coupling exists between the mode shapes and it is difficult to accurately determine which frequency corresponds to each mode. Calculations were made to keep track of the modes and associated frequencies and the results appear to confirm the characteristic described above. Although this behavior does not influence critical values of flutter parameters for weak or strong instabilities, it is an interesting phenomenon and should be investigated in detail in future studies.

Moisture-temperature gradient does not appear to have much influence on the critical value of the flutter parameter for laminate 4, but increases the critical values for laminates 5-7. This beneficial effect, however, is not due to increased damping. Moisture-temperature gradient actually reduces the loss tangents of bending as well as shear stiffness of all laminates as is clear from the values of  $\bar{\omega}_I$  at  $\bar{\lambda} = 0$ . This is a consequence of the type of master curve assumed (fig. 38) and the shift hypothesis. Loss tangents for the epoxy matrix reduce with decreasing frequency up to  $\omega \approx 10$ . Increased temperature and moisture effects cause a shift towards the left in figure 38 by the shift hypothesis, which causes a reduction in loss tangent. For the same reason, the storage modulus increases due to moisture-temperature effects. This increase in storage modulus increases the shear stiffness. It appears that this increase in shear stiffness is reflected in the increased values of  $\bar{\lambda}_{cr}$  in laminates 5-7 where shear deformations have significant influence. Since  $\bar{\lambda}_{cr}$  for laminate 4 is not strongly influenced by shear deformations, no increase is noticed in this case.

The approach based on calculation of complex eigenvalues should yield values of  $\bar{\lambda}_{cr}$  which are more accurate than those obtained in the previous subsection by the use of the condition



$\Delta_R = \Delta_I = 0$ . Therefore, the effect of various damping levels (table 2) was reinvestigated by the use of these refined calculations. Results are tabulated in table 4. For laminate 5,  $\bar{\lambda}_{cr1}$  and  $\bar{\lambda}_{cr2}$  appear to increase as damping level is increased from 1 to 3. For no damping there does not appear to be any point of incipient flutter corresponding to  $\bar{\lambda}_{cr3}$  for cases with damping. This point  $\bar{\lambda}_{cr3}$  is, however, not a point of severe instability. For laminate 4  $\bar{\lambda}_{cr}$  sharply drops from the value of 340 for zero damping to 157, 150, 150 for damping levels 1, 2, and 3, respectively. The reason for a higher value of  $\bar{\lambda}_{cr}$  for level 1 as compared to those for levels 2 and 3 is not clear. This trend is different from that in other results in tables 3 and 4, which show some increase or no change in  $\bar{\lambda}_{cr}$  as damping is increased from level 1 to 3. It should be noted, however, that the imaginary part of  $\bar{\lambda}$  sharply changes from negative to positive in the case of laminate 4 (see fig. 39) as it passes through  $\bar{\lambda}_{cr}$  and the properties used for calculations are obtained by linear interpolation from those given in a tabular form. In view of these facts, the small difference discussed above does not appear to be significant. In general, the conclusions which can be drawn from the present results are the same as those discussed in the previous subsection. It should be pointed out, however, that the drop in  $\bar{\lambda}_{cr}$  by introduction of small damping is significantly higher when shear deformation effects are small ( $a/h$  is large) as compared to the cases when such effects are dominant ( $a/h$  is small).

A simple way to assess the severity of flutter is to examine how the magnitude of the imaginary part of  $\omega$  increases after it becomes negative. The imaginary parts of  $\omega$  are plotted in figures 39-42 for laminates 4-7 which clearly show that severe flutter does not always set in at the values of  $\bar{\lambda}_{cr}$  given in these figures. Another approach of judging whether the instability is severe or not is to use the concept of amplitude ratio  $A_R$  or logarithmic increment (refs. 40 and 47). The amplitude ratio

$A_R$  is defined as the increase in amplitude in one cycle, which is equal to  $e^{2\pi\omega I/\omega R}$  and the logarithmic increment is  $\text{Log}_e A_R$ .  $\text{Log}_e A_R$  is plotted against  $\lambda$  for laminate 6 in figure 43, which clearly shows that beyond  $\bar{\lambda}_{cr}$  the amplitude does not increase too rapidly with  $\bar{\lambda}$ . The values of  $\bar{\lambda}$  near which amplitudes are expected to increase rapidly are higher than  $\bar{\lambda}_{cr}$  and should be close to, but less than, the critical flutter parameter for no damping. These observations are in agreement with those in reference 47. Figure 43 also shows the effect of environment (moisture-temperature gradient), aerodynamic damping, and prestress. Moisture-temperature gradient appears to stabilize the system. It has also been pointed out earlier that structural damping effects are less when moisture-temperature gradient is present in the laminate, which is a consequence of the master curve of epoxy used in calculations. The stabilization effect is caused by (i) reduced structural damping and (ii) increased shear stiffness, but the increase in  $\bar{\lambda}_{cr}$  is possibly entirely due to increase in shear stiffness.

Figure 43 also illustrates that  $\bar{\lambda}_{cr}$  ( $\bar{\lambda}$  at  $\text{log}_e A_R = 0$ ) is significantly increased by the introduction of aerodynamic damping but the amplitude ratio versus  $\bar{\lambda}$  plot does not differ significantly from the one with no aerodynamic damping for high values of  $A_R$ . The stabilization effects of aerodynamic damping have been observed in other studies (ref. 40). Effects of prestress have been studied for two values of the ratio of prestress to static buckling load, namely 0.5 and 0.8.  $\bar{\lambda}_{cr}$  is not significantly altered due to the presence of prestress, but severe flutter sets in at loads lower than that with no prestress. Effects of environment, prestress, and aerodynamic damping on  $\bar{\lambda}_{cr}$  are given in table 5.

The following important observations can be made from the results presented in this and the previous subsection:

1. Small damping lowers the flutter load from the value for no damping. The reduction is very significant when shear deformation effects are small or span-to-depth ratio of the panel is large. For small span-to-depth ratios, this reduction is not that significant. In general, higher damping increases the flutter load. Shear deformation effects have strong influence on analytical estimates of the flutter characteristics of a laminate.
2. When damping is present, instability is not always severe at points of incipient flutter. Values of  $\bar{\lambda}$  where instability is severe are usually close to  $\bar{\lambda}_{cr}$  for no damping.
3. For the type of master curve and shift hypothesis used in this study, moisture-temperature gradient in a laminate may increase the value of  $\bar{\lambda}_{cr}$  as well as  $\bar{\lambda}$  for a prescribed amplitude ratio  $A_R$ . However, the results are strongly dependent on the type of master curve and shift characteristics of the constituents.
4. Aerodynamic damping stabilizes the system and significant increase is noticed in the critical value of  $\bar{\lambda}_{cr}$  as the damping is increased. Prestress destabilizes the system but the effect on  $\bar{\lambda}_{cr}$  is not pronounced for values of prestress less than the static buckling load.
5. Bending-extension coupling effects introduced due to the presence of moisture-temperature gradient do not have any significant influence on the flutter characteristics of symmetric laminates.



### CONCLUDING REMARKS

The problem of panel flutter of epoxy matrix composite laminates is investigated here. Emphasis is placed upon incorporating into the analysis an appropriate constitutive relation for the composite laminate. This requires consideration of coupling effects between extension and bending and bending and twisting. It also requires consideration of shear deformation effects as a function of laminate construction and stacking sequence, and frequency-dependent dynamic viscoelastic behavior of composite laminates. In addition, an approach for the determination of the effects of moisture and temperature on the laminate constitutive equations is outlined. Finally, the panel flutter of symmetric laminates in cylindrical bending is investigated in order to assess the effects of the composite material parameters such as laminate construction, shear deformation, and damping upon the critical flutter parameter.

Effects of aerodynamic damping and prestress are also studied in a cursory fashion. Although the results given here are for symmetric laminates only, the methods utilized are applicable to cylindrical bending of laminates which are not necessarily symmetric.

The correspondence principle for vibrations of viscoelastic composites is utilized for the determination of lamina/laminate complex properties from the constituent complex properties. It is observed that if the effective elastic moduli are of a form such that they are explicitly obtained from the constituent properties, the dynamic correspondence principle is particularly simple to apply. Typical results for lamina/laminates show that their matrix-dominated stiffnesses are essentially governed by the epoxy matrix complex properties.

An analytical/numerical procedure to obtain the shear correction factors associated with the transverse shear stiffnesses is developed. The approach consists of obtaining the cut-off frequencies of propagation of plane waves in the thickness-shear mode for a laminated plate from a "refined" shear deformation

theory as well as "exact elasticity solution" and then equating them to obtain unknown values of the shear correction factors. In addition, a method is also formulated for evaluating the transverse shear coupling term. The shear correction factors for a limited number of composite laminates are presented. It is seen that as the number of layers in a laminate increases, the shear correction factors approach the classical value of  $\frac{\pi}{12}$  for a homogeneous plate, and the magnitude of the shear coupling term decreases. The ratio  $r$  ( $G_{23}/G_{12}$ ) also influences the magnitude of the shear correction factors. For values of  $r$  not close to unity and for a small number of layers in a laminate, the correction factors may differ significantly from the classical value.

The investigation of panel flutter characteristics of symmetric laminates indicates that both shear deformation and damping have significant effects. In general, introduction of little structural damping lowers the flutter load considerably from the case when there is no damping. Further increase in damping causes the flutter load to increase. These observations are in agreement with the well-known results of destabilizing effect of damping in nonconservative elastic systems. Introduction of aerodynamic damping, on the other hand, stabilizes the system and compressive prestress has a destabilizing effect. In cases where effects of shear deformation are small, i.e. span-to-depth ratio is large, the destabilization phenomenon caused by small structural damping discussed above is more pronounced than that in laminates with lower span-to-depth ratio. Severe instability does not always set in at points of incipient flutter when damping is present. Effects of environment on flutter characteristics are strongly dependent on the type of master curve and shift hypothesis used to estimate constituent properties for various temperature and moisture concentration levels. Experimental data on constituent properties are very limited and only a small number of problems have been studied here. However, the usefulness of the analytical techniques presented to study various

environmental factors has been clearly demonstrated. Bending extension coupling effects introduced due to nonsymmetric temperature and moisture distribution do not appear to have much influence on flutter characteristics of symmetric laminates.

Finally, a solution procedure for the moisture diffusion equation in the case of temperature/moisture dependent variable diffusivities across the thickness has been developed by the use of a finite-difference scheme and a predictor-corrector technique. Such an analysis in conjunction with the available data in the literature for moisture/temperature effects on lamina/laminate properties would provide the means of assessing the effects of environment on panel flutter, under transient as well as steady-state conditions.



APPENDIX A.  
EFFECTIVE COMPLEX MODULI OF LAMINA/LAMINATE

CORRESPONDENCE PRINCIPLE FOR VIBRATIONS OF VISCOELASTIC COMPOSITES

A theory of quasi-static viscoelastic behavior of fiber-reinforced materials has been developed (see, for example, ref. 1). The basic tool in the analysis is the correspondence principle which relates effective elastic moduli of composites to effective relaxation moduli and creep compliances of viscoelastic composites. Subsequently, it was demonstrated in reference 1 that the effective complex moduli (characterizing the dynamic behavior of viscoelastic composites) can also be related to the effective elastic moduli of composites by a correspondence principle. It is worthwhile here to reconstruct the logic developed in reference 1 to establish this dynamic viscoelastic correspondence principle. The effective relaxation moduli of a statistically homogeneous viscoelastic composite may be defined by

$$\bar{\sigma}_{ij}(t) = \int_{-\infty}^t C_{ijkl}^* (t - \tau) \frac{\partial \bar{\epsilon}_{kl}}{\partial \tau} d\tau \quad (A1)$$

where  $\bar{\sigma}_{ij}$  and  $\bar{\epsilon}_{ij}$  are the average stress and strain tensors, respectively, and  $C_{ijkl}^*$  is the effective relaxation moduli tensor. Assume that the average strain field varies with time in the form

$$\bar{\epsilon}_{ij} = \tilde{\epsilon}_{ij} e^{i\omega t} \quad (A2)$$

where  $\omega$  is the frequency and  $\tilde{\epsilon}_{ij}$  is time independent but may be complex and a function of  $\omega$ . Substitution of equation (A2) in equation (A1) results in

$$\bar{\sigma}_{ij}(t) = i\omega \tilde{\epsilon}_{ij} \int_{-\infty}^t C_{ijkl}^*(t - \tau) e^{i\omega\tau} d\tau. \quad (A3)$$

If  $t - \tau = t'$ , one obtains

$$\bar{\sigma}_{ij}(t) = \tilde{\sigma}_{ij} e^{i\omega t} \quad (A4)$$

where

$$\tilde{\sigma}_{ij} = D_{ijkl}^*(i\omega) \tilde{\epsilon}_{kl} \quad (A5)$$

and

$$D_{ijkl}^*(i\omega) = i\omega \int_0^{\infty} C_{ijkl}^*(t') e^{-i\omega t'} dt'. \quad (A6)$$

Equation (A5) resembles the elastic stress-strain law and  $D_{ijkl}^*$  are the effective complex moduli.  $D_{ijkl}^*$  can be separated into real and imaginary parts. Thus

$$D_{ijkl}^*(i\omega) = D_{ijklR}^*(\omega) + iD_{ijklI}^*(\omega) \quad (A7)$$

The real part of equation (A7) is called the storage modulus while the imaginary part is termed as the loss modulus. The ratio of the imaginary part to the real part is defined as the loss factor.

Consider now the Laplace transform (LT) of the effective relaxation moduli

$$\hat{C}_{ijkl}^*(p) = \int_0^{\infty} C_{ijkl}^*(t) e^{-pt} dt \quad (A8)$$

Then the LT of equation (A1) is given by:

$$\hat{\sigma}_{ij} = \Gamma_{ijkl}^*(p) \hat{\epsilon}_{kl}(p) \quad (A9)$$

where

$$\Gamma_{ijkl}^*(p) = p \hat{C}_{ijkl}^*(p). \quad (A10)$$

$\Gamma_{ijkl}^*$  is the transform domain (TD) effective moduli. From equations (A5), (A8), and (A10), it can be concluded that

$$D_{ijkl}^*(i\omega) = \Gamma_{ijkl}^*(i\omega)$$

and

$$D_{ijkl}^*(p) = \Gamma_{ijkl}^*(p). \quad (A11)$$

The static correspondence principle for viscoelastic composites states that the effective TD moduli of a viscoelastic composite are obtained by the replacement of phase elastic moduli by TD phase moduli in the expression for the effective elastic moduli of a composite with identical phase geometry. In other words, if the effective elastic moduli is defined as

$$e_{C_{ijkl}}^* = e_{C_{ijkl}}^* \{ \text{phase moduli, phase geometry} \} \quad (A12)$$

then the effective TD moduli are

$$\Gamma_{ijkl}^*(p) = e_{C_{ijkl}}^* \{ \text{TD phase moduli, phase geometry} \}. \quad (A13)$$

From equations (A11) and (A13), it is evident that

$$D_{ijkl}^*(i\omega) = e_{C_{ijkl}}^* \{ \text{TD phase moduli } (i\omega), \text{ phase geometry} \}. \quad (A14)$$



But the TD phase moduli on the RHS of equation (A14) are merely the same as the phase complex moduli from equation (A11). Consequently, equation (A14) is rewritten as

$$D_{ijkl}^*(i\omega) = e_{C_{ijkl}}^* \{ \text{phase complex moduli, phase geometry} \} \quad (A15)$$

Thus, the effective complex moduli of a viscoelastic composite are obtained by replacing the phase elastic moduli by the phase complex moduli in the expressions for the effective elastic moduli with identical phase geometry. If the effective elastic moduli are of a form such that they are explicitly obtained from the constituent properties, the above correspondence principle is particularly simple to apply. The complex phase moduli are generally obtained as a function of frequency from dynamic tests. In what follows, it will be assumed that the complex phase moduli of fiber and matrix are known for the frequency range under consideration and also for various temperature and moisture content.

#### LAMINA COMPLEX MODULI FROM CONSTITUENT COMPLEX MODULI

To obtain the complex moduli of unidirectional composite lamina, the correspondence principle of vibration of viscoelastic composites as discussed above and in reference 1 will be utilized. If analytical expressions for effective elastic moduli are known, it is possible to obtain the effective complex moduli in a rather straightforward manner. In general, closed-form analytical expressions for effective elastic moduli are difficult to obtain. Several approximate expressions are available in literature and use of these relations is likely to yield approximate expressions for the complex moduli. The closed-form expressions of the upper bound results for the effective elastic moduli based on the composite cylinder assemblage model (refs. 7 and 8) will be used here. It is well known that for a transversely isotropic unidirectional composite, the composite cylinder assemblage model yields coincident upper and lower bounds for four of the five independent

moduli. Also, the upper bound results for the other modulus are found to be close to experimental results. Therefore, the results given here should yield good approximate results for the complex moduli. It should also be pointed out that the expressions for four of the five independent moduli are correct within the limitations of the composite cylinder assemblage model.

The results obtained by the use of the procedure described above are given below.

$$\begin{aligned}
 \tilde{E}_A^* &= v^f \tilde{E}_A^f + v^m \tilde{E}_A^m + \frac{4(\tilde{v}_A^f - \tilde{v}_A^m)^2 v^f v^m}{\frac{v^m}{\tilde{K}^f} + \frac{v^f}{\tilde{K}^m} + \frac{1}{\tilde{G}_T^m}} \\
 \tilde{v}_A^* &= v^f \tilde{v}_A^f + v^m \tilde{v}_A^m + \frac{v^f v^m (\tilde{v}_A^f - \tilde{v}_A^m) \left( \frac{1}{\tilde{K}^m} - \frac{1}{\tilde{K}^f} \right)}{\frac{v^m}{\tilde{K}^f} + \frac{v^f}{\tilde{K}^m} + \frac{1}{\tilde{G}_T^m}} \\
 \tilde{G}_A^* &= \tilde{G}_A^m \frac{v^m \tilde{G}_A^m + (1 + v^f) \tilde{G}_A^f}{(1 + v^f) \tilde{G}_A^m + v^m \tilde{G}_A^f} \\
 \tilde{K}^* &= \frac{v^m \tilde{K}^m (\tilde{K}^f + \tilde{G}_T^m) + v^f \tilde{K}^f (\tilde{K}^m + \tilde{G}_T^m)}{v^m (\tilde{K}^f + \tilde{G}_T^m) + v^f (\tilde{K}^m + \tilde{G}_T^m)} \\
 \tilde{G}_T^* &= \tilde{G}_T^m \frac{c_1}{c_2}
 \end{aligned}
 \tag{A16}$$

$$\tilde{E}_T^* = \frac{4\tilde{K}^* \tilde{G}_T^*}{\tilde{K}^* + (1 + \frac{4\tilde{K}^* \tilde{v}_A^* \tilde{v}_A^*}{\tilde{E}_A^*}) \tilde{G}_T^*}$$

$$\tilde{v}_T^* = \frac{\tilde{E}_T^*}{2\tilde{G}_T^*} - 1 \quad (A16)$$

where  $v^m$  and  $v^f$  are the volume fractions of matrix and fibers in the fiber bundle, respectively, and

$$C_1 = (\frac{\gamma + \beta^m}{\gamma - 1} + \beta^m v^f) (1 + (\frac{\beta^m - \gamma \beta^f}{1 + \gamma \beta^f}) (v^f)^3) - 3v^f (v^m)^2 (\beta^m)^2 ,$$

$$C_2 = (\frac{\gamma + \beta^m}{\gamma - 1} - v^f) (1 + \frac{\beta^m - \gamma \beta^f}{1 + \gamma \beta^f} (v^f)^3) - 3v^f (v^m)^2 (\beta^m)^2 ,$$

$$\gamma = \frac{\tilde{G}_T^f}{\tilde{G}_T^m} ,$$

$$\beta^m = \frac{1}{1 + \frac{2\tilde{G}_T^m}{\tilde{K}^m}} \quad \text{and} \quad \beta^f = \frac{1}{1 + \frac{2\tilde{G}_T^f}{\tilde{K}^f}} .$$

In the above equations,  $E$ ,  $\nu$ ,  $G$ , and  $K$  are the Young's modulus, Poisson's ratio, shear modulus, and plane strain bulk modulus, respectively. Superscripts "f" and "m" refer to the fiber and matrix material and subscripts "A" and "T" refer to the fiber bundle axial and transverse directions. Superscript "\*" denotes



the effective fiber bundle property. The fibers and matrix materials are considered to be transversely isotropic. Also, the symbol "~" over a quantity indicates that the quantity is complex. The complex moduli for a composite at a given frequency, temperature, and moisture content can be obtained by using the expressions given above.

#### LAMINATE COMPLEX STIFFNESSES

Approximate expressions for effective complex stiffnesses  $\tilde{A}_{ij}$ ,  $\tilde{B}_{ij}$  and  $\tilde{D}_{ij}$  for a laminated plate are obtained by the use of the displacement field in equation (B13) of Appendix B, the laminated plate theory of reference 24, and the correspondence principle outlined above. The expressions for these complex stiffnesses are given below:

$$\{\tilde{A}_{ij}(\omega), \tilde{B}_{ij}(\omega), \tilde{D}_{ij}(\omega)\} = \int_{-H/2}^{H/2} \tilde{Q}_{ij}(\omega)(1, z, z^2) dz, \quad (i, j = 1, 2, 6) \quad (A17)$$

$$\tilde{A}_{ij}(\omega) = \int_{-H/2}^{H/2} \tilde{C}_{ij}(\omega) dz, \quad (i, j = 4, 5)$$

$$\text{and } \tilde{K}_{ij}(\omega) = k_{ij} \tilde{A}_{ij}(\omega) \quad (i, j = 4, 5)$$

where

$$\tilde{Q}_{ij}(\omega) = \tilde{C}_{ij}(\omega) - \frac{\tilde{C}_{i3}(\omega)}{\tilde{C}_{33}(\omega)} \tilde{C}_{3\alpha}(\omega) \quad \begin{array}{l} \text{(plane stress reduced} \\ \text{stiffnesses; } i, j = 1, 2, 3, 6; \\ \alpha = 1, 2, 6) \end{array}$$

$$\tilde{C}_{ij}(\omega) = \text{frequency-dependent lamina complex stiffness matrix,}$$

and

$$k_{ij} = \text{shear correction factors for transverse shear which are functions of laminate construction and stacking sequence}$$

The method of calculation of effective properties for the laminate in shear  $\tilde{K}_{ij}$  ( $i, j = 4, 5$ ) is discussed in Appendix B.

APPENDIX B.  
DETERMINATION OF SHEAR CORRECTION FACTORS  
FOR COMPOSITE LAMINATES

One of the objectives of the present program is to develop laminate constitutive relations which consider the effect of laminate stacking sequence. In a conventional laminate analysis, the bending ( $D_{ij}, i, j=1, 2, 6$ ) and bending-extension coupling ( $B_{ij}, i, j=1, 2, 6$ ) stiffnesses are functions of stacking sequence while the extensional stiffnesses ( $A_{ij}, i, j=1, 2, 6, 4$  and  $5$ ) are not. Hence, the stiffnesses associated with the transverse shear deformation ( $A_{44}$ ,  $A_{45}$  and  $A_{55}$ ) are insensitive to the manner in which the laminae are stacked together. In addition, the shear correction factor,  $k$ , used with the  $A_{44}$ ,  $A_{45}$  and  $A_{55}$  stiffnesses is generally a constant ( $\pi^2/12$  or  $5/6$ ). An approach to consider the stacking sequence effect is to formulate a higher order plate theory. But this would be inappropriate and cumbersome for use in structural dynamics problems such as panel flutter. An alternate, and perhaps more convenient, approach is to determine the shear correction factors as a function of laminate construction and stacking sequence by using a refined or "exact elasticity" theory and to utilize these shear correction factors in conjunction with a simple shear deformation laminate plate theory of the type in references 12-14 and 23. The analytical/numerical procedure to obtain the correction factors (associated with the transverse shear stiffnesses  $A_{44}$ ,  $A_{45}$  and  $A_{55}$ ) is described subsequently. The basic approach is to obtain the cut-off (infinite wave length) frequencies for propagation of plane waves in the thickness-shear mode for a laminated plate, both from the shear-deformation theory and the "exact elasticity solution" and then equate them to obtain the unknown values of the shear correction factors  $k_{44}$  and  $k_{55}$ . In addition, a method has been formulated for evaluating the transverse shear coupling term  $k_{45}A_{45}$ .

# THICKNESS SHEAR MODE CUT-OFF FREQUENCIES FROM THE ELASTICITY SOLUTION

Consider a laminated plate consisting of  $m$  layers of total thickness  $H$ , as shown in figure 2. Assume, for example, the case of plane waves propagating in the  $x$ -direction. Then the displacements are of the form

$$u = u(x, z), \quad v = v(x, z), \quad w = w(x, z) \quad (B1)$$

The constitutive relations for each orthotropic layer (at a fiber orientation  $\theta$  with respect to the  $x$ -axis) in the laminate coordinate system  $xyz$  are

$$\begin{bmatrix} \sigma_{xx} \\ \sigma_{yy} \\ \sigma_{zz} \\ \tau_{xy} \end{bmatrix} = \begin{bmatrix} C_{11} & C_{12} & C_{13} & C_{16} \\ C_{12} & C_{22} & C_{23} & C_{26} \\ C_{13} & C_{23} & C_{33} & C_{36} \\ C_{16} & C_{26} & C_{36} & C_{66} \end{bmatrix} \begin{bmatrix} \epsilon_{xx} \\ \epsilon_{yy} \\ \epsilon_{zz} \\ \gamma_{xy} \end{bmatrix}$$

and

$$\begin{bmatrix} \tau_{yz} \\ \tau_{xz} \end{bmatrix} = \begin{bmatrix} C_{44} & C_{45} \\ C_{45} & C_{55} \end{bmatrix} \begin{bmatrix} \gamma_{yz} \\ \gamma_{xz} \end{bmatrix} \quad (B2)$$

where the strain components are the engineering strains. From the linear stress-strain relationships and the equations of motion from the theory of elasticity, the governing field equations for each layer are

$$C_{11}u_{,xx} + C_{55}u_{,zz} + C_{16}v_{,xx} + C_{45}v_{,zz} + (C_{13} + C_{55})w_{,xz} = \rho u_{,tt},$$

$$C_{16}u_{,xx} + C_{45}u_{,zz} + C_{66}v_{,xx} + C_{44}v_{,zz} + (C_{36} + C_{45})w_{,xz} = \rho v_{,tt}, \quad (B3)$$



$$(C_{13} + C_{55})u_{,xz} + (C_{36} + C_{45})v_{,xz} + C_{55}w_{,xx} + C_{33}w_{,zz} = \rho w_{,tt}, \quad (B3)$$

where a comma followed by a subscript indicates a differentiation and  $\rho$  is the mass density. The boundary conditions on the laminate surfaces ( $z = \pm H/2$ ) are:

$$\tau_{xz} = \tau_{yz} = 0 \quad (B4)$$

and

$$\sigma_{zz} = 0. \quad (B5)$$

The continuity of displacements and stresses at the interface requires that  $\sigma_{zz}$ ,  $\tau_{xz}$ ,  $\tau_{yz}$ ,  $u$ ,  $v$ , and  $w$  be continuous at the interfaces.

A solution for the displacements in each layer for the problem of plane wave propagation can be assumed to be

$$\begin{aligned} u &= U(z)e^{i\omega(t-fx)} \\ v &= V(z)e^{i\omega(t-fx)} \\ w &= W(z)e^{i\omega(t-fx)} \end{aligned} \quad (B6)$$

where  $f = \pi/\lambda\omega$  and  $\lambda$  is the wave length. For infinitely large wave lengths and for the thickness shear mode of wave propagation ( $w = 0$ ), equations (B3) reduce to

$$\begin{aligned} C_{55}U_{,zz} + C_{45}V_{,zz} + \rho\omega^2U &= 0 \\ C_{45}U_{,zz} + C_{44}V_{,zz} + \rho\omega^2V &= 0 \end{aligned} \quad (B7)$$

For the solution of equation (B7), only the boundary conditions in equation (B4) need to be satisfied, in addition to the continuity of  $\tau_{xz}$ ,  $\tau_{yz}$ ,  $u$ , and  $v$  at the layer interfaces. It should be noted that equation (B7) holds for any direction of wave propagation.

After solving for  $U(z)$  and  $V(z)$  in equations (B7), a relationship can be established between the interface tractions ( $\tau_{xz}$  and  $\tau_{yz}$ ) and displacements ( $U$  and  $V$ ) with reference to a local cartesian coordinate system  $xyz_{1,...m}$  (see fig.2).  $z_{1,...m}$  is defined such that the layer thickness  $h$  is bounded by the planes  $z_i = \pm h/2$ . The relationship between the surface tractions and the displacements is

$$\begin{bmatrix} \tau_{xz}^+ \\ \tau_{yz}^+ \\ \tau_{xz}^- \\ \tau_{yz}^- \end{bmatrix} = \frac{\omega}{2(1-d_1 d_2)} [\bar{K}] \begin{bmatrix} U^+ \\ V^+ \\ U^- \\ V^- \end{bmatrix} e^{i\omega t} \quad (B8)$$

where the + and - signs indicate the quantities at  $z_i = h/2$  and  $z_i = -h/2$ , respectively. The elements  $\bar{k}_{ij}$  of the matrix  $[\bar{K}]$  are listed below:

$$\begin{aligned} \bar{k}_{11} &= \bar{k}_{33} = C'_{55} (s_1 - t_1) + C'_{44} d_2^2 (s_2 - t_2) \\ \bar{k}_{12} &= \bar{k}_{21} = \bar{k}_{34} = \bar{k}_{43} = C'_{55} d_1 (t_1 - s_1) + C'_{44} d_2 (t_2 - s_2) \\ \bar{k}_{13} &= \bar{k}_{31} = -C'_{55} (t_1 + s_1) - C'_{44} d_2^2 (t_2 + s_2) \\ \bar{k}_{14} &= \bar{k}_{41} = \bar{k}_{23} = \bar{k}_{32} = C'_{55} d_1 (t_1 + s_1) + C'_{44} d_2 (t_2 + s_2) \\ \bar{k}_{22} &= \bar{k}_{44} = C'_{55} d_1^2 (s_1 - t_1) + C'_{44} (s_2 - t_2) \\ \bar{k}_{24} &= \bar{k}_{42} = -C'_{55} d_1^2 (t_1 + s_1) - C'_{44} (t_2 + s_2) \end{aligned} \quad (B9)$$

where  $C'_{55}, C'_{44}, d_1, d_2, t_1, t_2, s_1$  and  $s_2$  are obtained from

$$2(C_{44}C_{55} - C_{45}^2)\gamma_{1,2}^2 = \rho[(C_{55} + C_{44}) \pm \sqrt{(C_{55} - C_{44})^2 + 4C_{45}^2}] \quad (B10)$$

$$d_{1,2} = C_{45}\gamma_{1,2}^2 / (\rho - C_{55,44}\gamma_{1,2}^2)$$

$$C'_{55} = \gamma_1(C_{55} + d_2C_{45})$$

$$C'_{44} = \gamma_2(C_{44} + d_1C_{45}) \quad (B11)$$

$$\begin{aligned} t_i &= \tan(\gamma_i \omega h / 2) \\ s_i &= \cot(\gamma_i \omega h / 2) \end{aligned} \quad ; i = 1, 2 \quad (B12)$$

$\gamma_i^2$  are the characteristic roots for the differential equations (B7). The expressions in equations (B12) are valid if  $\gamma_i^2$  ( $i=1,2$ ) as evaluated from equation (B10) are positive. If one of them is negative, then  $\gamma_i$  in equation (B12) is calculated as the square root of the absolute value of  $\gamma_i^2$  and the trigonometric functions are replaced by their hyperbolic counterparts.

Once the stiffness matrix  $[\bar{K}]$  for each layer is obtained, the global stiffness matrix for the laminate made of a finite number of layers is constructed by considering the free surface and interface conditions. Since the laminate surfaces are stress free, the cut-off frequencies  $\omega$  are obtained by equating the determinant of the global stiffness matrix to zero. Because of the complicated manner in which  $\omega$  enters in each element of the matrix, a trial and error procedure is employed. The local and global stiffness matrices are to be obtained for each trial value of  $\omega$ . The size of this global stiffness matrix is  $(2m') \times (2m')$  where  $(m'-1)$  is the number of layers. The size of the global stiffness matrix can be reduced for the case of mid-plane symmetric laminates or for the case when all the laminae material axes coincide with the laminate x-y axes.



# THICKNESS SHEAR MODE CUT-OFF FREQUENCIES FROM LAMINATED PLATE SHEAR DEFORMATION THEORY

The shear deformation theory utilized here is the one developed in reference 12 for isotropic, homogeneous plates and for laminated plates in references 13 and 14. Referring again to figure 2, the displacement field is assumed to be of the form

$$u = u^0(x, y, t) + z\psi_x(x, y, t)$$

$$v = v^0(x, y, t) + z\psi_y(x, y, t)$$

$$w = w^0(x, y, t) \tag{B13}$$

where  $u^0$ ,  $v^0$ , and  $w^0$  are displacements at the reference surface (center) of the laminate. It is evident that the local layer rotations are assumed equal and "thickness stretch" is ignored.

The stress and moment resultants for the laminate, each per unit length, are defined in the usual way; that is,

$$\begin{aligned} (N_x, N_y, N_{xy}, Q_x, Q_y) &= \int_{-H/2}^{H/2} (\sigma_x, \sigma_y, \tau_{xy}, \tau_{xz}, \tau_{yz}) dz \\ (M_x, M_y, M_{xy}) &= \int_{-H/2}^{H/2} (\sigma_x, \sigma_y, \tau_{xy}) z dz \end{aligned} \tag{B14}$$

By substituting the stress-strain relationships of equation (B1) and the displacement field of equation (B13) in conjunction with the strain-displacement relations of linear elasticity, in equation (B14), the plate constitutive relations are obtained as:

$$\begin{bmatrix} N_x \\ N_y \\ N_{xy} \\ M_x \\ M_y \\ M_{xy} \end{bmatrix} = \begin{bmatrix} A & B \\ B & D \end{bmatrix} \begin{bmatrix} u,0 \\ u,x \\ v,0 \\ v,y \\ u,y + v,x \\ \psi_{x,x} \\ \psi_{y,y} \\ \psi_{x,y} + \psi_{y,x} \end{bmatrix} \quad (B15)$$

and

$$\begin{bmatrix} Q_y \\ Q_x \end{bmatrix} = \begin{bmatrix} k_{44}A_{44} & k_{45}A_{45} \\ k_{45}A_{45} & k_{55}A_{55} \end{bmatrix} \begin{bmatrix} w,y + \psi_y \\ w,x + \psi_x \end{bmatrix} \quad (B16)$$

$$\text{where } A_{ij}, B_{ij}, D_{ij} = \int_{-H/2}^{H/2} Q_{ij}(1, z, z^2) dz \quad (i, j = 1, 2, 6)$$

$$A_{ij} = \int_{-H/2}^{H/2} C_{ij} dz \quad (i, j = 4, 5),$$

$$Q_{i\alpha} = C_{i\alpha} - \frac{C_{i3}}{C_{33}} C_{3\alpha} \quad (i = 1, 2, 3, 6; \alpha = 1, 2, 6) \quad (B17)$$

and  $k_{44}, k_{55}, k_{45}$  = shear correction factors.

In the contracted notation  $\sigma_1 = \sigma_x, \sigma_2 = \sigma_y, \sigma_3 = \sigma_z, \sigma_4 = \tau_{yz}, \sigma_5 = \tau_{xz},$  and  $\sigma_6 = \tau_{xy}$ . In general, the shear correction factors are assumed to be equal; that is,  $k_{44} = k_{55} = k_{45} = k$ .

Referring to equations (B13), it is evident that the transverse shear strain is constant across the laminate thickness, thus making the interlaminar shear stresses discontinuous at the interfaces. This is a violation of the continuity of stress. In reference 23, the shear stress is assumed continuous and constant

across the thickness and the shear strain is allowed to be discontinuous. This is achieved in the following manner. From equation (B2), the shear strains  $\gamma_{yz}$  and  $\gamma_{xz}$  in a layer are related by the relationship (in contracted notation)

$$\gamma_i^{(m)} = S_{ij}^{(m)} \sigma_j, \quad i, j = 4, 5 \quad (B18)$$

where  $S_{ij}^{(m)}$  are the compliances of layer  $m$ .  $\sigma_4$  and  $\sigma_5$  are continuous across the thickness of the plate, while the strains  $\gamma_4, \gamma_5$  are discontinuous. Integration of equation (B18) yields

$$\Gamma_i = L_{ij} Q_j \quad (i, j = 4, 5) \quad (B19)$$

where

$$\Gamma_i = \frac{1}{H} \int_{-H/2}^{H/2} \gamma_i^{(m)} dz,$$

$$L_{ij} = \frac{1}{H^2} \int_{-H/2}^{H/2} S_{ij}^{(m)} dz$$

and

$$Q_j = H \sigma_j.$$

$\Gamma_i$  can be interpreted as average laminate transverse shear strains. Equation (B19), on inversion, results in

$$Q_j = A'_{ij} \Gamma_i \quad (B20)$$

where  $A'_{ij} = L_{ij}^{-1}$ .



It is now assumed that the displacement field in equation (B13) represents the average plate displacements. Thus

$$\begin{bmatrix} Q_4 \\ Q_5 \end{bmatrix} = \begin{bmatrix} Q_y \\ Q_x \end{bmatrix} = \begin{bmatrix} k'_{44}A'_{44} & k'_{45}A'_{45} \\ k'_{45}A'_{45} & k'_{55}A'_{55} \end{bmatrix} \begin{bmatrix} w',_y + \psi_y \\ w',_x + \psi_x \end{bmatrix} \quad (B21)$$

where  $k'_{44}$ ,  $k'_{55}$ , and  $k'_{45}$  are the modified shear correction factors and are distinct from  $k_{44}$ ,  $k_{55}$ , and  $k_{45}$  in equation (B16). In general, one may define the following relationship

$$\begin{bmatrix} Q_y \\ Q_x \end{bmatrix} = \begin{bmatrix} K_{44} & K_{45} \\ K_{45} & K_{55} \end{bmatrix} \begin{bmatrix} w',_y + \psi_y \\ w',_x + \psi_x \end{bmatrix} \quad (B22)$$

where

$$K_{44} = k_{44}A_{44} = k'_{44}A'_{44}$$

$$K_{45} = k_{45}A_{45} = k'_{45}A'_{45}$$

and

$$K_{55} = k_{55}A_{55} = k'_{55}A'_{55} \quad (B23)$$

The equations of motion in terms of stress and moment resultants can now be written as:

$$N_{x,x} + N_{xy,y} = Pu^0_{,tt} + R\psi_{x,tt}$$

$$N_{xy,x} + N_{y,y} = Pv^0_{,tt} + R\psi_{y,tt}$$

$$Q_{x,x} + Q_{y,y} = Pw_{,tt} \quad (B24)$$

$$M_{x,x} + M_{xy,y} - Q_x = Ru^0_{,tt} + I\psi_{x,tt}$$

and

$$M_{xy,x} + M_{y,y} - Q_y = Rv_{,tt}^0 + I\psi_{y,tt}$$

$$\text{where } (P, R, I) = \int_{-H/2}^{H/2} \rho(1, z, z^2) dz \quad (B25)$$

For the particular case of plane wave propagation in the x direction, the above equations of motions are rewritten in terms of displacement variables (from ref.14 )

$$A_{11}u_{,xx}^0 + A_{16}v_{,xx}^0 + B_{11}\psi_{x,xx} + B_{16}\psi_{y,xx} = Pu_{,tt}^0 + R\psi_{x,tt}$$

$$A_{16}u_{,xx}^0 + A_{66}v_{,xx}^0 + B_{16}\psi_{x,xx} + B_{66}\psi_{y,xx} = Pv_{,tt}^0 + R\psi_{y,tt}$$

$$K_{55}(\psi_{x,x} + w_{,xx}) + K_{45}\psi_{y,x} = Pw_{,tt}$$

$$B_{11}u_{,xx}^0 + B_{16}v_{,xx}^0 + D_{11}\psi_{x,xx} + D_{16}\psi_{y,xx} - K_{55}(\psi_x + w_{,x})$$

$$-K_{45}\psi_y = Ru_{,tt}^0 + I\psi_{x,tt}$$

and

$$B_{16}u_{,xx}^0 + B_{66}v_{,xx}^0 + D_{16}\psi_{x,xx} + D_{66}\psi_{y,xx}$$

$$-K_{45}(\psi_x + w_{,x}) - K_{44}\psi_y = Rv_{,tt}^0 + I\psi_{y,tt} \quad (B26)$$

Solutions to these equations can be written in the following form:

$$u^0 = Ue^{i\omega(t-fx)}$$

$$v^0 = Ve^{i\omega(t-fx)}$$

$$\psi_x = \Psi_x e^{i\omega(t-fx)}$$

$$\psi_y = \Psi_y e^{i\omega(t-fx)} \quad (B27)$$

and

$$w = W e^{i\omega(t-fx)} \quad (B27)$$

where  $f = \pi/\lambda\omega$ ;  $\omega$  is the frequency and  $\lambda$  the wavelength.

For the thickness-shear mode of wave propagation ( $\lambda$  infinitely large and  $w = 0$ ), equations (B26) further reduce to

$$\begin{aligned} (I'\omega^2 - K_{55})\psi_x - K_{45}\psi_y &= 0 \\ -K_{45}\psi_x + (I'\omega^2 - K_{44})\psi_y &= 0 \end{aligned} \quad (B28)$$

where  $I' = I - R^2/P$ .

Solution of equations (B28) yields the cut-off frequencies  $\omega_{1,2}^2$

$$2I'\omega_{1,2}^2 = (K_{44} + K_{55}) \pm [(K_{55} - K_{44})^2 + 4K_{45}^2]^{1/2} \quad (B29)$$

Note again that  $\omega_{1,2}^2$  are independent of the direction of wave propagation because of the assumption that  $\lambda$  approaches infinity. Also, unless otherwise stated, it will be assumed that in mode 1,  $\psi_x$  is the predominant displacement while in mode 2,  $\psi_y$  assumes that role.

If the cut-off frequencies  $\omega_{1,2}$  are known from the "exact elasticity" solution as described earlier, then the quantities  $K_{44}$  and  $K_{55}$  are obtained from equation (B30); that is,

$$2K_{55,44} = I'(\omega_1^2 + \omega_2^2) \pm [I'^2(\omega_1^2 - \omega_2^2)^2 - 4K_{45}^2]^{1/2} \quad (B30)$$

provided that  $K_{45}$  is known. An approximate procedure for estimating  $K_{45}$  is described subsequently. Having obtained the values of  $K_{44}$ ,  $K_{55}$  and  $K_{45}$  for a particular laminate in this fashion, the shear-deformation theory can be used for calculating the response of a laminated plate under various loading conditions.



# DETERMINATION OF THE TRANSVERSE SHEAR COUPLING STIFFNESS

It is observed in equation (B30) that the shear correction factors  $k_{44}$  and  $k_{55}$  can be obtained when the thickness shear cut-off frequencies  $\omega_{1,2}^2$  (from the exact elasticity solution) and the coupling term  $K_{45}$  ( $=k_{45}A_{45}$  or  $k'_{45}A'_{45}$ ) are known. By using the approach in reference 16, the term  $K_{45}$  can be obtained to be

$$K_{45} = (k_{44}k_{55})^{1/2}A_{45}. \quad (B31)$$

Since the stiffness  $A_{45}$  is known, both  $K_{44}$  and  $K_{55}$  can now be determined from equation (B30). Based on the displacement field in equation (B13),  $A_{45}$  is zero for orthotropic, symmetric and  $[\pm\theta]$  laminates ( $\pm\theta$  laminates having equal percentages of  $+\theta$  and  $-\theta$  layers). Thus, the coupling stiffness  $K_{45}$  also vanishes for these laminates. In reality, however, the transverse shear force  $Q_x$  will induce both  $\gamma_{xz}(z)$  and  $\gamma_{yz}(z)$  shear strains, although the magnitude of the latter will be smaller than that of the former. The actual coupling is expected to reduce for laminates which are more homogeneous ( $K_{45} = 0$  for homogeneous, orthotropic laminates). In the present investigation, the magnitude of this coupling is ascertained from the procedure outlined below.

The two lowest values of the cut-off frequencies  $\omega_{1,2}^2$  are obtained initially from the exact elasticity solution. From the eigenfunctions corresponding to each of these two frequencies, the following integrals are evaluated for each layer:

$$\int_{-h/2}^{h/2} \tau_{xz} dz = [C_{55}(U^+ - U^-) + C_{45}(V^+ - V^-)] e^{i\omega t}$$

and

$$\int_{-h/2}^{h/2} \tau_{yz} dz = [C_{45}(U^+ - U^-) + C_{44}(V^+ - V^-)] e^{i\omega t} \quad (B32)$$

These integrals are summed for all the  $m$  layers of the laminate giving the shear forces  $Q_{x_{1,2}} e^{i\omega t}$  and  $Q_{y_{1,2}} e^{i\omega t}$  for the two modes. The average shear strains  $\psi_{x_{1,2}}$  and  $\psi_{y_{1,2}}$  are then estimated by utilizing equation (B28). They are:

$$\begin{aligned}\psi_{x_i} &= Q_{x_i} / I' \omega_i^2 \\ \psi_{y_i} &= Q_{y_i} / I' \omega_i^2\end{aligned}\quad i = 1, 2 \quad (B33)$$

Having obtained  $\psi_{x_i}$  and  $\psi_{y_i}$ , equations (B22) are rewritten as

$$\begin{aligned}K_{55}^* \psi_{x_i} + K_{54}^* \psi_{y_i} &= Q_{x_i} \\ K_{45}^* \psi_{x_i} + K_{44}^* \psi_{y_i} &= Q_{y_i}\end{aligned}\quad i = 1, 2 \quad (B34)$$

The unknowns are  $K_{55}^*$ ,  $K_{44}^*$ ,  $K_{45}^*$ , and  $K_{54}^*$ .

The coupling term to be used in equation (B30) is taken to be

$$K_{45} = (K_{45}^* K_{54}^*)^{1/2}. \quad (B35)$$

Thus, the shear correction factors can be obtained either from equations (B35) and (B30) or directly from equations (B34). The differences between the shear correction factors determined from both the approaches are insignificant. Hence, the procedure for the determination of  $K_{45}$  in equation (B35) appears to be reasonable.

It should be noted that in a few cases when  $K_{44}^*$  and  $K_{55}^*$  are almost the same, substitution of  $K_{45}$  from equation (B35) in (B30) yields a very small negative number under the square

root sign in the right-hand side of equation (B30). This discrepancy has been neglected in the results reported herein. Also, for laminates with  $A_{45}' = 0$ , use of equation (B23) yields  $K_{45} = 0$ . Use of a zero value for  $K_{45}$  in equation (B30) yields  $K_{44}$  and  $K_{55}$ , which are significantly different from  $K_{44}^*$  and  $K_{55}^*$  as obtained from equations (B34). This is due to the limitation of the plate theory (which yields  $K_{45} = 0$ ) and can be avoided by techniques described in this section.



APPENDIX C.  
PANEL FLUTTER ANALYSIS OF VISCOELASTIC LAMINATED PLATES  
IN CYLINDRICAL BENDING

An important objective of this study is to investigate the effects of environment, damping (dynamic viscoelastic properties) and coupling properties, and shear deformation in composite laminates on panel flutter. The panel flutter problem is a complex one and is influenced by various factors such as type of aerodynamic theory used, aspect ratio of the panel and boundary conditions, flow angle, prestress, etc. For panels made of composite laminates, the variables in the analysis are increased significantly. Therefore, the emphasis here is on the material parameters rather than on the aerodynamic or geometric aspects of the problem. Hence, it is logical to consider a simple geometry and an aerodynamic theory which is amenable to a straightforward solution procedure. To that end, the problem of panel flutter in cylindrical bending is investigated here. The aerodynamic loading and damping is determined from linear piston theory. A shear deformation laminated plate theory which considers unique shear correction factors for a given laminate construction and stacking sequence (see Appendix B) is employed and material damping is included by considering complex lamina stiffnesses (see Appendix A). The effects of these material parameters on the panel flutter characteristics (critical aerodynamic pressure or speed) can then be evaluated.

GOVERNING EQUATIONS AND METHOD OF ANALYSIS

The panel flutter problem is illustrated in figure 21, which shows supersonic flow over a flat plate at an angle  $\Lambda$  with the x-axis. The linear, small-deflection shear-deformation laminate theory in conjunction with frequency dependent complex laminate properties is used to characterize the panel response. Since the panel is constrained to deform in cylindrical bending, the analysis variables are independent of the y coordinate. Following reference 14 and the displacement field in equation (B13), the

governing equations for panel flutter can be written as:

$$\begin{aligned}
 \tilde{A}_{11} u_{,xx}^0 + \tilde{A}_{16} v_{,xx}^0 + \tilde{B}_{11} \psi_{x,xx} + \tilde{B}_{16} \psi_{y,xx} &= P u_{,tt}^0 + R \psi_{x,tt} \\
 \tilde{A}_{16} u_{,xx}^0 + \tilde{A}_{66} v_{,xx}^0 + \tilde{B}_{16} \psi_{x,xx} + \tilde{B}_{66} \psi_{y,xx} &= P v_{,tt}^0 + R \psi_{y,tt} \\
 \tilde{K}_{55} (\psi_{x,x} + w_{,xx}) + \tilde{K}_{45} \psi_{y,x} &= \frac{2q}{\bar{\beta}} \cos \Lambda w_{,x} \\
 &+ \rho_a c w_{,t} + N_{xx}^0 w_{,xx} + P w_{,tt} \\
 \tilde{B}_{11} u_{,xx}^0 + \tilde{B}_{16} v_{,xx}^0 + \tilde{D}_{11} \psi_{x,xx} + \tilde{D}_{16} \psi_{y,xx} - \tilde{K}_{55} (\psi_x + w_{,x}) \\
 - \tilde{K}_{45} \psi_y &= R u_{,tt}^0 + I \psi_{x,tt} \\
 \tilde{B}_{16} u_{,xx}^0 + \tilde{B}_{66} v_{,xx}^0 + \tilde{D}_{16} \psi_{x,xx} + \tilde{D}_{66} \psi_{y,xx} - \tilde{K}_{45} (\psi_x + w_{,x}) \\
 - \tilde{K}_{44} \psi_y &= R v_{,tt}^0 + I \psi_{y,tt}
 \end{aligned} \tag{C1}$$

where

$\rho_a$  = free stream air density,

$c$  = free stream speed of sound,

$q$  = dynamic pressure of the airstream,

$\bar{\beta}$  = compressibility factor =  $\sqrt{M^2 - 1}$

$M$  = Mach number

$N_{xx}^0$  = panel prestress

$P, R, I$  = inertial terms defined in equation (B25)

and

$\tilde{A}_{ij}, \tilde{B}_{ij}, \tilde{D}_{ij}$  ( $i, j = 1, 2, 6$ ) and  $\tilde{K}_{ij}$  ( $i, j = 4, 5$ ) are the complex, frequency-dependent laminate stiffnesses derived in Appendices A and B.

The aerodynamic loading is obtained from the linear piston theory (ref. 39). The piston theory gives a simple expression

for the aerodynamic loading and has been shown to be applicable for Mach numbers greater than 1.6 (ref. 38). The expression  $\frac{2q}{\beta} \cos \Lambda w, x$  is the aerodynamic pressure term, while the term  $\rho_a c w, t$  represents aerodynamic damping. It is also assumed that the prestress is unaffected by the displacements in the plate.

The boundary conditions at  $x = 0, a$  (fig. 21) for a simple panel are

$$\begin{aligned}
 w &= 0, \\
 N_{xx} &= \tilde{A}_{11} u, x^0 + \tilde{A}_{16} v, x^0 + \tilde{B}_{11} \psi_{x,x} + \tilde{B}_{16} \psi_{y,x} = 0, \\
 N_{xy} &= \tilde{A}_{16} u, x^0 + \tilde{A}_{66} v, x^0 + \tilde{B}_{16} \psi_{x,x} + \tilde{B}_{66} \psi_{y,x} = 0, \\
 M_{xx} &= \tilde{B}_{11} u, x^0 + \tilde{B}_{16} v, x^0 + \tilde{D}_{11} \psi_{x,x} + \tilde{D}_{16} \psi_{y,x} = 0, \\
 \text{and} \\
 M_{xy} &= \tilde{B}_{16} v, x^0 + \tilde{B}_{66} v, x^0 + \tilde{D}_{16} \psi_{x,x} + \tilde{D}_{66} \psi_{y,x} = 0.
 \end{aligned} \tag{C2}$$

In what follows, the following nondimensional quantities will be utilized:

$$X, U_0, V_0, W = (x, u_0, v_0, w)/a$$

$$A_{ij}, B_{ij}, D_{ij}, K_{ij} = (a^2 \tilde{A}_{ij}, a \tilde{B}_{ij}, \tilde{D}_{ij}, a^2 \tilde{K}_{ij})/D_0$$

$$\bar{P}, \bar{R}, \bar{I} = (a^4 P, a^3 R, a^2 I)/D_0$$

$$\bar{\lambda} = \frac{2a^3 q \cos \Lambda}{\beta D_0}, \quad S = \frac{a^4 \rho_a c}{D_0} \quad \text{and} \quad \bar{N}_{xx} = \frac{a^2 N_{xx}^0}{D_0} \tag{C3}$$

and

$D_0$  = a real constant with the same unit as  $\tilde{D}_{11}$ . For convenience, a number close to the real part of the bending stiffness  $\tilde{D}_{11}$  corresponding to the first frequency in the chosen frequency range may be selected.



The governing differential equations in terms of displacements  $U_0$ ,  $V_0$ ,  $W$  and rotations  $\psi_x, \psi_y$  are the same as equation (C1) with all the quantities replaced by their nondimensional counterparts in equations (C3).

The Galerkin method will be used to solve the differential equations (C1). In this particular application of the method, a series solution for the dependent variables is chosen which satisfies all the boundary conditions and the coefficients of the series are determined so that each term of the series is orthogonal to the exact solution. The series functions assumed for this analysis are

$$w = -e^{i\omega t} \sum_{n=1}^{\infty} \frac{a_n}{\alpha_n} \sin \alpha_n x$$

$$\psi_x + W_{,x} = e^{i\omega t} \sum_{n=1}^{\infty} b_n \cos \alpha_n x$$

$$u^0 = e^{i\omega t} \sum_{n=1}^{\infty} c_n \cos \alpha_n x$$

$$\psi_y = e^{i\omega t} \sum_{n=1}^{\infty} d_n \cos \alpha_n x$$

and

$$v^0 = e^{i\omega t} \sum_{n=1}^{\infty} e_n \cos \alpha_n x \quad (C4)$$

where  $\alpha_n = n\pi$ . The boundary conditions are identically satisfied by the functions in equations (C4). Use of the Galerkin procedure in conjunction with equations (C1), (C2), and (C4) yields

$$\{ [K_n] - \frac{\omega^2}{\alpha_n^2} [M_n] \} \{ A_n \} + 4\bar{\lambda} \{ L_n \} = 0 ; n = 1, 2, \dots \infty \quad (C5)$$

where

$$[K_n] = \begin{bmatrix} (D_{11} - \bar{N}_{xx}/\alpha_n^2 + iS\omega/\alpha_n^4) & D_{11} & B_{11} & D_{16} & B_{16} \\ D_{11} & (D_{11} + K_{55}/\alpha_n^2) & B_{11} & (D_{16} + K_{45}/\alpha_n^2) & B_{16} \\ B_{11} & B_{11} & A_{11} & B_{16} & A_{16} \\ D_{16} & (D_{16} + K_{45}/\alpha_n^2) & B_{16} & (D_{66} + K_{44}/\alpha_n^2) & B_{66} \\ B_{16} & B_{16} & A_{16} & B_{66} & A_{66} \end{bmatrix} \quad (C6)$$

$$[M_n] = \begin{bmatrix} \bar{P}/\alpha_n^2 + \bar{I} & \bar{I} & \bar{R} & 0 & 0 \\ \bar{I} & \bar{I} & \bar{R} & 0 & 0 \\ \bar{R} & \bar{R} & \bar{P} & 0 & 0 \\ 0 & 0 & 0 & \bar{I} & \bar{R} \\ 0 & 0 & 0 & \bar{R} & \bar{P} \end{bmatrix} \quad (C7)$$

$$[A_n] = \begin{bmatrix} a_n \\ b_n \\ c_n \\ d_n \\ e_n \end{bmatrix}, \quad \text{and} \quad L_n^0 = \begin{bmatrix} \sum_{m=1, n-m=\text{odd}}^{\infty} \frac{e_m}{(\alpha_n^2 - \alpha_m^2)\alpha_n^2} \\ 0 \\ 0 \\ 0 \\ 0 \end{bmatrix} \quad (C8)$$

If one truncates each of the series in equation (C4) at  $n \leq N$ , equation (C5) yields a set of  $5N$  homogeneous equations. For a nontrivial solution, the determinant of the coefficients  $a_n, b_n, c_n, d_n, e_n$  ( $n = 1, 2, \dots, N$ ) must equal zero. Standard eigenvalue routines cannot be used to calculate the eigenvalues  $\omega_n^2$  (for given  $\bar{\lambda}$ , the flutter parameter) since the elements of the matrix  $[K_n]$  are frequency dependent. Hence, a trial and error procedure must be employed.

In general, the frequencies  $\omega_n$  are complex; that is,

$$\omega = \omega_R + i \omega_I \quad (C9)$$

The panel behavior is characterized by the variation of  $(\omega_R + i \omega_I)$  with  $\bar{\lambda}$ . Since the time dependence is defined by the term  $e^{i\omega t}$ , it is clear that if the imaginary part,  $\omega_I$ , is negative, a divergent motion ensues. If, on the other hand,  $\omega_I$  is positive, the result is a damped harmonic motion. Thus, flutter is considered to occur for the lowest value of  $\bar{\lambda}$  at which the imaginary part of the frequency changes sign, or in other words, vanishes. This condition corresponds to sustained simple harmonic motion and represents incipient flutter.

For  $\bar{\lambda} = 0$ , the imaginary parts of all the frequencies are positive (damped motion). As  $\bar{\lambda}$  is increased to the point of flutter, the imaginary part of the one of the frequencies will be equal to zero. For a further increase in  $\bar{\lambda}$ , the imaginary part will become negative. However, in some cases, a phenomenon termed here as "weak coalescence" (of two modes) may occur. In such a case, the imaginary part of the frequency tends to become zero again with increase in  $\bar{\lambda}$  and careful consideration should be given to select the correct flutter parameter from the point of view of practical applications.

It has been pointed out earlier that for numerical calculations, it is necessary to truncate the system of equations (C5)



at  $n = N$  and investigate the possibility of coalescence of any two of the  $5N$  modes. Usually, the real parts of frequencies corresponding to the modes dominated by the in-plane displacements  $u^0(c_n, n = 1, 2, \dots, N)$  and  $v^0(e_n, n = 1, 2, \dots, N)$  as well as the average rotations due to shear  $\psi_x + w_{,x}(b_n, n = 1, 2, \dots, N)$  and  $\psi_y(d_n, n = 1, 2, \dots, N)$  are high. Therefore, the possibility of flutter as a result of coalescence of a majority of the modes dominated by  $c_n, e_n, b_n$ , and  $d_n$  ( $n = 1, 2, \dots, N$ ) with each other or with those in which the terms  $a_n$  (corresponding to the displacement  $w$ ) are dominant can be ruled out and, except for the first few of the constants  $b_n, c_n, d_n$ , and  $e_n$  ( $n = 1, 2, \dots, N$ ), all others may be assumed to be zero without any loss in accuracy. A simple procedure for elimination of some of these constants is to estimate the real parts of the frequencies (for  $\bar{\lambda} = 0$ ) dominated by these modes and compare them with the highest flexural frequency. Based on this comparison, the relative importance of these terms can be easily determined. The rows and columns corresponding to the terms which are not important may then be omitted from the system of equations in (C5).

#### Panel Flutter of [0/90] Laminate

For a laminate made of orthotropic layers with their material axes parallel to the  $x$  and  $y$  directions, the solutions associated with  $v^0$  and  $\psi_y$  are uncoupled. Hence, the constants  $d_n$  and  $e_n$  ( $n = 1, 2, \dots, N$ ) can be removed from equation (C5). Also,  $b_n$  and  $c_n$  ( $n = 1, 2, \dots, N$ ) can be eliminated from equation (C5) provided that

$$\Delta_n = (\tilde{A}_{11}\alpha_n^2 - \bar{P}\omega^2)(\tilde{D}_{11}\alpha_n^2 + \tilde{K}_{55} - \bar{I}\omega^2) - (\tilde{B}_{11}\alpha_n^2 - \bar{R}\omega^2)^2 \neq 0,$$

$$n = 1, 2, \dots, N \quad (C10)$$

This process of elimination yields

$$\begin{aligned}
 & [\alpha_n^2 \{ \tilde{K}_{55} - \frac{\tilde{K}_{55}(\tilde{A}_{11}\alpha_n^2 - \bar{P}\omega^2)}{\Delta_n} - \bar{N}_{xx} \} + iS\omega - \bar{P}\omega^2] a_n \\
 & + 4\bar{\lambda} \sum_{\substack{m=1 \\ n-m=\text{odd}}}^N \frac{a_m \alpha_n^2}{\alpha_n^2 - \alpha_m^2} = 0, \quad n = 1, 2, \dots, N \quad (C11)
 \end{aligned}$$

Equation (C11) is a system of  $N$  homogeneous equations and for a nontrivial solution, the determinant of the coefficients  $a_n$  must vanish. The critical flutter parameter,  $\bar{\lambda}_{cr}$ , may be determined as the lowest value of  $\bar{\lambda}$  for which the real and imaginary parts of the determinant are zero. The determinant is evaluated for a range of values of real  $\omega$  and  $\bar{\lambda}$  to determine these quantities at which both the real and imaginary parts of the determinant vanish.

APPENDIX D.  
SOLUTION OF THE MOISTURE DIFFUSION PROBLEM

The governing differential equation of the one-dimensional moisture diffusion equation is

$$\frac{\partial C}{\partial t} = \frac{\partial}{\partial x} \left( \mu \frac{\partial C}{\partial x} \right) \quad (D1)$$

where  $C$  is the moisture concentration. If the derivatives with respect to space coordinate  $x$  are replaced by finite differences, the partial differential equation (D1) can be converted to a set of ordinary differential equations

$$\frac{\partial C_i}{\partial t} = \delta_{i-1} C_{i-1} + \delta_i C_i + \delta_{i+1} C_{i+1}, \quad i = 2, 3, \dots, n \quad (D2)$$

where

$$\begin{aligned} \delta_{i-1} &= (4\mu_i - \mu_{i+1} + \mu_{i-1})/4d^2 \\ \delta_i &= -2\mu_i/d^2 \\ \delta_{i+1} &= (4\mu_i + \mu_{i+1} - \mu_{i-1})/4d^2 \\ \mu_i &= \text{diffusivity at node } i \end{aligned} \quad (D3)$$

$d$  = mesh size =  $H/n$  when all meshes are of equal size,  $H$  is the laminate thickness and  $n+1$  = total number of nodes including the boundary points.

With prescribed boundary conditions  $C_1$  and  $C_{n+1}$  as well as initial distribution of  $C$  known, the set of equations (D2) can be easily solved by a predictor corrector scheme. With the use of this scheme, the diffusivities  $\mu_i$  may be considered to be dependent on  $C_i$ .



To consider jump discontinuities in diffusivities, the equation (D2) at the node  $k$  which coincides with the interface between layers  $m$  and  $m+1$ , is modified by the use of the following values of  $\delta_{i-1}$ ,  $\delta_i$  and  $\delta_{i+1}$ .

$$\begin{aligned}\delta_{i-1} &= (\mu_k^m + \mu_{k-1}^m) / [d_m (d_m + d_{m+1})] \\ \delta_i &= -[(\mu_k^m + \mu_{k-1}^m) / d_m + (\mu_k^{m+1} + \mu_{k+1}^{m+1}) / d_{m+1}] / (d_m + d_{m+1}) \quad (D4) \\ \delta_{i+1} &= (\mu_k^{m+1} + \mu_{k+1}^{m+1}) / [d_{m+1} (d_m + d_{m+1})]\end{aligned}$$

where  $d_m$  and  $d_{m+1}$  are the mesh sizes in layers  $m$  and  $m+1$ , respectively. These values are obtained on the assumption that the moisture concentration at node  $k$  is the same in layers  $m$  and  $m+1$ . The following relations have been made use of to obtain equation (D4):

$$\begin{aligned}d_m \frac{\partial C_k}{\partial t} &= (\mu_k^m - \mu_{k-1}^m) (C_k - C_{k-1}) / d_m + \mu_k^m (C_k - 2C_{k-1} \\ &\quad + C_{k-2}) / d_m \quad (D5)\end{aligned}$$

$$\begin{aligned}d_{m+1} \frac{\partial C_k}{\partial t} &= (-\mu_k^{m+1} + \mu_{k+1}^{m+1}) (C_{k+1} - C_k) / d_{m+1} + \mu_k^{m+1} \\ &\quad (C_k - 2C_{k+1} + C_{k+2}) / d_{m+1} \quad (D6)\end{aligned}$$

$$\begin{aligned}\mu_k^m (3C_k - 4C_{k-1} + C_{k-2}) / 2d_m &= \mu_k^{m+1} (-3C_k + 4C_{k+1} \\ &\quad - C_{k+2}) / 2d_{m+1} \quad (D7)\end{aligned}$$

Equations (D5) and (D6) are obtained from (D1) by the use of backward and forward difference formulae at node k in layers m and m+1, respectively. A mass conservation condition (moisture transfer) across the interface, i.e.  $\mu_k^m \frac{\partial C_k^m}{\partial x} = \mu_k^{m+1} \frac{\partial C_k^{m+1}}{\partial x}$

in the form of a higher order difference formula yields the relation (D7). The addition of equations (D5) and (D6) and the use of (D7) result in (D4).

In the present form, the computer program solves the system of equations (D2) - (D4) for prescribed initial and boundary conditions as well as a given temperature distribution. Diffusivities at various temperatures and moisture concentrations are input in a tabular form and linear interpolation is used to calculate diffusivity for any temperature and moisture concentration.

#### REFERENCES

1. Z. Hashin, Theory of Fiber Reinforced Materials, NASA CR-1974, 1972.
2. C. W. Bert and S. Chang, In-Plane, Flexural, Twisting and Thickness-Shear Coefficients for Stiffness and Damping of a Monolayer Filamentary Composite, Final Report (Part I), NASA Grant NGR-37-003-055, School of Aerospace, Mechanical and Nuclear Engineering, Univ. of Oklahoma, Norman, Oklahoma, 1972.
3. C. W. Bert and C. C. Siu, Vibration and Damping of Laminated, Composite-Material Plates Including Thickness Shear Effects, Final Report (Part II), NASA Grant NGR-37-003-055, School of Aerospace, Mechanical and Nuclear Engineering, Univ. of Oklahoma, Norman, Oklahoma, 1972.
4. A. B. Schultz and S. W. Tsai, "Dynamic Moduli and Damping Ratios in Fiber-Reinforced Composites," J. Composite Materials, Vol. 2, p. 368, 1968.
5. R. R. Clary, "Vibration Characteristics of Unidirectional Filamentary Composite Material Panels," ASTM STP 497, p. 415, 1972.
6. A. B. Schultz and S. W. Tsai, "Measurements of Complex Dynamic Moduli of Laminated Fiber Reinforced Composites," J. Composite Materials, Vol. 3, p. 434, 1969.
7. Z. Hashin and B. W. Rosen, "The Elastic Moduli of Fiber Reinforced Materials," J. Applied Mechanics, Vol. 31, p. 233, 1964; errata, Vol. 32, p. 219, 1965.
8. B. W. Rosen, "Thermomechanical Properties of Fibrous Composites" Proc. Royal Society London (A), Vol. 319, p. 79, 1970.
9. E. Reissner and Y. Stavsky, "Bending and Stretching of Certain Types of Heterogeneous Anisotropic Elastic Plates," J. Applied Mechanics, Vol. 28, p. 402, 1961.
10. J. M. Whitney and A. W. Leissa, "Analysis of Heterogeneous Anisotropic Plates," J. Applied Mechanics, Vol. 36, p. 261, 1969.
11. E. Reissner, "The Effect of Transverse Shear Deformation on the Bending of Elastic Plates," J. Applied Mechanics, Vol. 12, p. 69, 1945.
12. R. D. Mindlin, "Influence of Rotatory Inertia and Shear on Flexural Motions of Isotropic, Elastic Plates," J. Applied Mechanics, Vol. 18, p. 69, 1951.
13. P. C. Yang, C. H. Norris, Y. Stavsky, "Elastic Wave Propagation in Heterogeneous Plates," International J. Solids and Structures, Vol. 2, p. 665, 1966.



#### REFERENCES (Contd.)

14. J. M. Whitney and N. J. Pagano, "Shear Deformation in Heterogeneous Anisotropic Plates," J. Applied Mechanics, Vol. 37, p. 1031, 1970.
15. S. B. Dong, Studies Relating to the Structural Dynamic Behavior of Laminated Plates and Shells, UCLA-ENG-7236, 1972.
16. J. M. Whitney, "Stress Analysis of Thick Laminated Composite and Sandwich Plates," J. Composite Materials, Vol. 6, p. 426, 1972.
17. G. P. Cowper, "The Shear Coefficient in Timoshenko's Beam Theory," J. Applied Mechanics, Vol. 33, p. 335, 1966.
18. N. J. Pagano, "Exact Solutions for Composite Laminates in Cylindrical Bending," J. Composite Materials, Vol. 3, p. 398, 1969.
19. S. Srinivas, et al., "An Exact Analysis for Vibration of Simply Supported Homogeneous and Laminated Thick Rectangular Plates," J. Sound and Vibration, Vol. 12, p. 187, 1970.
20. S. V. Kulkarni and N. J. Pagano, "Dynamic Characteristics of Composite Laminates," J. Sound and Vibration, Vol. 23, p. 127, 1972.
21. C. T. Sun, J. D. Achenbach and G. Herrmann, "Continuum Theory for a Laminated Medium," J. Applied Mechanics, Vol. 29, p. 287, 1968.
22. C. T. Sun, "Theory of Laminated Plates," ASME Paper No. 70-WA/APM-25.
23. P. C. Chou and J. Carleone, "Transverse Shear in Laminated Plate Theories," J. Applied Mechanics, Vol. 40, p. 1333, 1973.
24. Anon., Proceedings of the Air Force Workshop on Durability Characteristics of Resin Matrix Composites, Battelle Columbus Laboratories, 1975.
25. J. R. Vinson, R. B. Pipes, W. J. Walker and D. R. Ulrich, ed., The Effects of Relative Humidity and Elevated Temperature on Composite Structures, AFOSR TR-77-0030, Center for Composite Materials, University of Delaware, 1976.
26. C. E. Browning, "The Effects of Moisture on the Properties of High Performance Structural Resins and Composites," Proceedings 28th Annual SPI Conference, 1973
27. E. L. McKague et al., Life Assurance of Composite Structures, AFML-TR-75-51, Vol. 1, 1975.

#### REFERENCES (Contd.)

28. J. M. Augl and R. Tarabocco, Environmental Degradation Studies on Carbon Fiber Reinforced Epoxies, Presented at the Technical Coordination Program, Panel 3 (UK, Canada and Australia), Australia, August 1975; also Naval Surface Weapons Center, White Oak Laboratory, Silver Spring, Maryland.
29. Anon., Advanced Composites Design Guide, Air Force Materials Laboratory, Third Edition (Second Revision), 1976.
30. R. A. Heller et al., "Temperature Dependence of the Complex Modulus for Fiber-Reinforced Materials," ASTM STP 580, p. 298, 1975.
31. D. Roylance and M. Roylance, "Influence of Outdoor Weathering on Dynamic Mechanical Properties of Glass/Epoxy Laminate," ASTM STP 602, p. 85, 1976.
32. G. S. Springer and C. H. Shen, Moisture Absorption and Desorption of Composite Materials, AFML-TR-76-102, 1976. Also see G. S. Springer, "Moisture Content of Composites Under Transient Conditions", Journal of Composite Materials, Vol. II, p. 107, 1977.
33. R. B. Pipes et al., "On the Hygrothermal Response of Laminated Composite Systems", J. Composite Materials, Vol. 10, p. 129, 1976.
34. R. L. Bisplinghoff and H. Ashley, Principles of Aeroelasticity, John Wiley, 1962.
35. Y. C. Fung, An Introduction to the Theory of Aeroelasticity, Dover Publications, 1969.
36. H. Ashley, "Aeroelasticity," Applied Mechanics Reviews, Vol. 23, p. 119, 1970.
37. L. E. Goodman and J. V. Rattaya, "Review of Panel Flutter and Effects of Aerodynamic Noise," Applied Mechanics Surveys, Spartan Books, 1966.
38. E. H. Dowell, "Panel Flutter: A Review of the Aeroelastic Stability of Plates and Shells," AIAA Journal, Vol. 8, p. 385, 1970.
39. J. M. Hedgepeth, "Flutter of Rectangular Simply Supported Panels at High Supersonic Speeds," J. Aeronautical Sciences, Vol. 24, p. 563, 1957.

REFERENCES (Contd.)

40. J. Dugundji, "Theroretical Considerations of Panel Flutter at High Supersonic Mach Numbers," AIAA Journal, Vol. 4, p. 1257, 1966.
41. C. P. Shore, Effects of Structural Damping on Flutter of Stressed Panels, NASA TN D-4990, 1969.
42. J. A. McElman, Flutter of Curved and Flat Sandwich Panels Subjected to Supersonic Flow, NASA TN D-2192, 1964.
43. L. L. Erickson, Supersonic Flutter of Sandwich Panels: Effects of Face Sheet Bending Stiffness, Rotary Inertia, and Orthotropic Core Shear Stiffness, NASA TN D-6427, 1971.
44. A. A. Permutter, On the Aeroelastic Stability of Orthotropic Panels in Supersonic Flow, J. Aerospace Sciences, Vol. 29, p. 1332, 1962.
45. R. L. Ramkumar and T. A. Weissar, "Flutter of Flat Rectangular Anisotropic Plates in High Mach Number Supersonic Flow," J. Sound and Vibration, Vol. 50, p. 587, 1977.
46. J. W. Sawyer, Flutter of Laminated Plates in Supersonic Flow, NASA TM X-72800, 1975.
47. G. Herrmann and I. C. Jong, "On the Destabilizing Effect of Damping in Nonconservative Elastic Systems," J. Applied Mechanics, Vol. 33, p. 592, 1965.
48. D. H. Kaelble, "Dynamic and Tensile Properties of Epoxy Resins", J. Appl. Polymer Sci., 9, 1213 (1965).
49. J. C. Halpin, Introduction to Viscoelasticity, Composite Materials Workshop, S. W. Tsai, J. C. Halpin and N. J. Pagano, Ed. Technomic Publication, 1968.



Table 1. Constituent Properties

Epoxy Matrix

Frequency	$E_R^*$ $\times 10^6 \text{ psi}$	$E_I^*$ $\times 10^4 \text{ psi}$	$\nu_R^*$	$\nu_I^*$
$10^1$	0.452	0.732	0.303	-0.0032
$10^2$	0.475	0.869	0.293	-0.0038
$10^3$	0.348	0.915	0.349	-0.0040
$10^4$	0.342	1.45	0.351	-0.0063
$10^5$	0.34	1.96	0.352	-0.0085
$10^6$	0.34	2.47	0.352	-0.0108
$10^7$	0.34	2.98	0.352	-0.0130

\*R - Real

\*I - Imaginary

Epoxy Matrix : K (Bulk Modulus) =  $0.3824 \times 10^6 \text{ psi}$

Boron Fiber :  $E = 53.7 \times 10^6 \text{ psi}$ ,  $\nu = 0.222$

Graphite Fiber:  $E_A = 34 \times 10^6 \text{ psi}$ ,  $E_T = 3 \times 10^6 \text{ psi}$ ,  $\nu_A = 0.26$ ,  $\nu_T = 0.4$ ,  $G_A = 3.2 \times 10^6$

Boron/Epoxy Mass Density  $\rho = 0.000194 \text{ lb-sec}^2/\text{in}^4$ ,  $\nu^f = 0.5$

Graphite/Epoxy Mass Density  $\rho = 0.00015 \text{ lb-sec}^2/\text{in}^4$ ,  $\nu^f = 0.5$

Table 2. Various Damping Levels for Epoxy Matrix

Level of Damping	Multiplication Factor
0	0
1	0.25
2 (Base; table 1)	1
3	2.5

Table 3. Effect of Damping Levels on Flutter Parameter  $\bar{\lambda}_{cr}$  for Laminates 1, 2, and 3.

Laminate 1. Boron/epoxy,  $[0/90]_s$ ,  $a = 0.6$  in,  $H = 0.06$  in

<u>Level of Damping</u>	<u>Figure No.</u>	<u><math>\bar{\lambda}_{cr1}</math></u>	<u><math>\bar{\lambda}_{cr2}</math></u>	<u><math>\bar{\lambda}_{cr3}</math></u>
0	23	94	130	-
1	24	87	100	40
2	25	89	103	48
3	26	97	108	60

Laminate 2. Boron/epoxy,  $[0/90]_{2s}$ ,  $a = 0.6$  in,  $H = 0.06$  in

<u>Level of Damping</u>	<u>Figure No.</u>	<u><math>\bar{\lambda}_{cr1}</math></u>	<u><math>\bar{\lambda}_{cr2}</math></u>	<u><math>\bar{\lambda}_{cr3}</math></u>
0	27	110	165	-
1	28	110	128	86
2	29	112	130	86

Laminate 3. Graphite/epoxy,  $[0/90]_{2s}$ ,  $a = 3.6$  in,  $H = 0.06$  in

<u>Level of Damping</u>	<u>Figure No.</u>	<u><math>\bar{\lambda}_{cr}</math></u>
0	30	330
1,2,3	31	130



Table 4. Effect of Damping Levels on Flutter Parameter  $\bar{\lambda}_{cr}$  for Laminates 4 and 5.

Laminate 4. Graphite/Epoxy  $[0/90]_{2s}$ ,  $a = 3.6$  in.,  $H = .06$  in.

Level of Damping	$\bar{\lambda}_{cr}$
0	340
1	157
2	150
3	150

Laminate 5. Graphite/Epoxy  $[0/90]_{2s}$ ,  $a = 0.6$  in.,  $H = .06$  in.

Level of Damping	$\bar{\lambda}_{cr1}$	$\bar{\lambda}_{cr2}$	$\bar{\lambda}_{cr3}$
0	148	205	-
1	139	152	48
2	141	152	48
3	152	155	48.5

Table 5. Effects of Environment, Aerodynamic Damping and Prestress on  $\bar{\lambda}_{cr}$  for Laminate 6.

	$\bar{\lambda}_{cr}$
Reference State	125
Moisture-Temperature Gradient	148
Aerodynamic Damping $\rho_a c = 10^{-4} \text{ lb}^{\text{sec}}/\text{in}^3$	176
Aerodynamic Damping $\rho_a c = 10^{-3} \text{ lb}^{\text{sec}}/\text{in}^3$	280
Prestress $N_{xx}^0 = 120 \text{ lb/in}$ $\sim 0.5 \times$ (static buckling load)	108
Prestress $N_{xx}^0 = 192 \text{ lb/in}$ $\sim 0.8 \times$ (static buckling load)	101

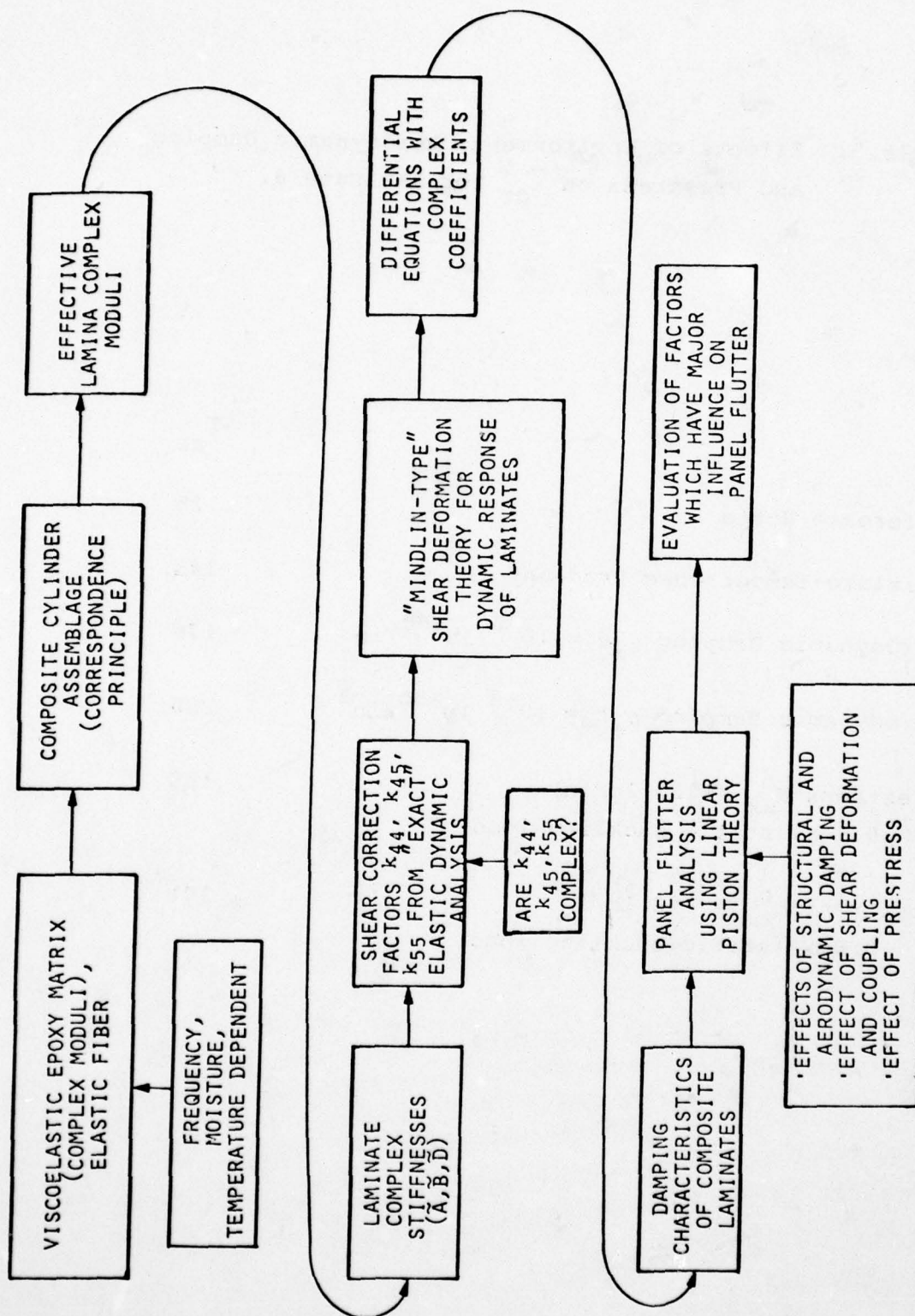


Figure 1. Various Modules in the Composite Laminate Panel Flutter Problem



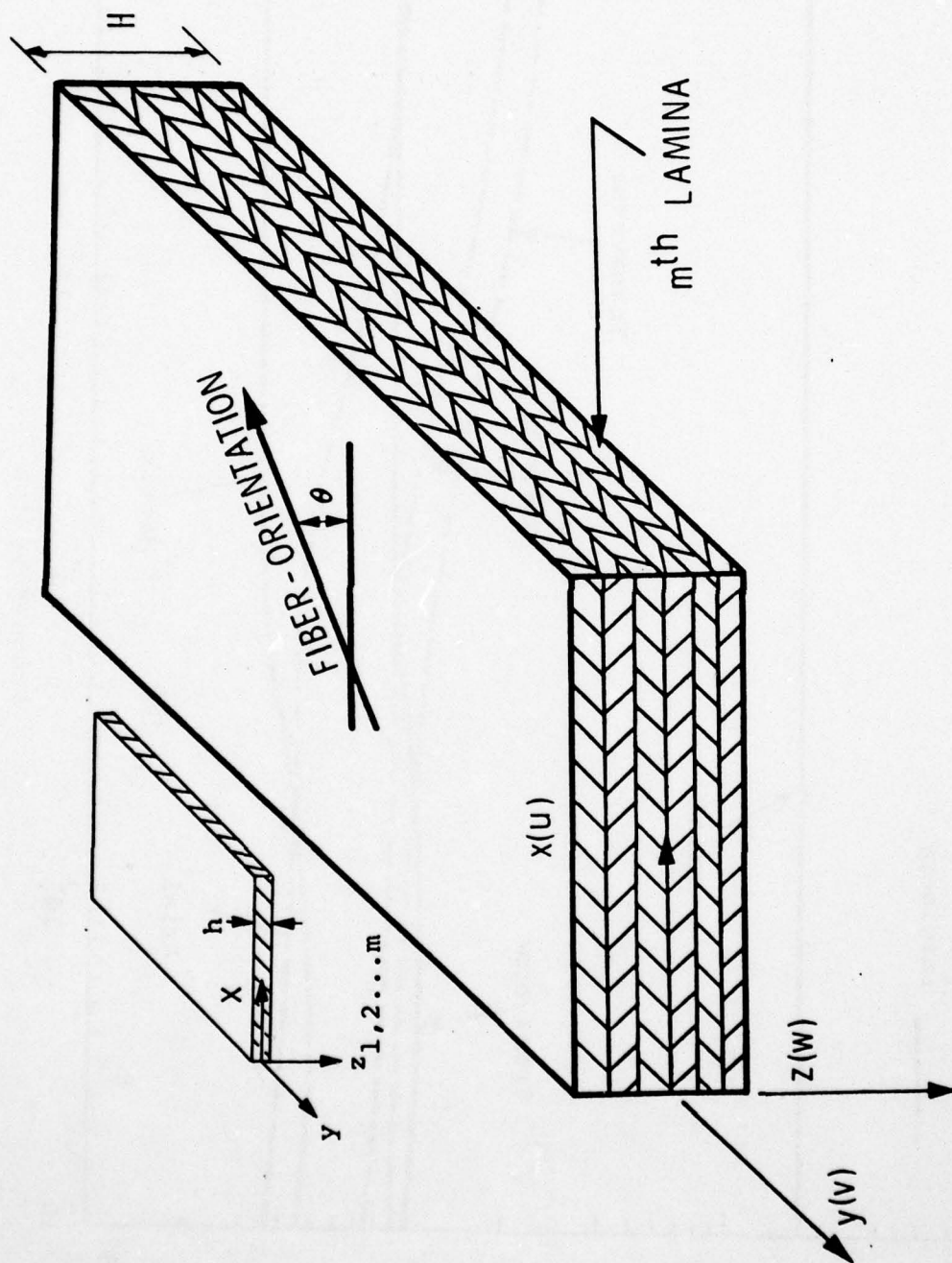


Figure 2. Composite Lamina/Laminate Coordinate Systems

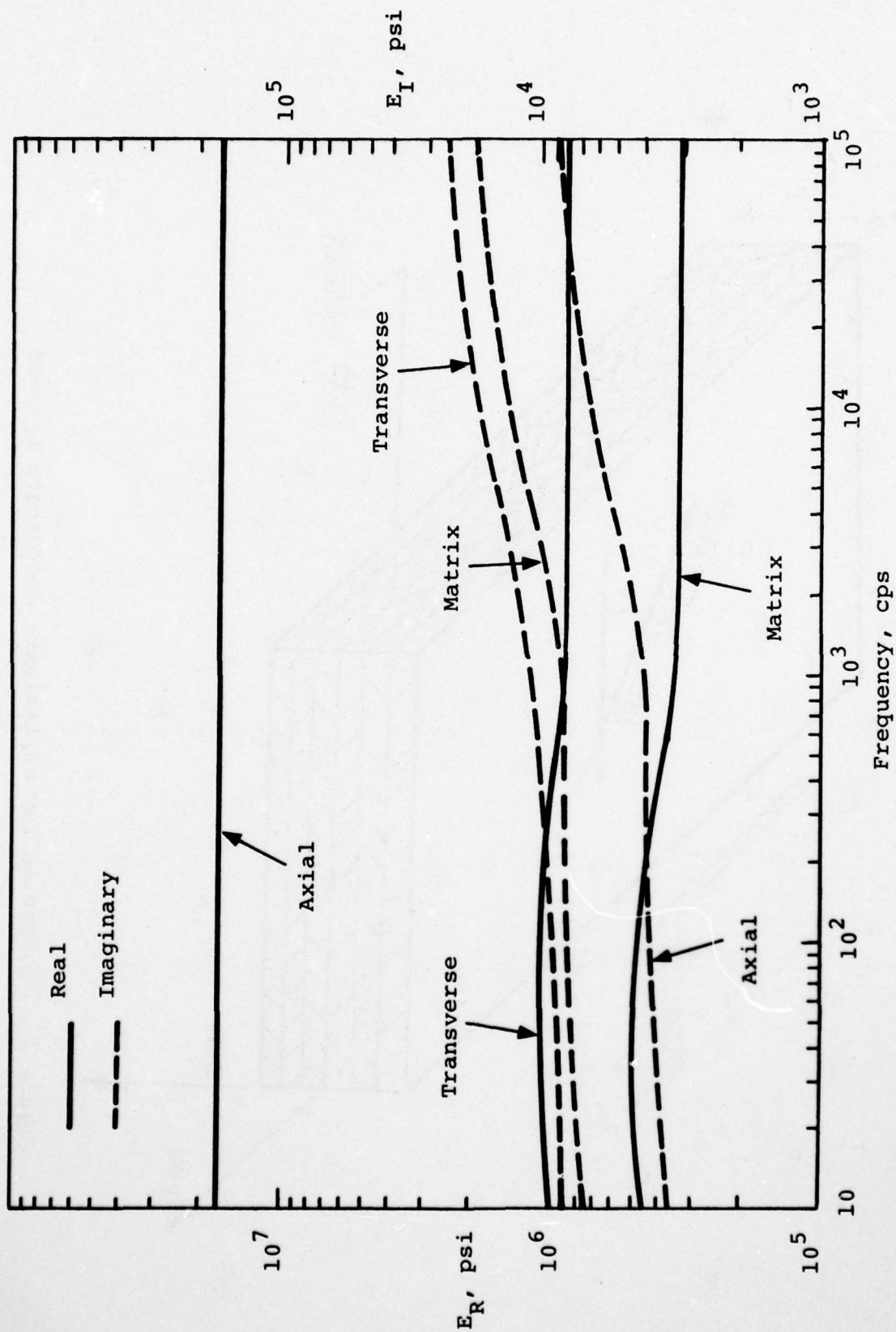


Figure 3. Variation of Lamina and Matrix Complex Young's Moduli With Frequency

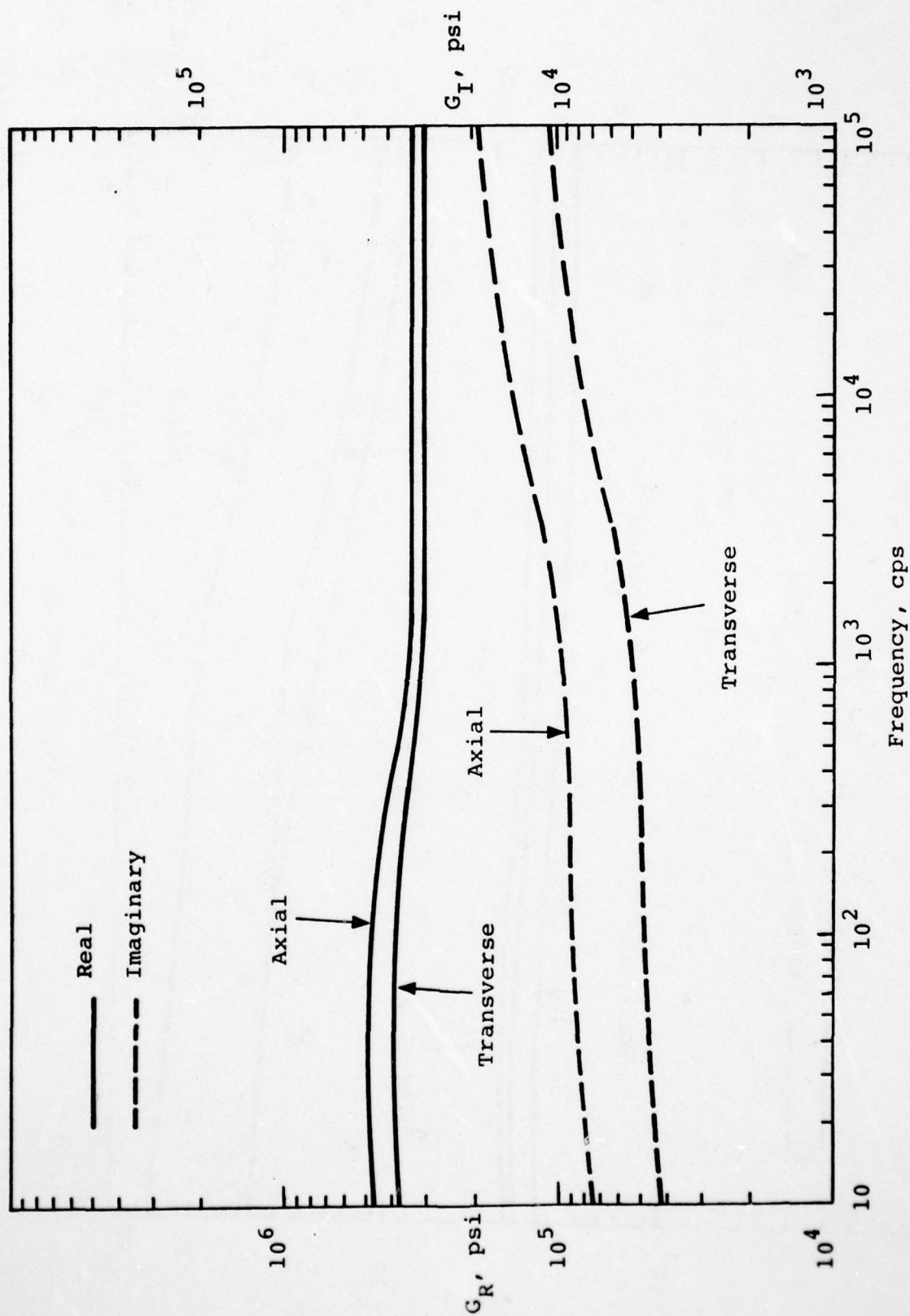


Figure 4. Variation of Lamina Complex Shear Moduli With Frequency



AD-A055 753

MATERIALS SCIENCES CORP BLUE BELL PA  
EFFECTS OF ENVIRONMENT, AND DAMPING AND COUPLING PROPERTIES OF --ETC(U)  
JAN 78 S N CHATTERJEE, S V KULKARNI

F/G 11/4

F44620-76-C-0080

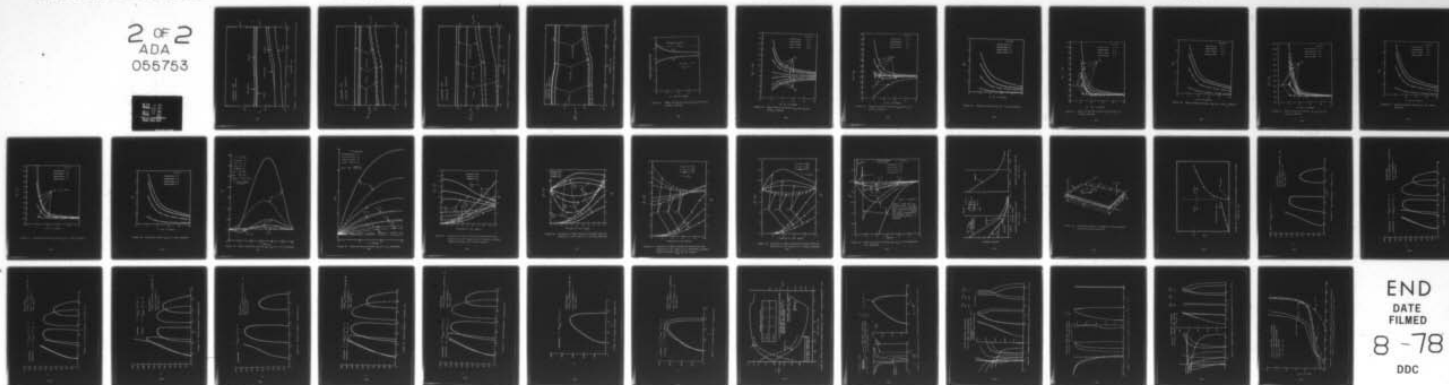
UNCLASSIFIED

MSC/TFR/802/1151

AFOSR-TR-78-1066

NL

2 OF 2  
ADA  
066753



END  
DATE  
FILMED  
8-78  
DDC

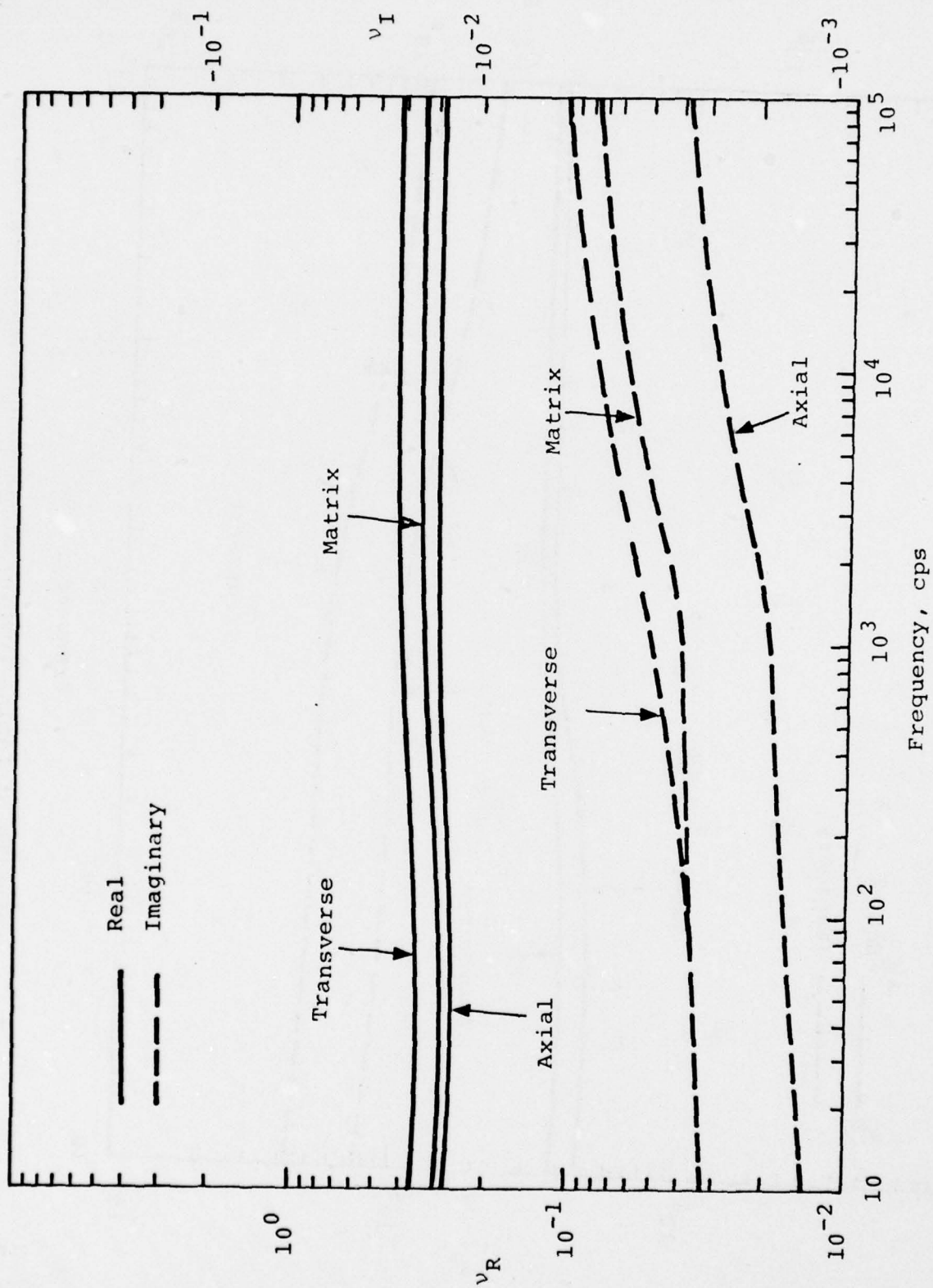


Figure 5. Variation of Lamina and Matrix Complex Poisson's Ratios With Frequency

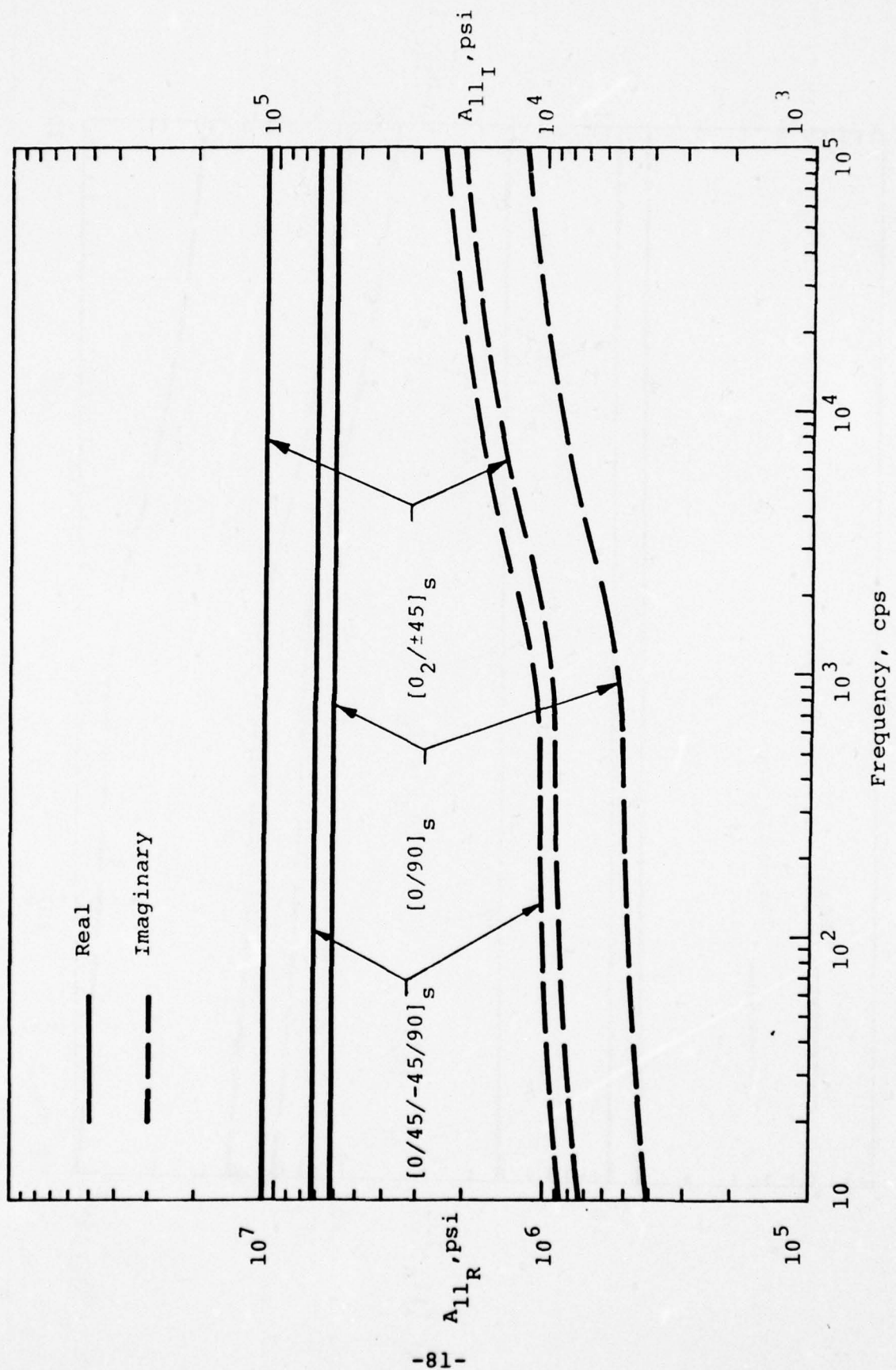


Figure 6. Variation of Laminate Extensional Stiffness  $A_{11}$  With Frequency



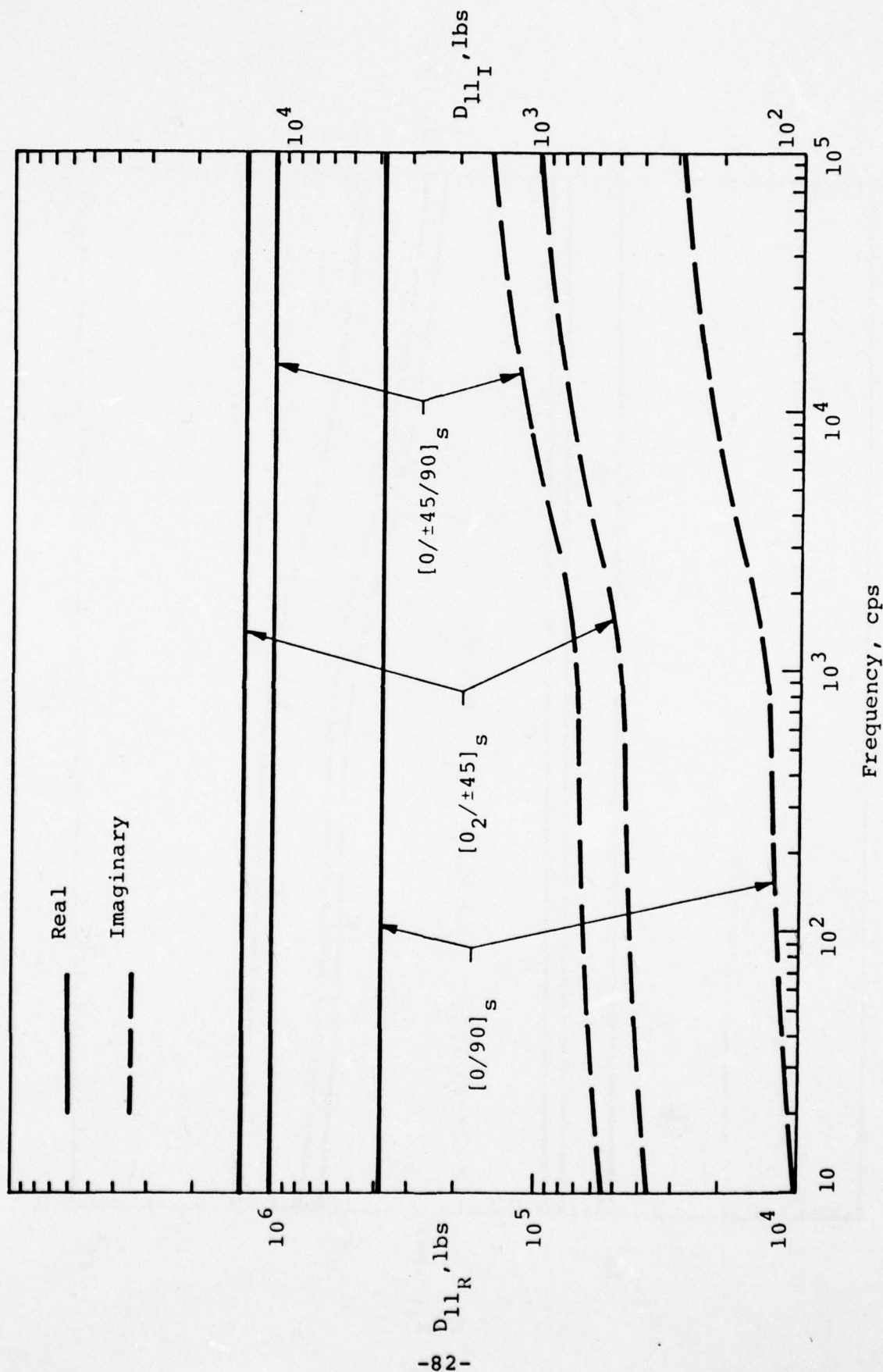


Figure 7. Variation of Laminate Bending Stiffness  $\bar{D}_{11}$  With Frequency

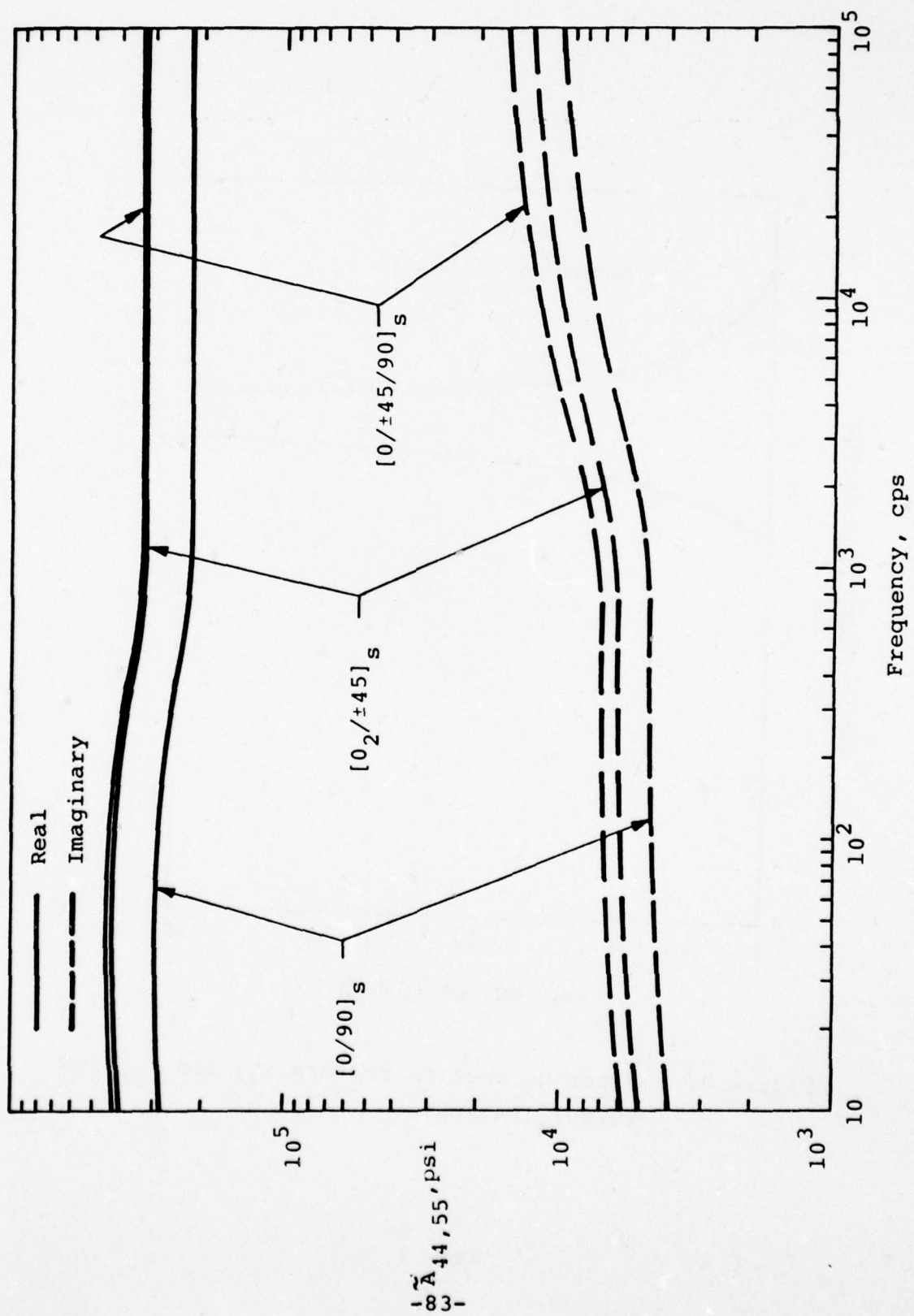


Figure 8. Variation of Laminate Transverse Shear Stiffnesses  $\bar{A}_{44,55}$  With Frequency

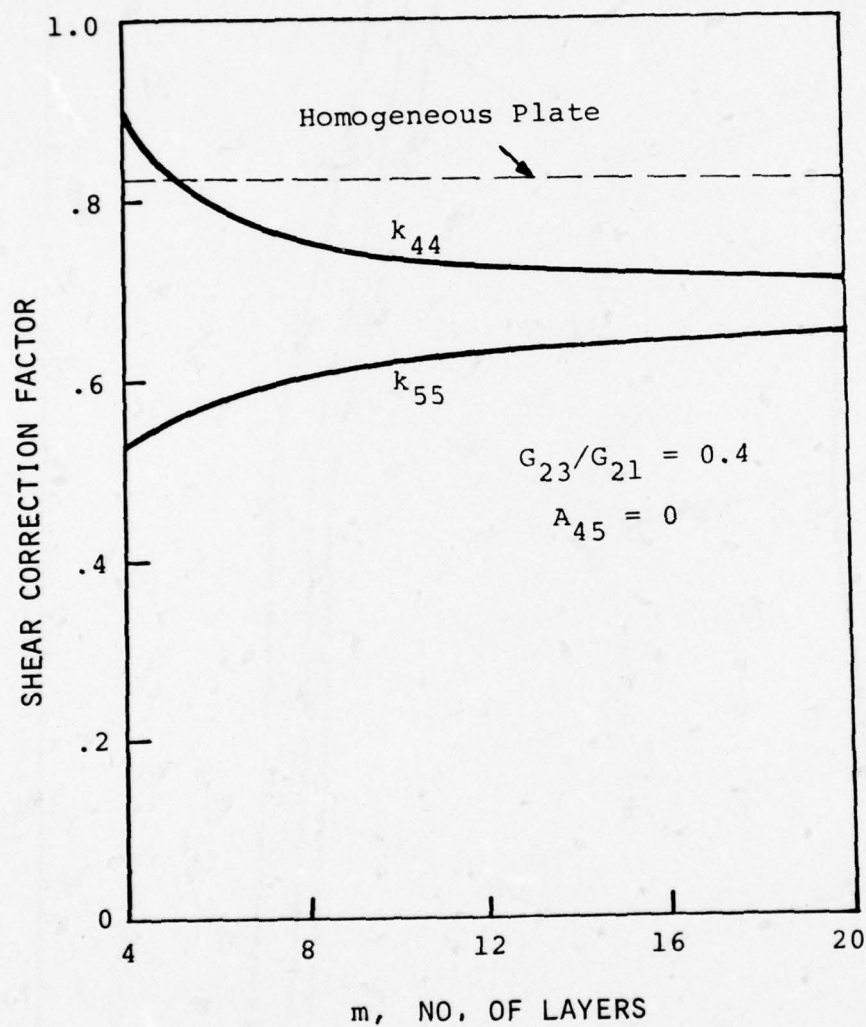


Figure 9. Shear Correction Factors  $k_{44}$  and  $k_{55}$  for  $[0/90]_s$  Laminate



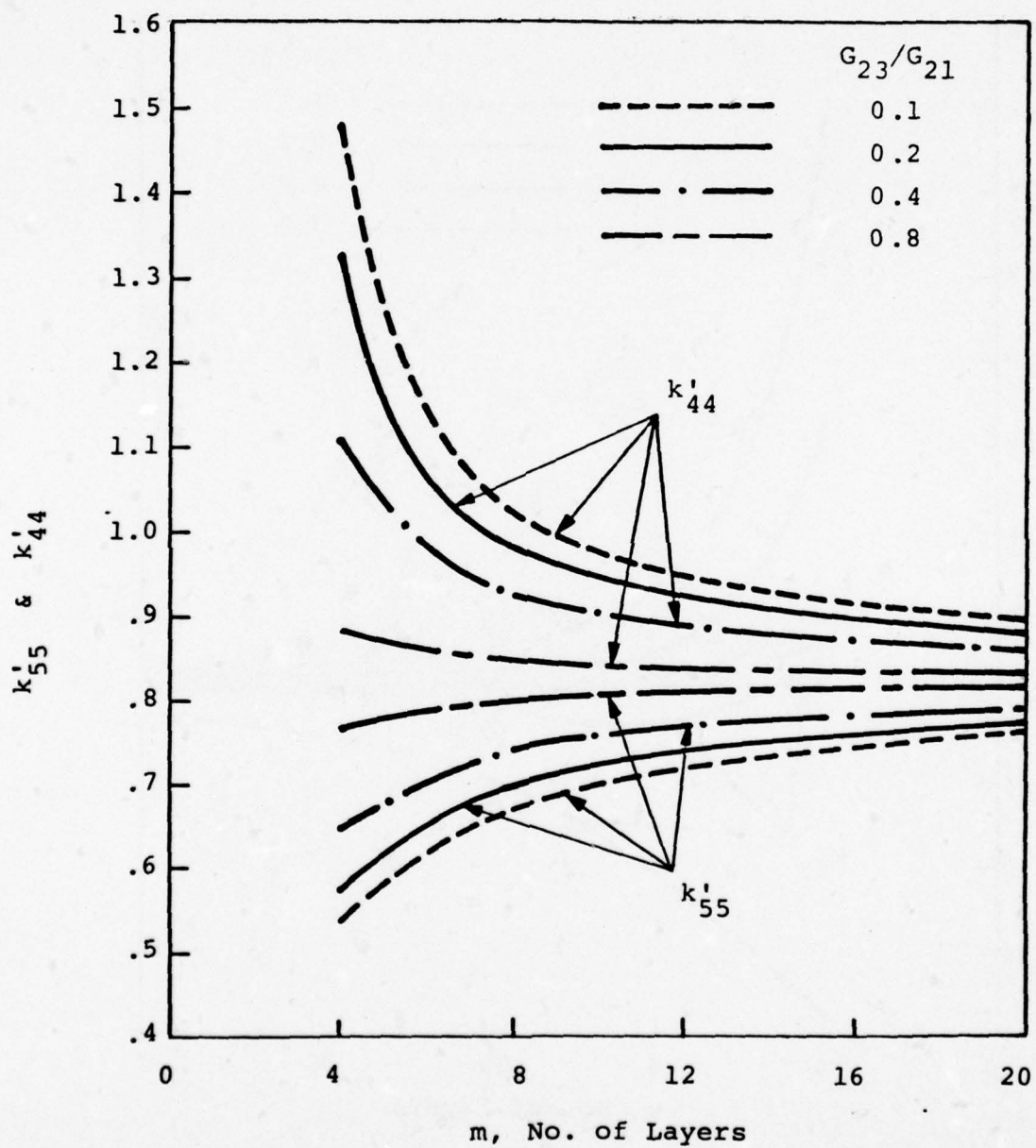


Figure 10. Shear Correction Factors  $k'_{44}$  and  $k'_{55}$  for  $[0/90]_s$  Laminate

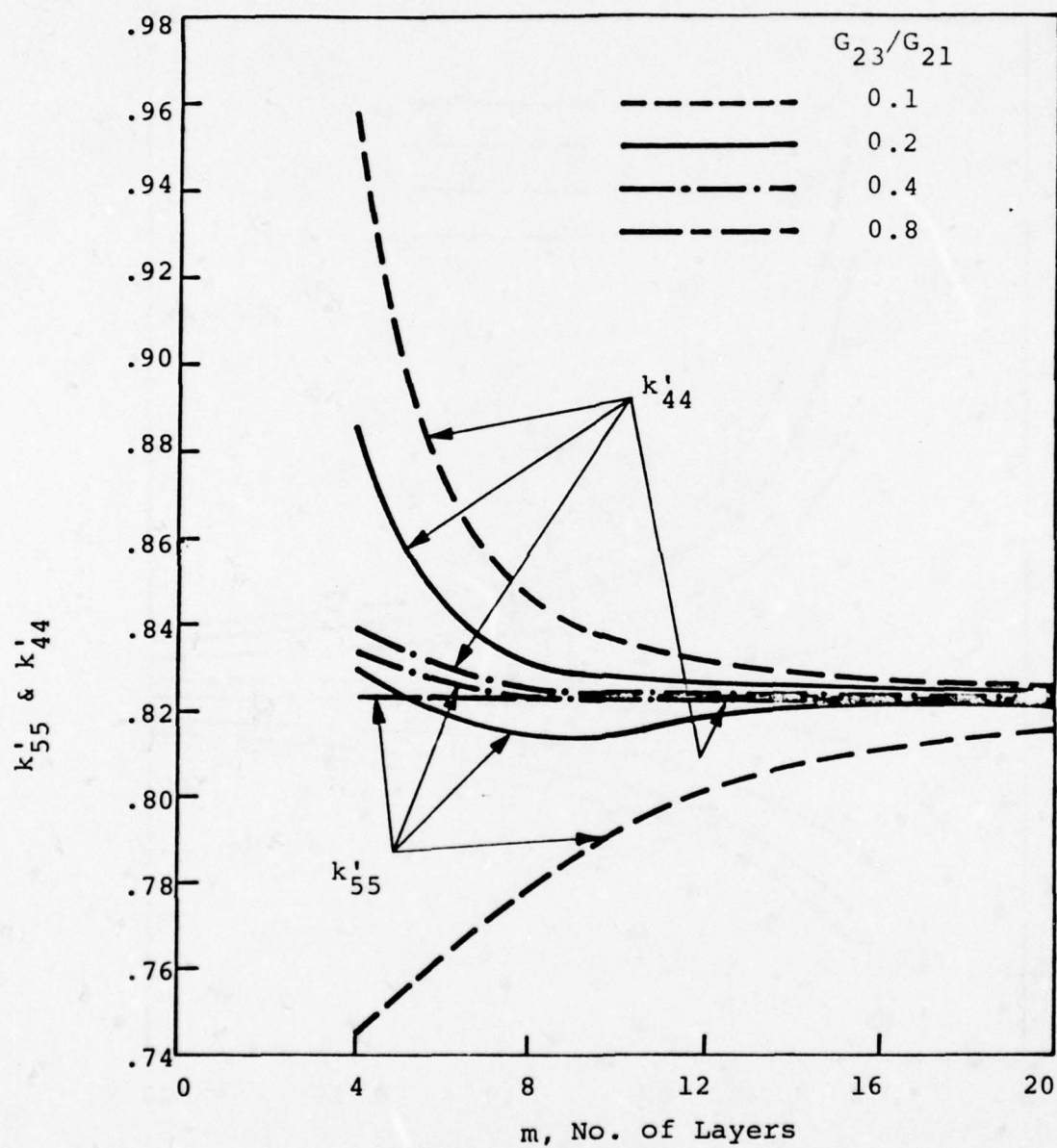


Figure 11. Shear Correction Factors  $k'_{44}$  and  $k'_{55}$  for  $[\pm 15^\circ]_s$  Laminate

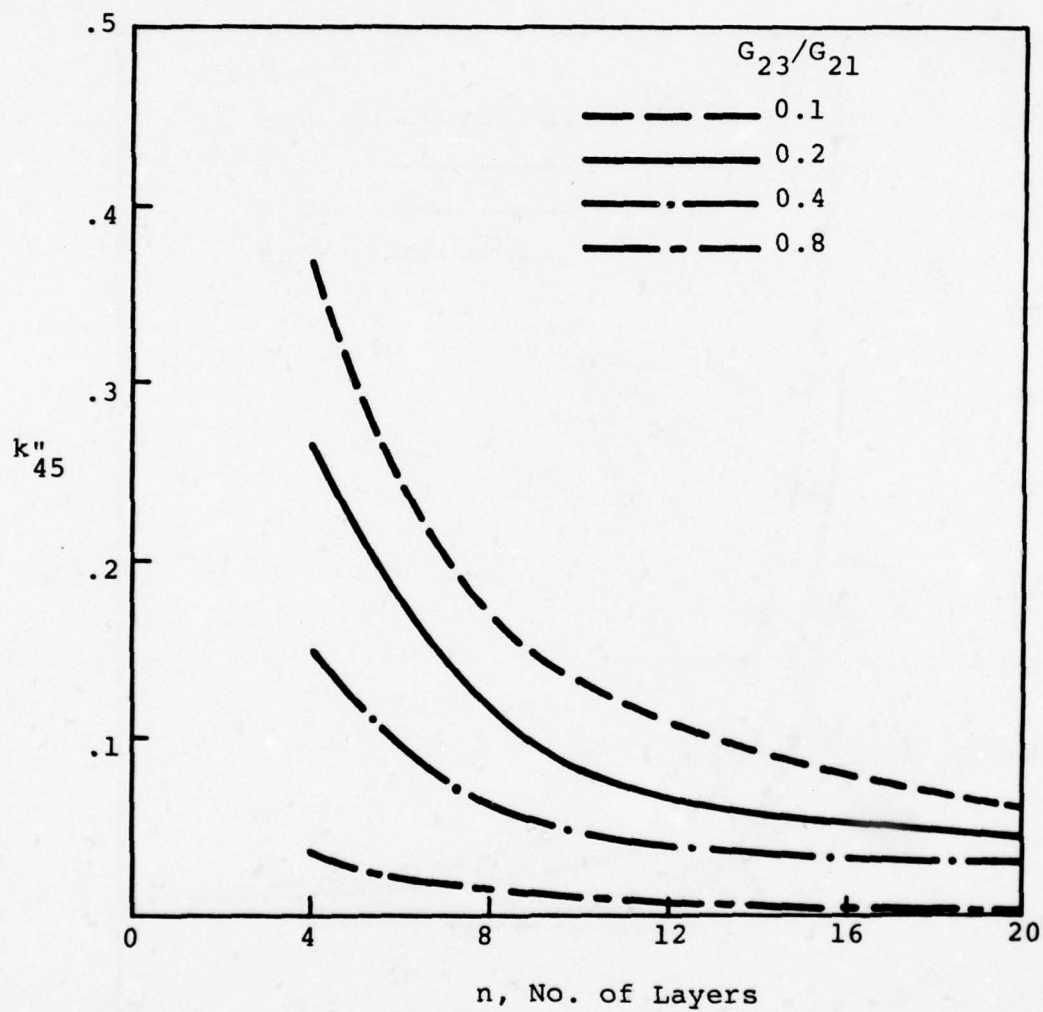


Figure 12. Correction Factor  $k''_{45}$  for  $[\pm 15^\circ]_s$  Laminate



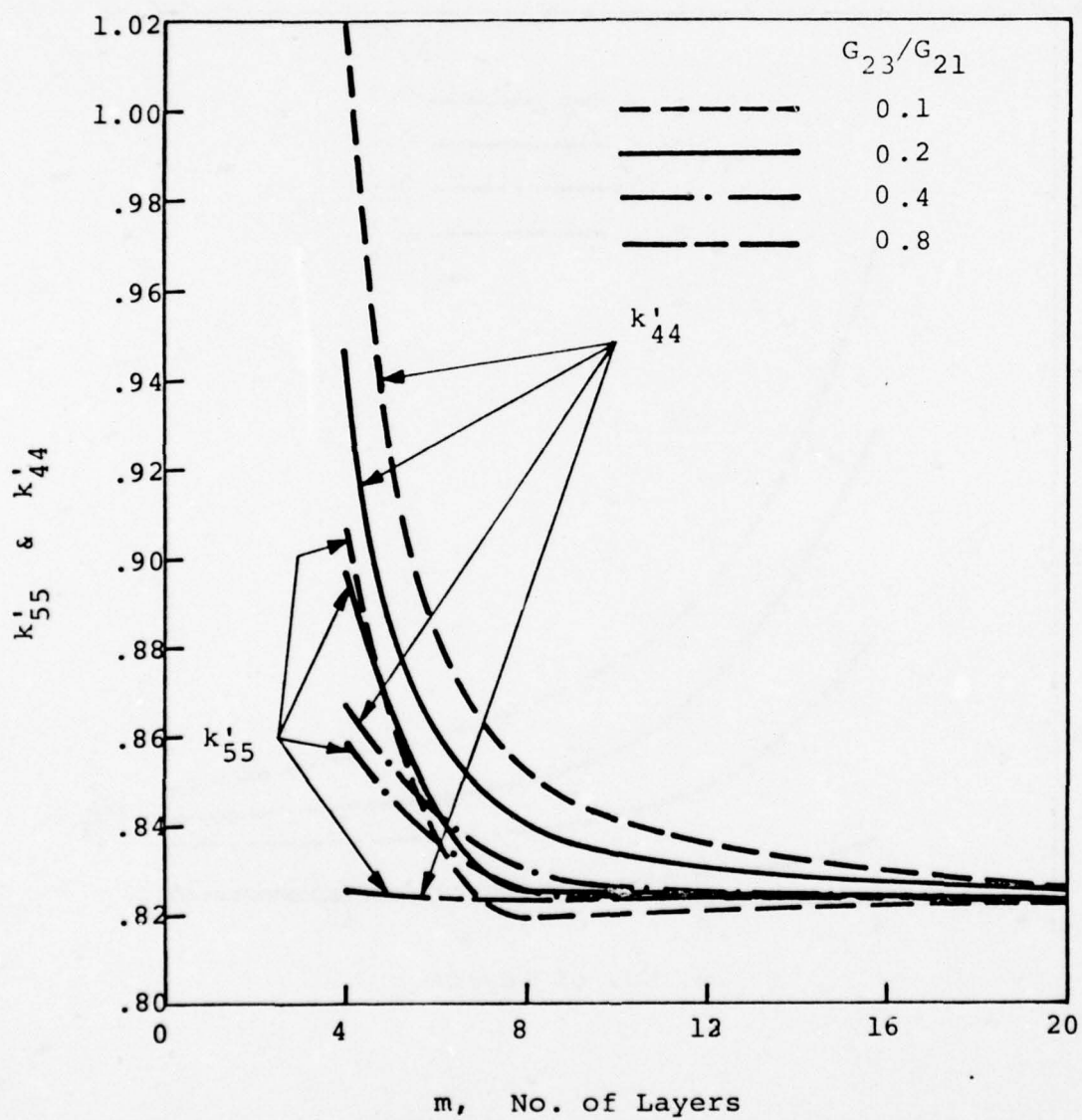


Figure 13. Shear Correction Factors  $k'_{44}$  and  $k'_{55}$  for  $[\pm 30^\circ]_s$  Laminate

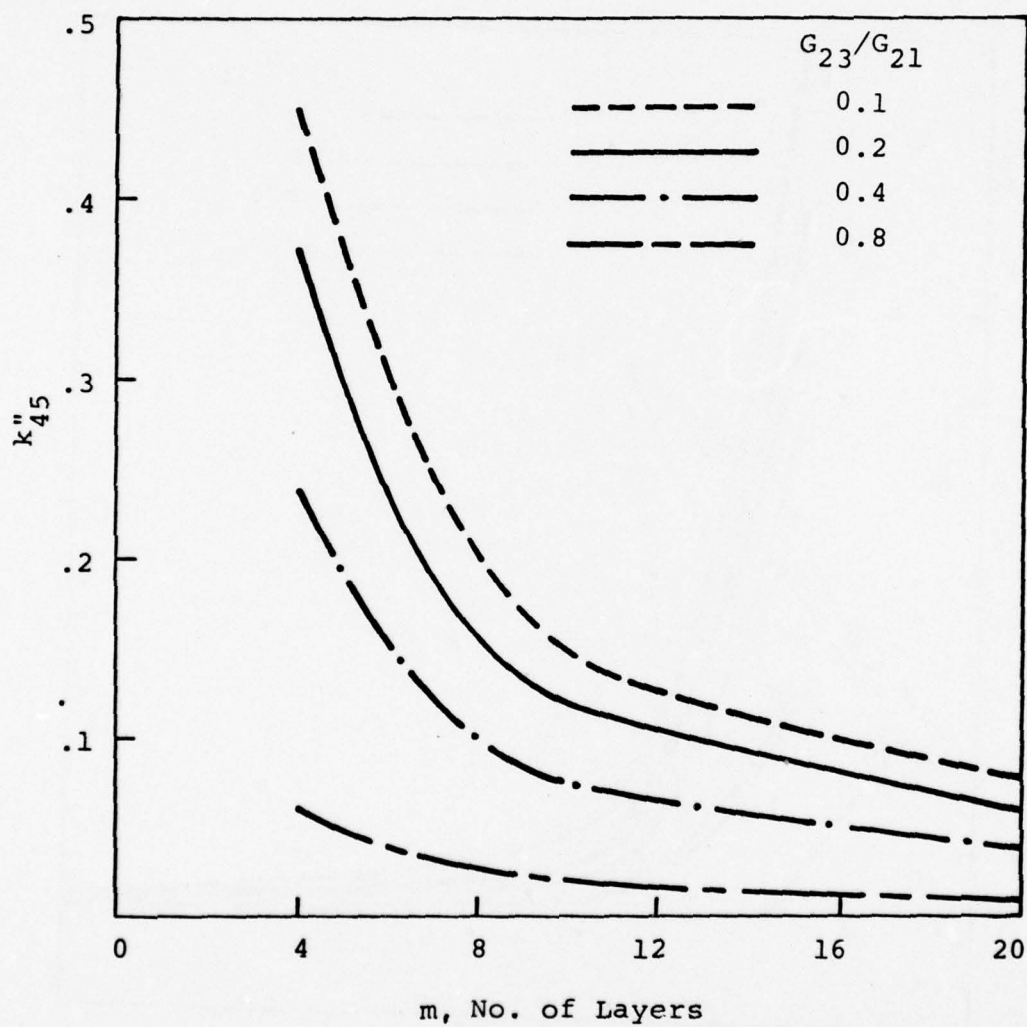


Figure 14. Shear Correction Factor  $k''_{45}$  for  $[\pm 30^\circ]_s$  Laminate

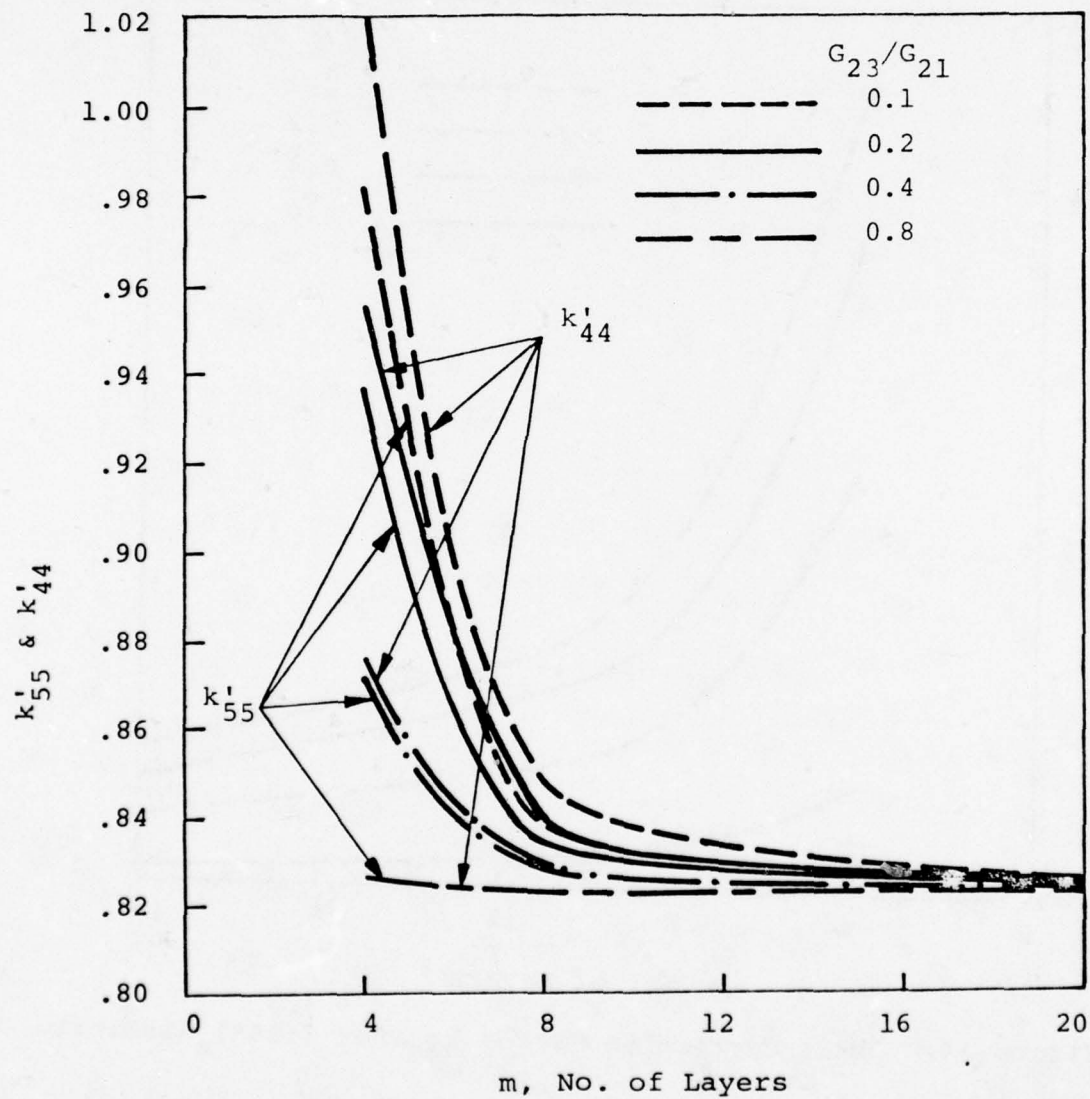


Figure 15. Shear Correction Factors  $k'_{44}$  and  $k'_{55}$  for  $[\pm 40^\circ]_s$  Laminate



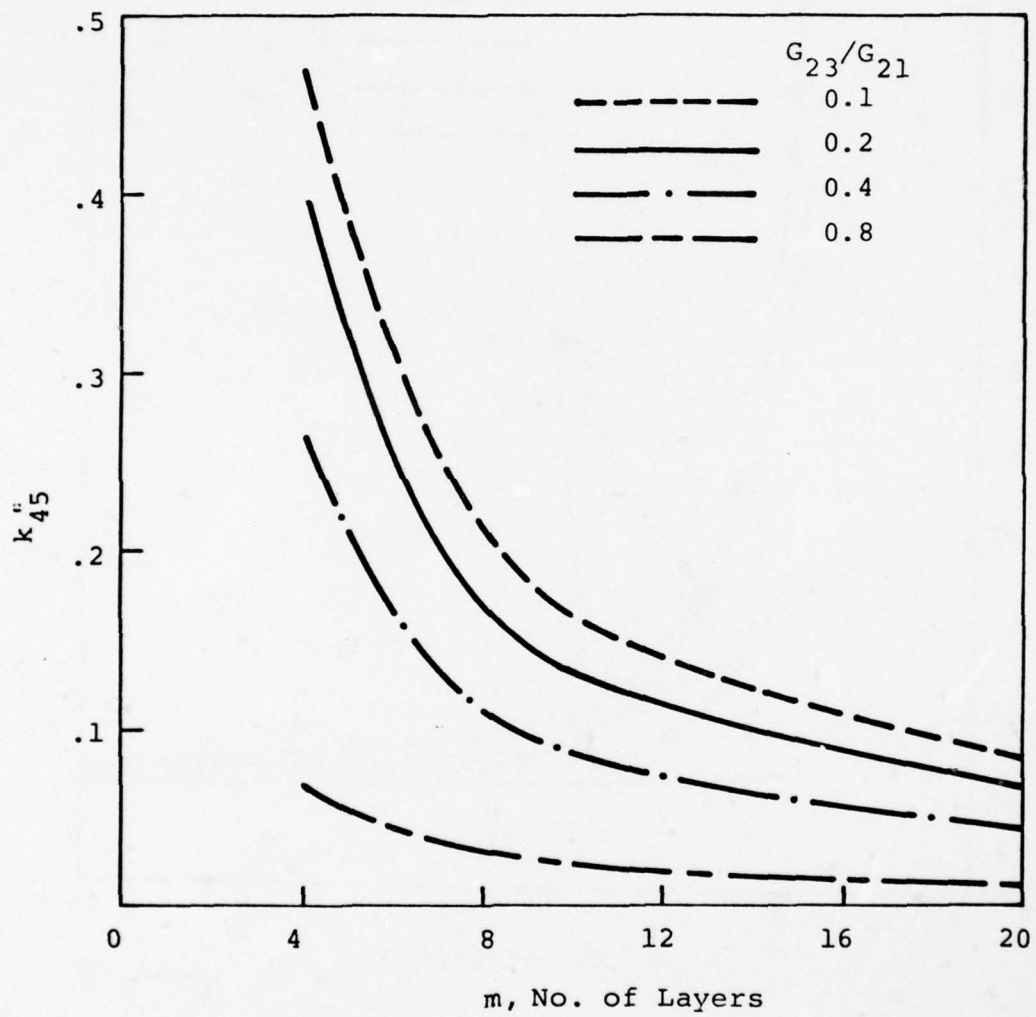


Figure 16. Shear Correction Factor  $k''_{45}$  for  $[\pm 40^\circ]_s$  Laminate

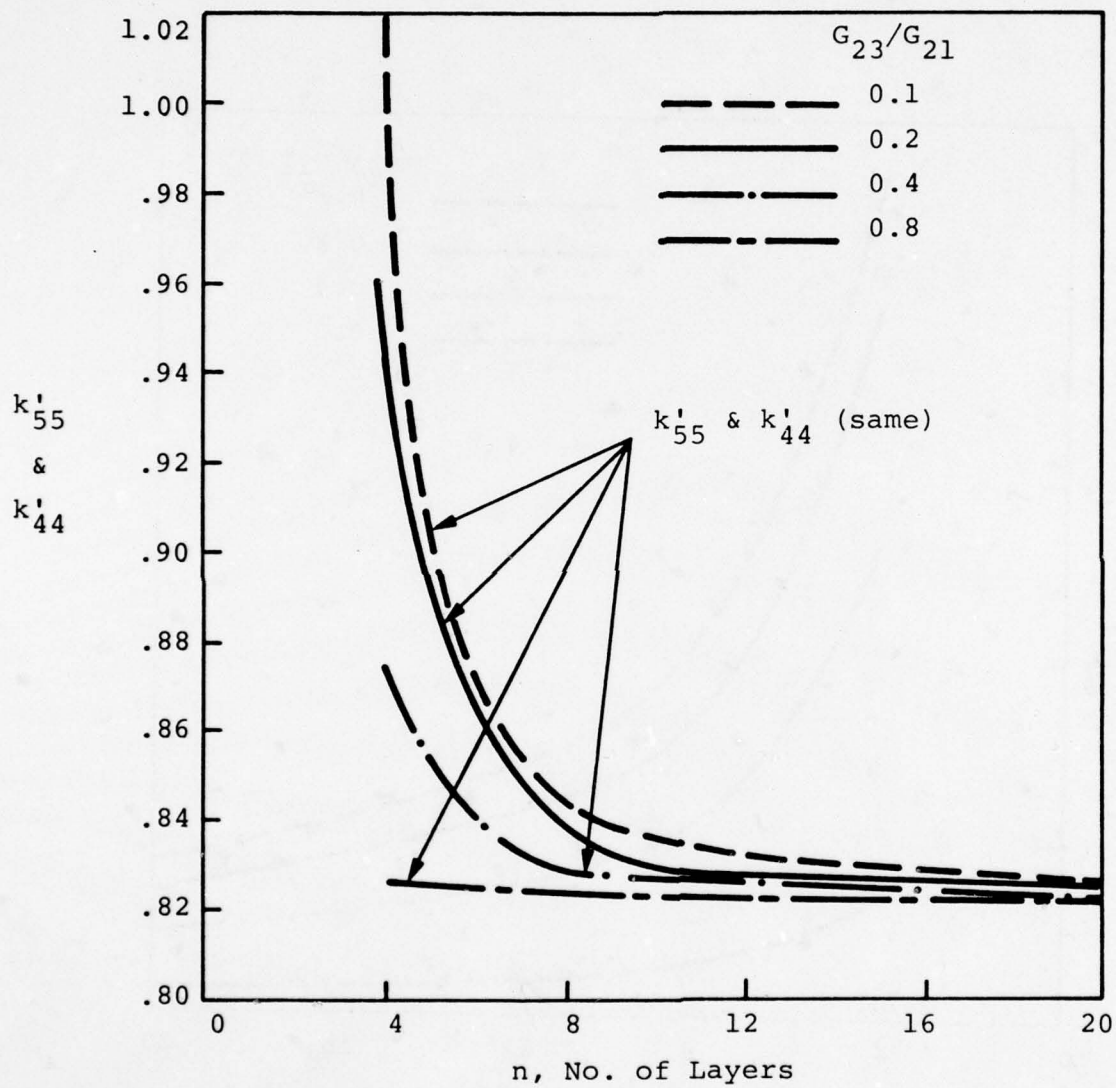


Figure 17. Correction Factor  $k'_{55}$  and  $k'_{44}$  for  $[\pm 45]_s$  Laminate

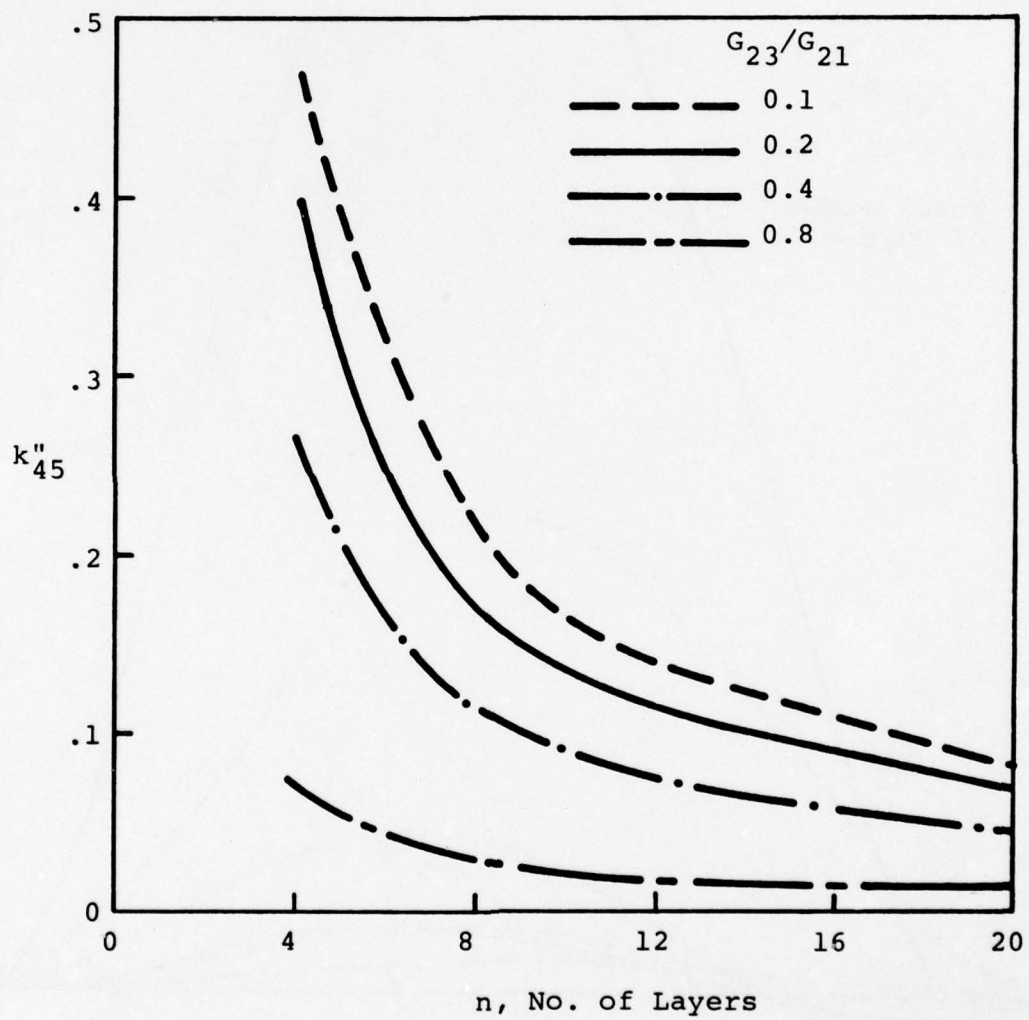


Figure 18. Correction Factor  $k''_{45}$  for  $[\pm 45]_s$  Laminate



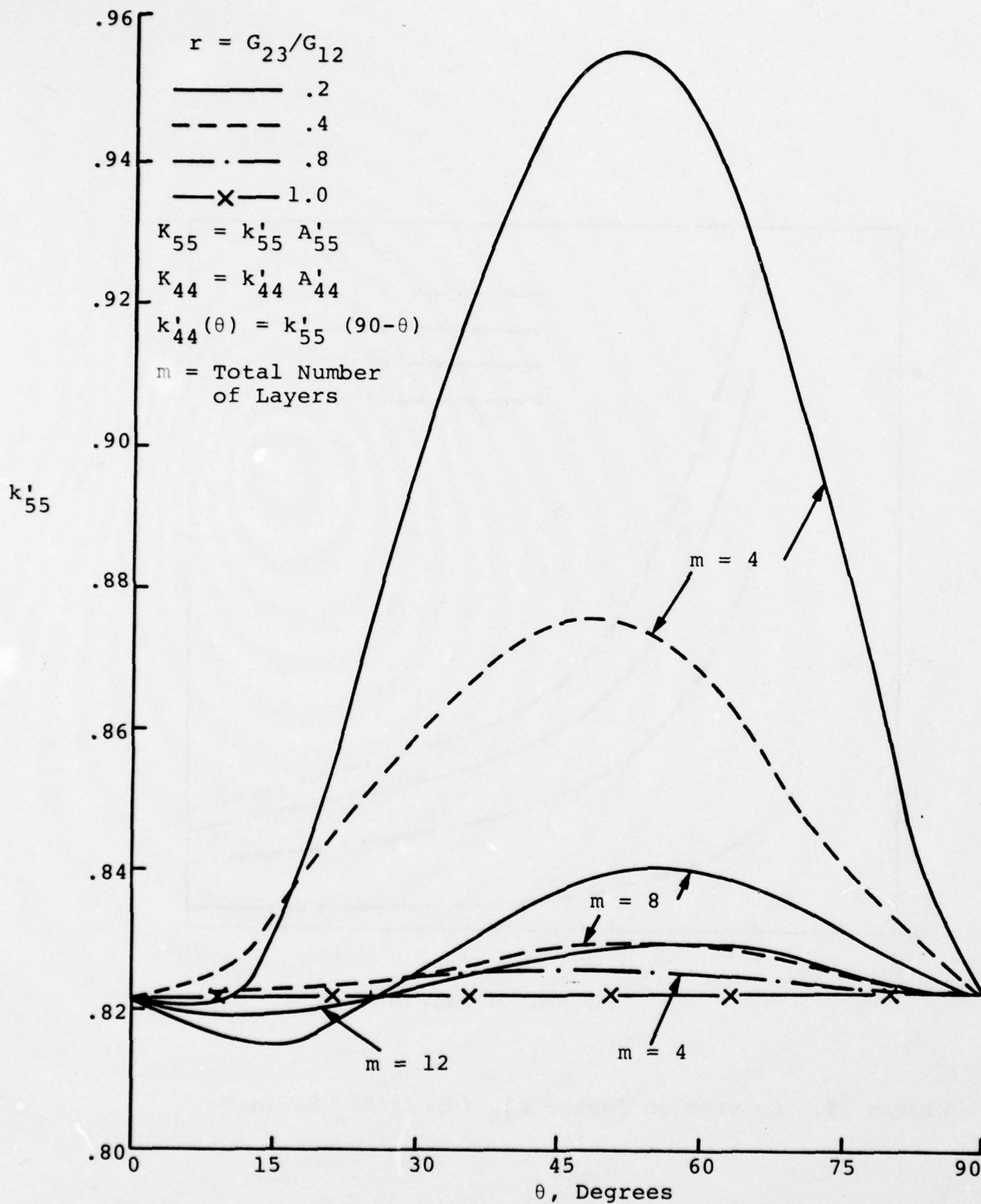


Figure 19. Shear Correction Factors  $k'_{55}$ ,  $k'_{44}$  for  $[\pm\theta]_s$  Laminates

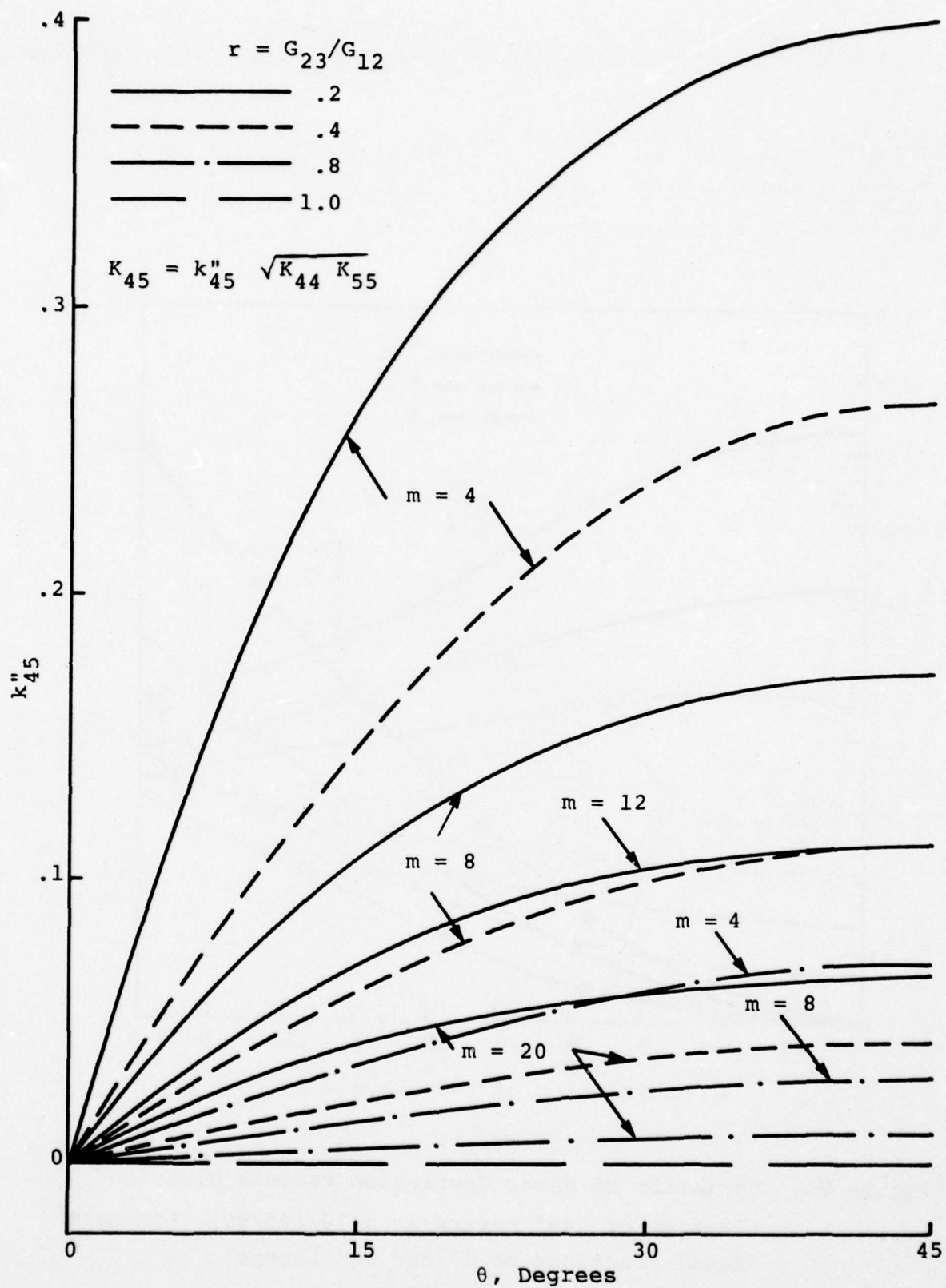


Figure 20. Shear Correction Factor  $k''_{45}$  for  $[\pm\theta]_s$  Laminates

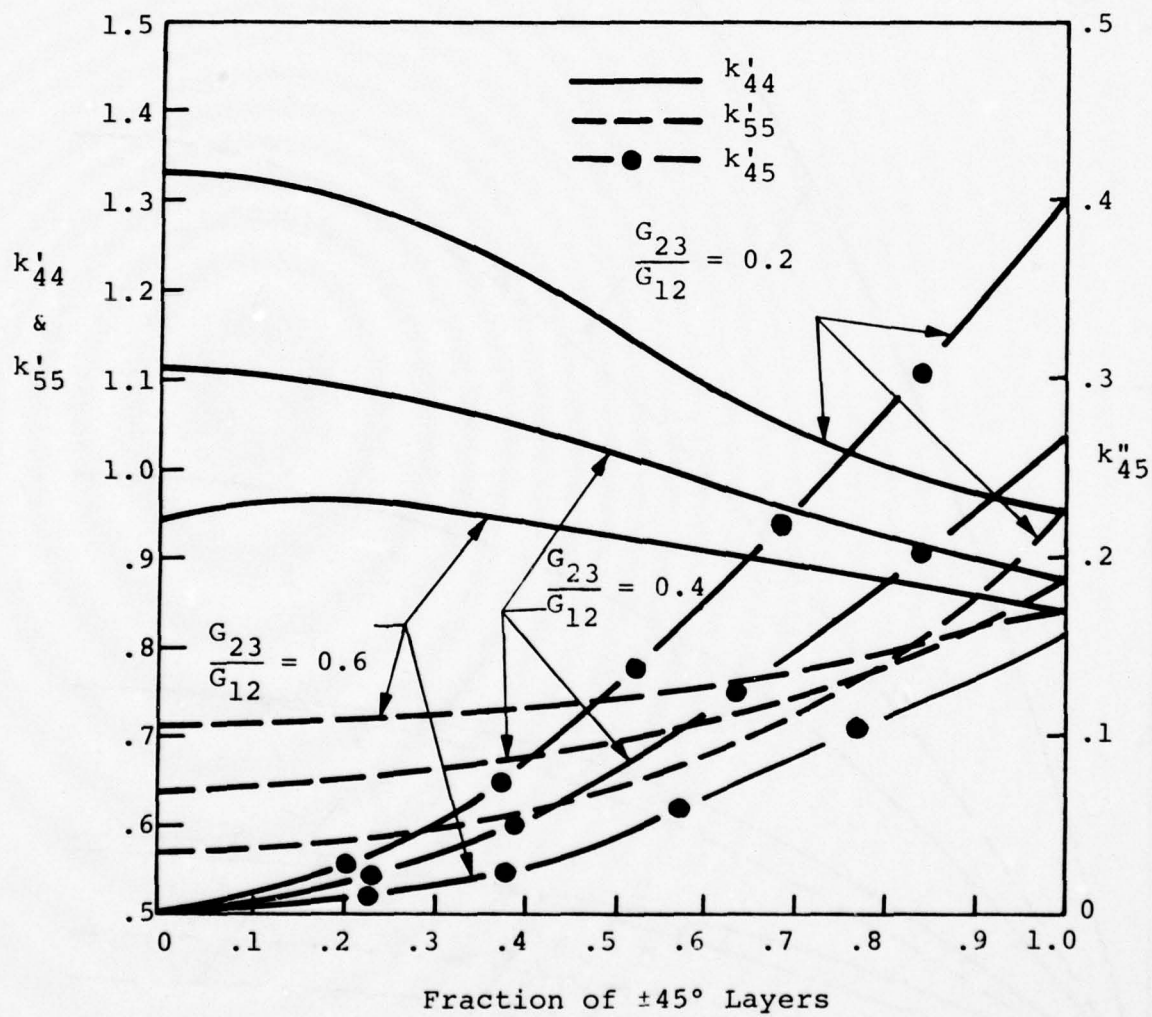


Figure 21. Variation of Shear Correction Factors With the Fraction of  $\pm 45^\circ$  Layers in a  $[0/\pm 45/90]_s$  Laminate (Equal Fractions of  $0^\circ$  and  $90^\circ$  Layers)



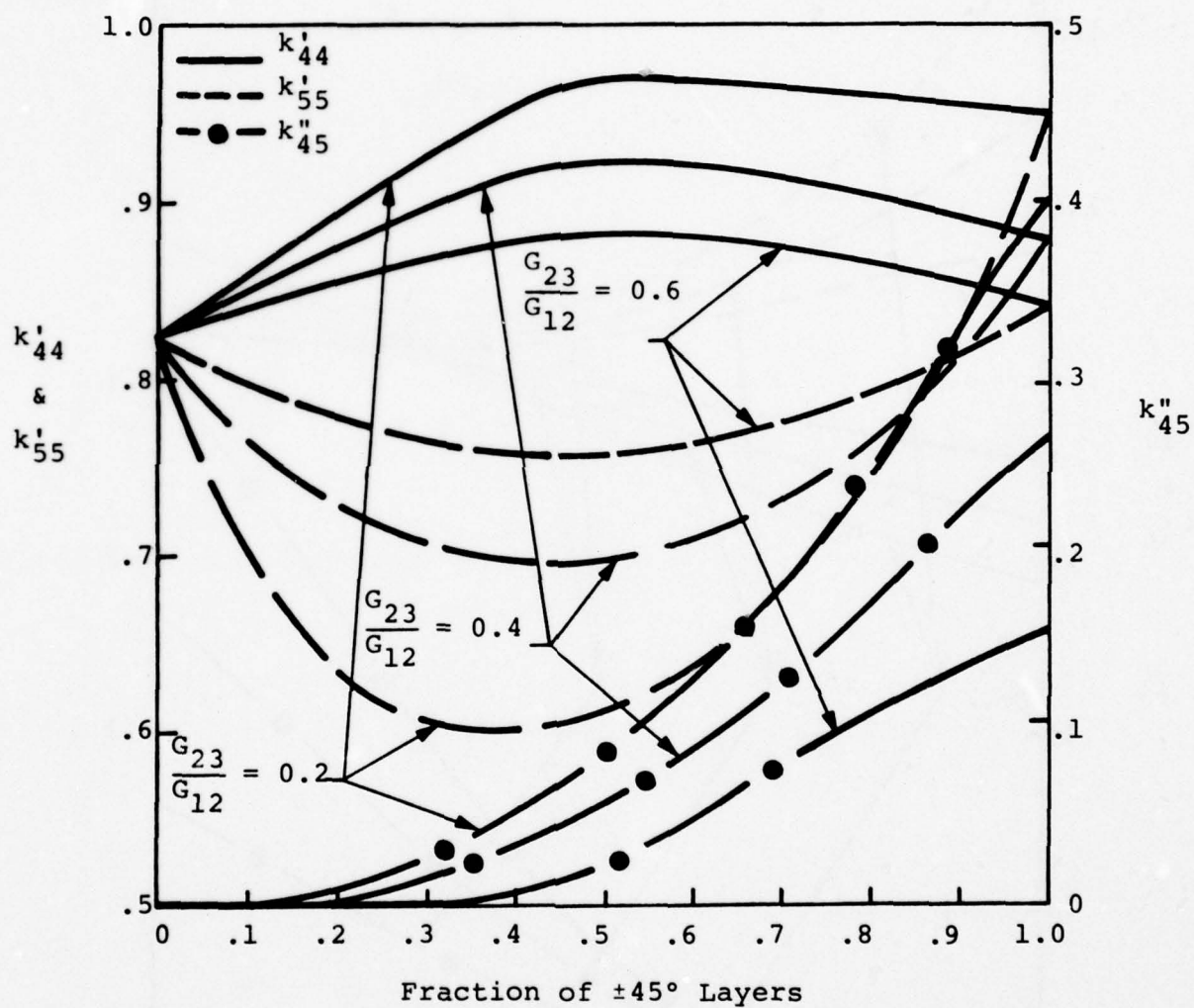


Figure 22. Variation of Shear Correction Factors With the Fraction of  $\pm 45^\circ$  Layers in a  $[0/\pm 45]_s$  Laminate

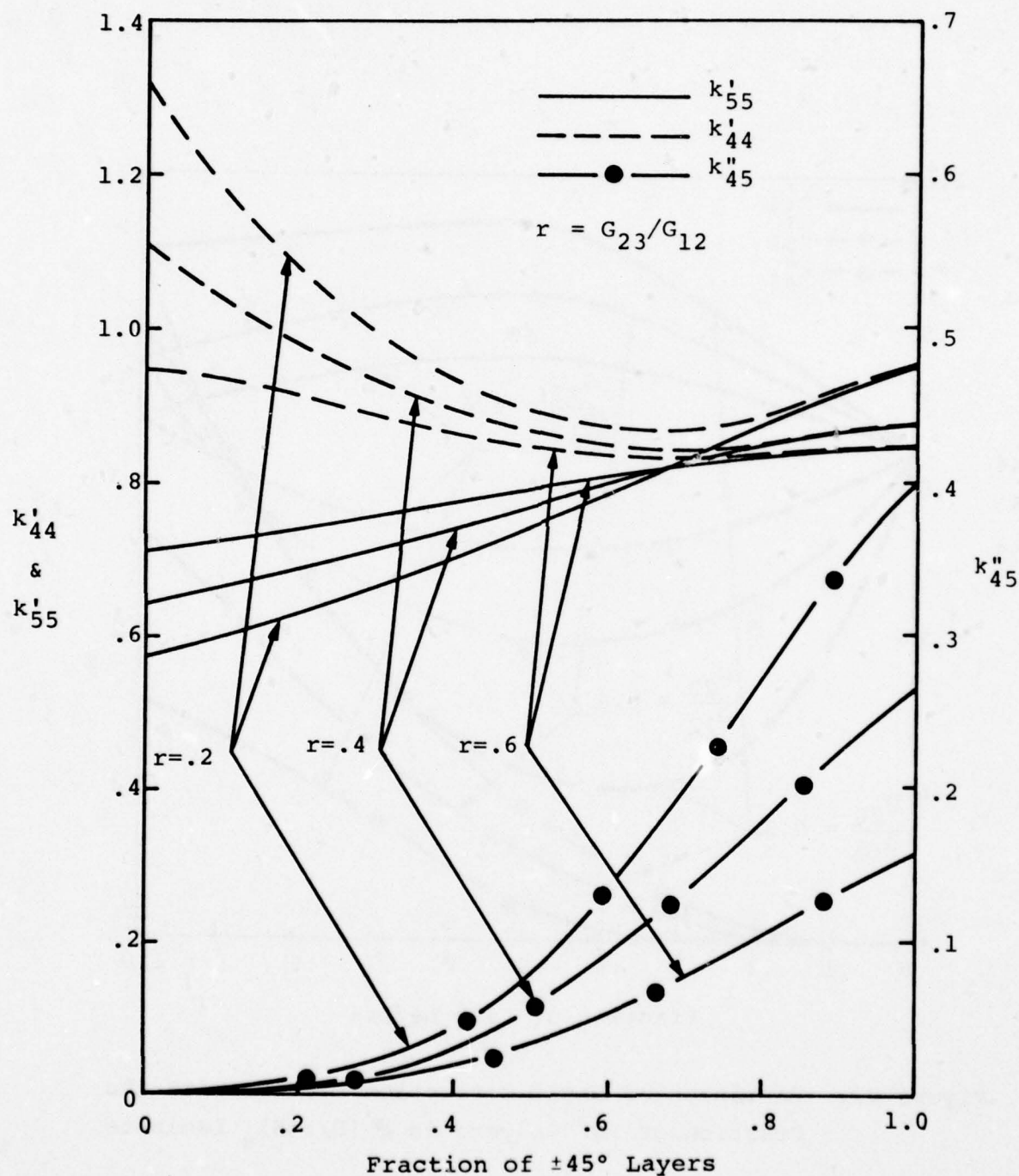


Figure 23. Variation of Shear Correction Factors With the Fraction of  $\pm 45^\circ$  Layers in a  $[\pm 45/0/90]_s$  Laminate (Equal Fractions of  $0^\circ$  and  $90^\circ$  Layers)

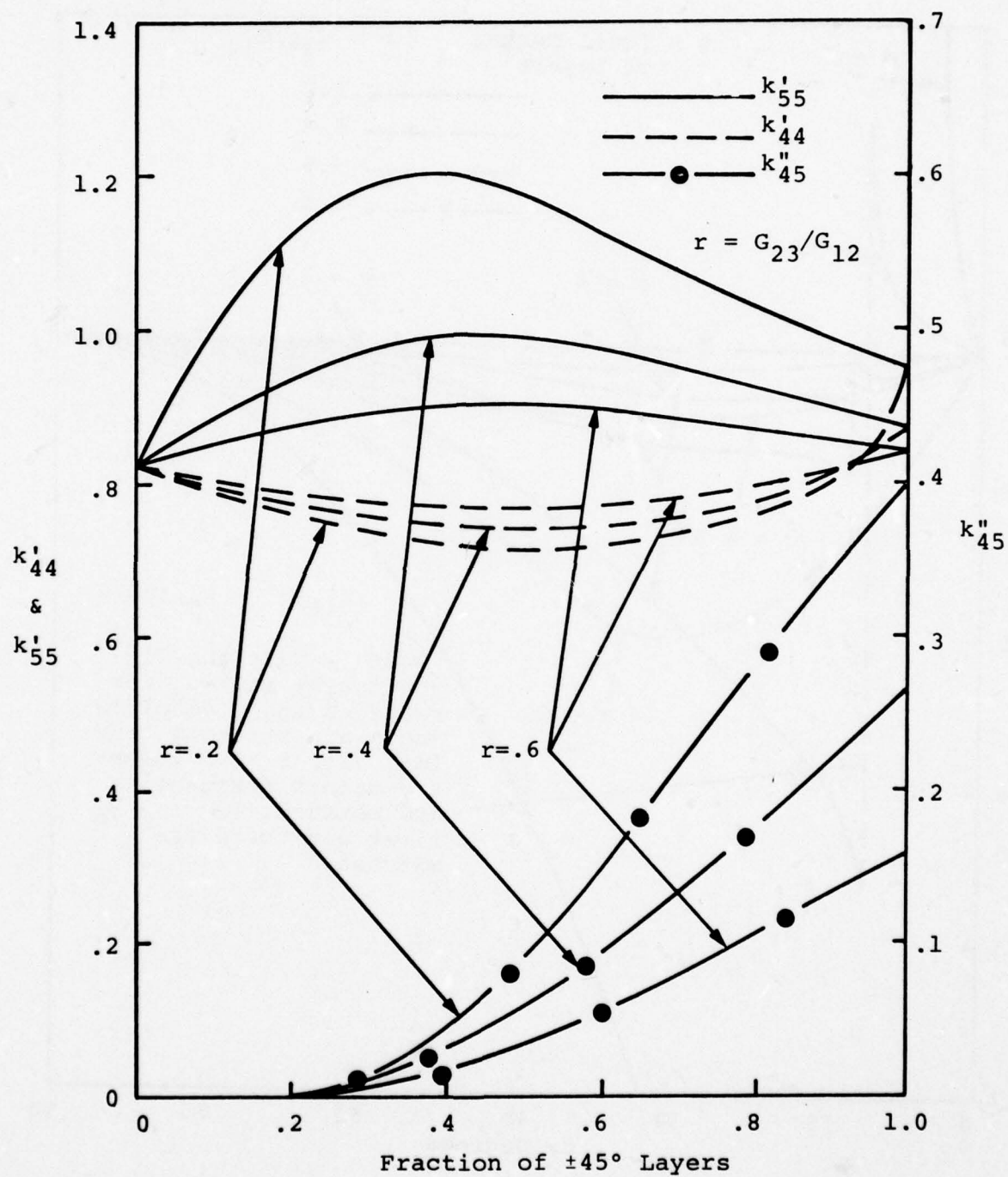


Figure 24. Variation of Shear Correction Factors With the Fraction of  $\pm 45^\circ$  Layers in a  $[\pm 45/0]_s$  Laminate



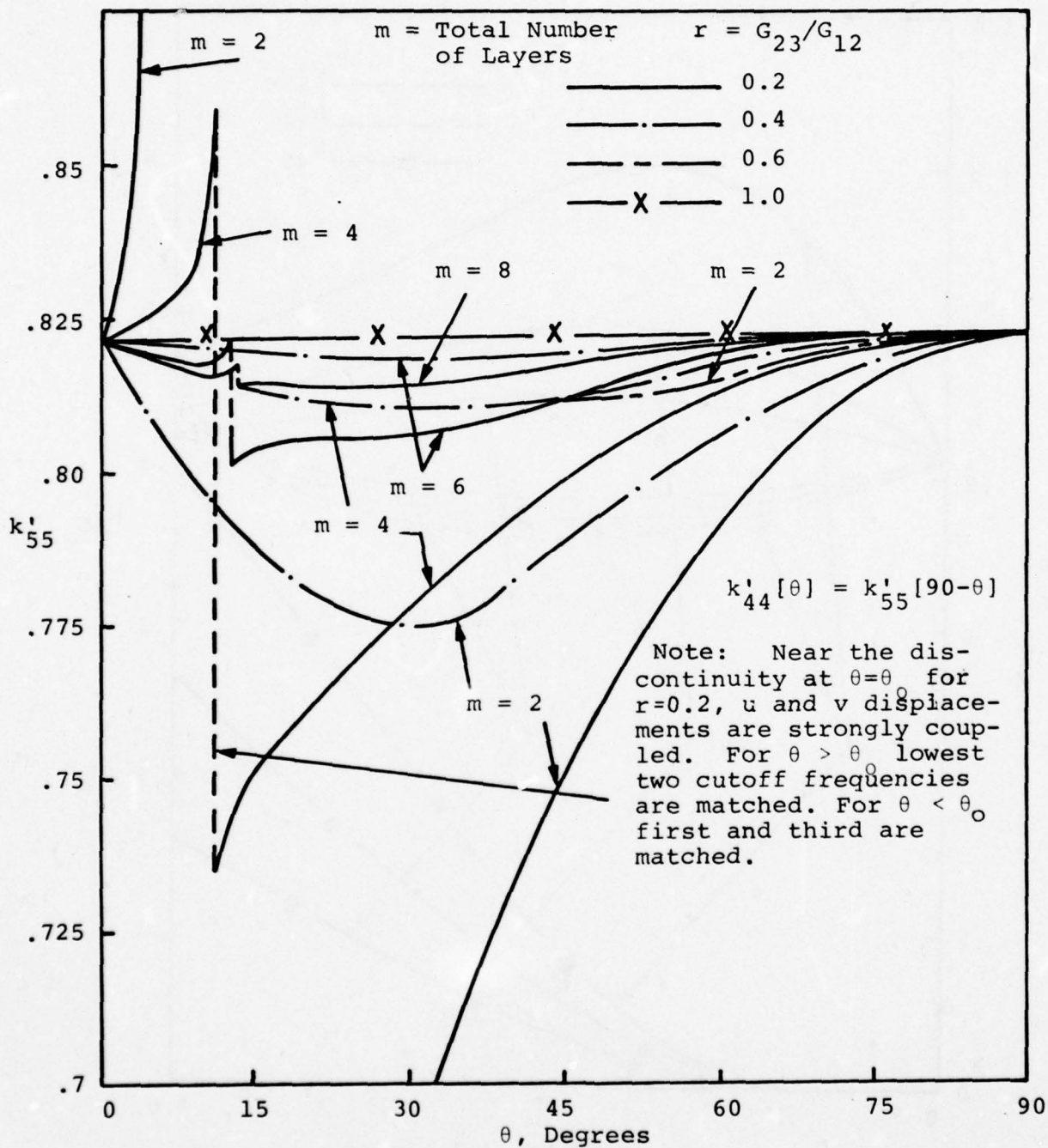


Figure 25. Shear Correction Factors  $k'_{55}$ ,  $k'_{44}$  for Antisymmetric  $[\pm\theta]$  Laminates

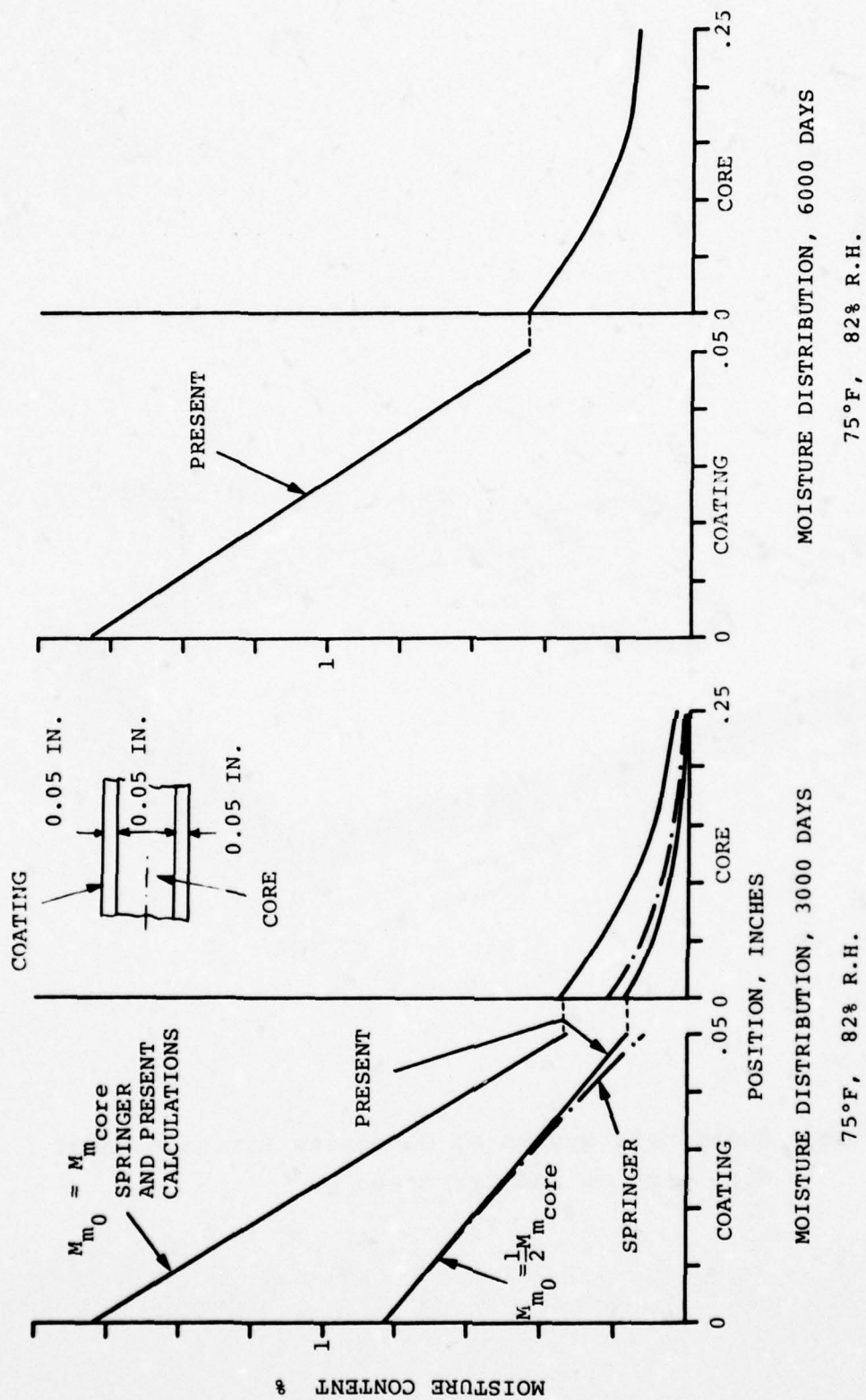


Figure 26. Moisture Distribution in a Coated Composite

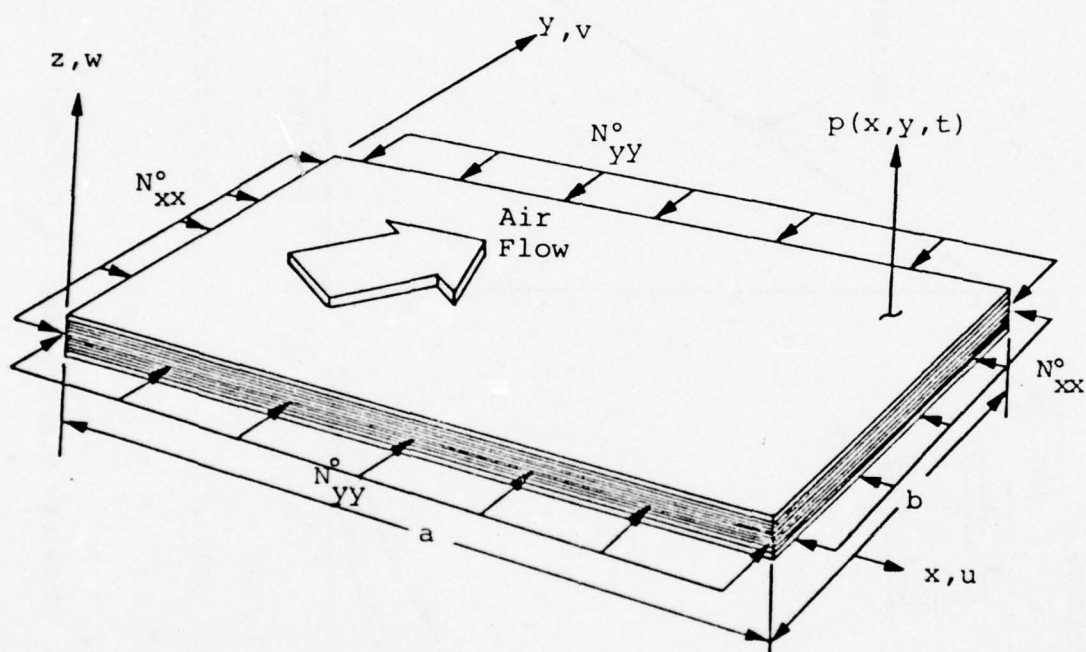


Figure 27. Coordinate System of Composite Laminate Panel With Airflow and Prestress



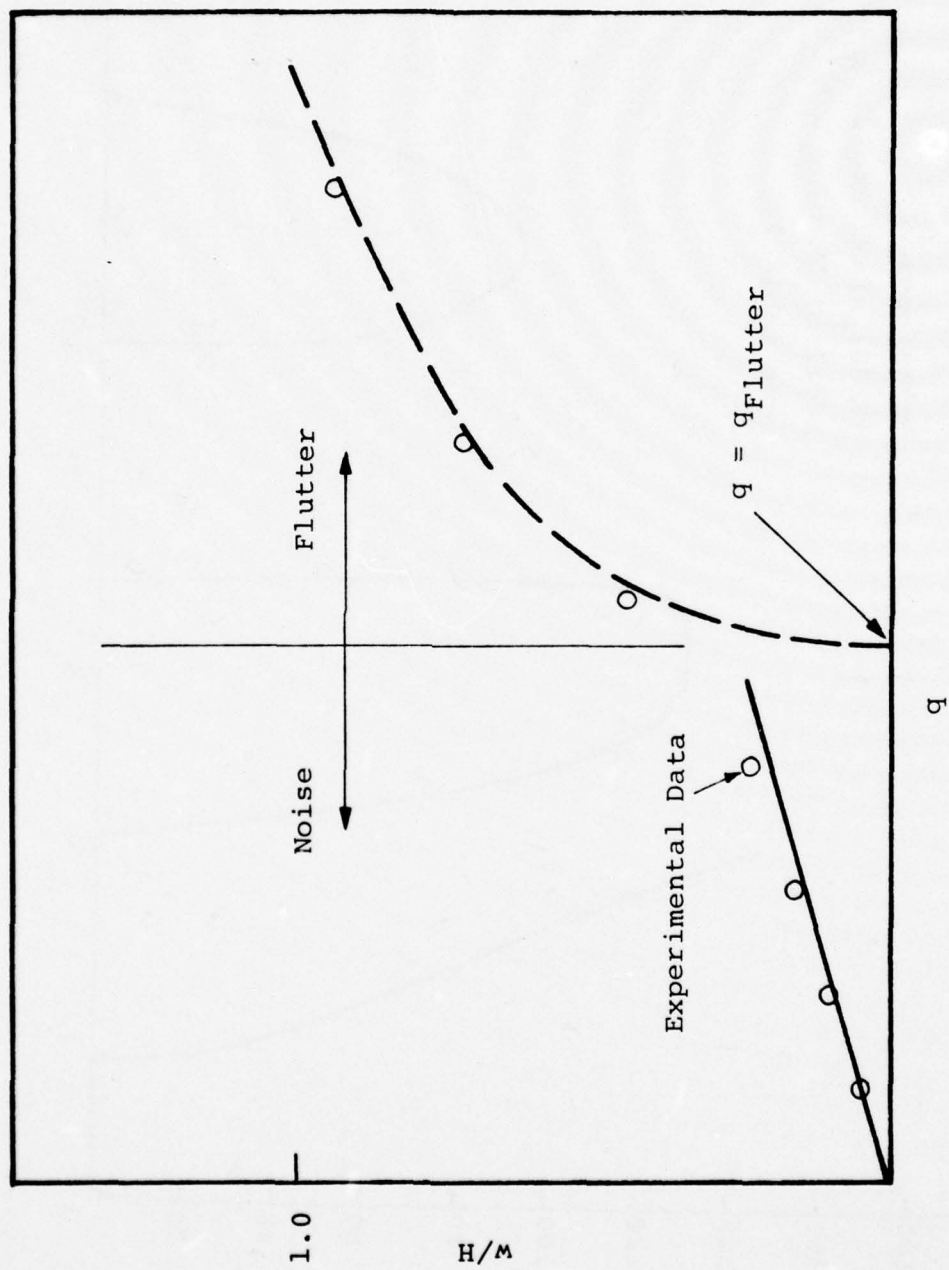


Figure 28. Schematic of Structural Response vs. Dynamic Pressure  
(from ref. 38)

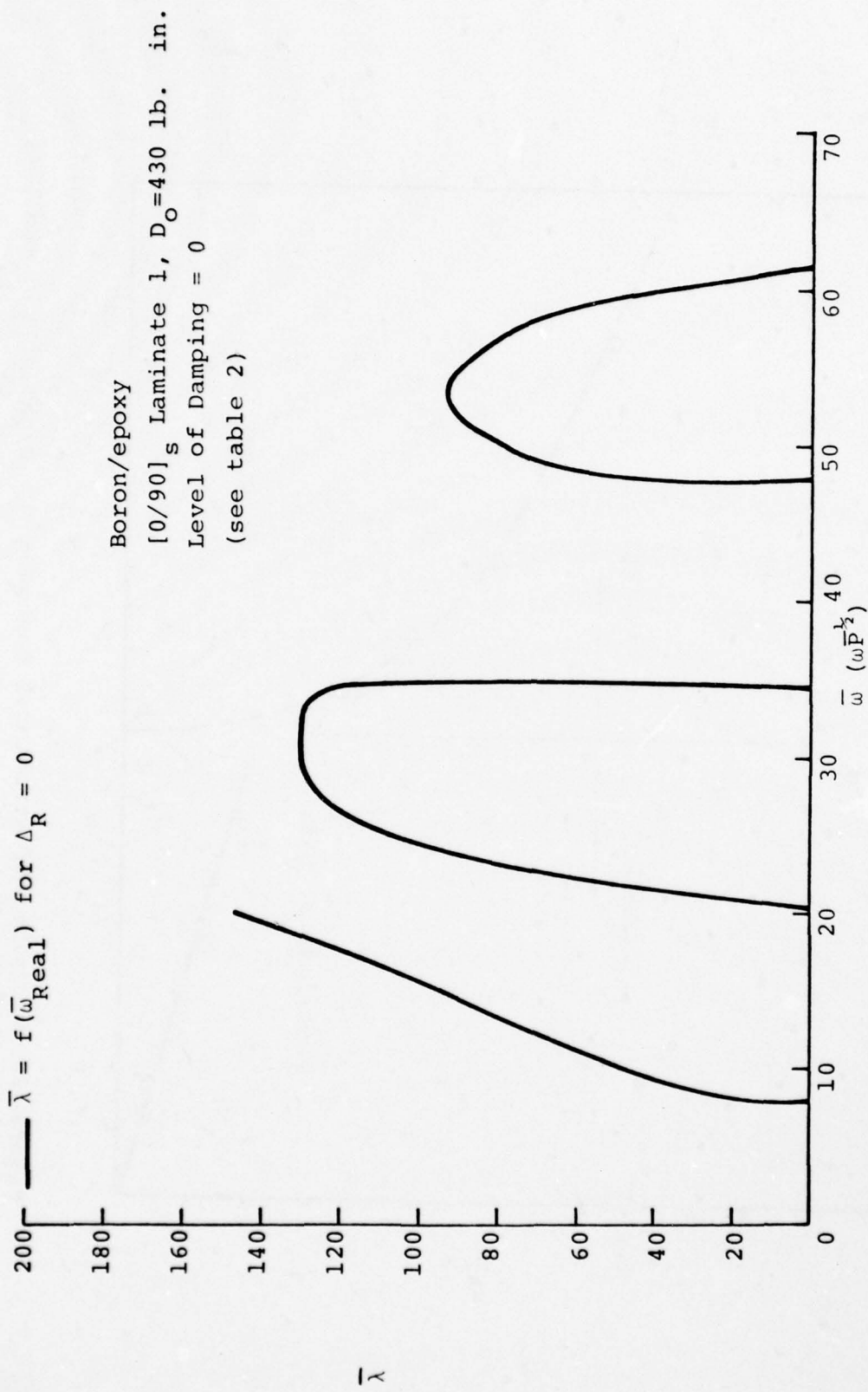


Figure 29. Flutter Parameter - Frequency Plot

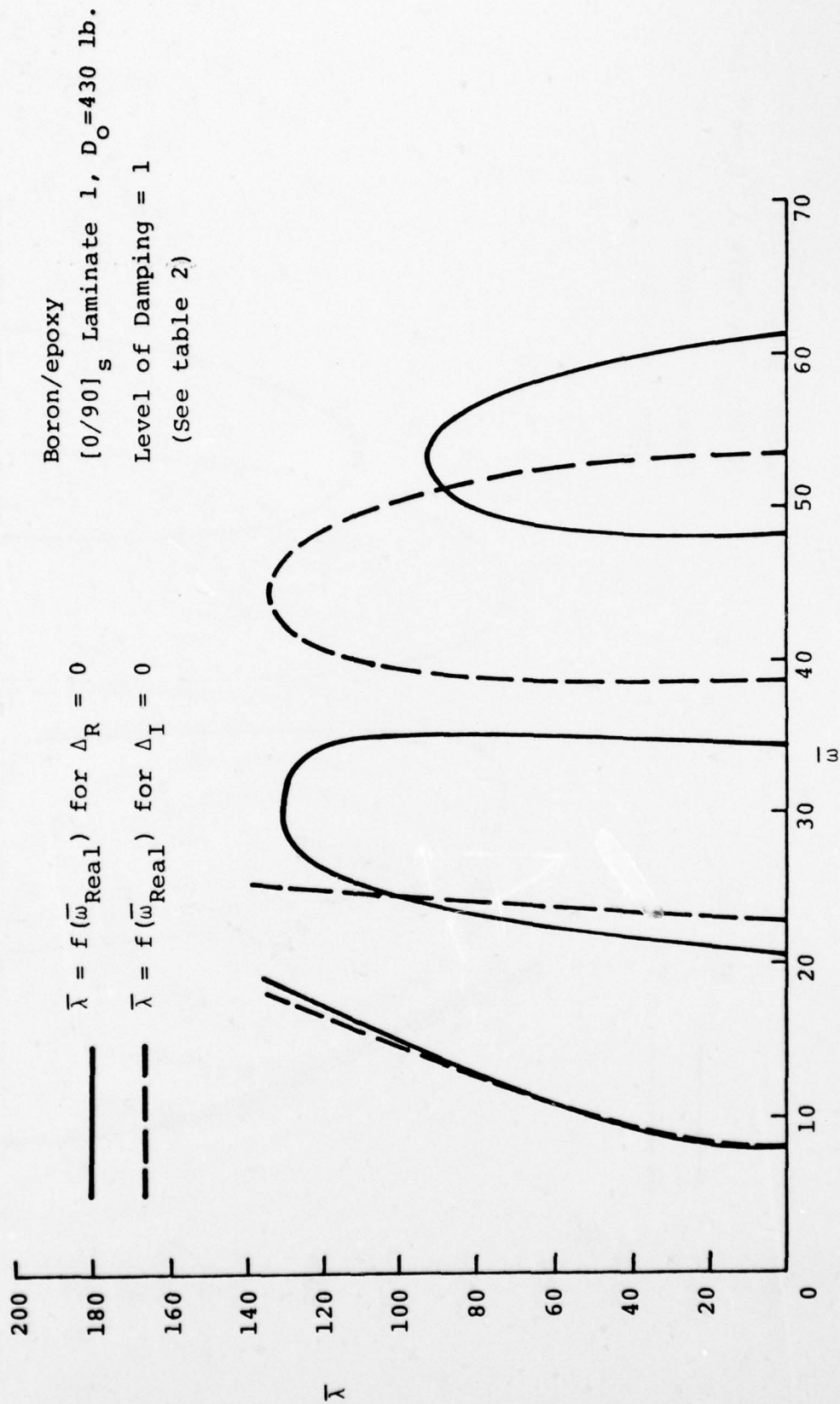


Figure 30. Flutter Parameter - Frequency Plot



Boron/epoxy  
 [0/90]<sub>s</sub> Laminate 1,  $D_0 = 430$  lb. in.  
 Level of Damping = 2  
 (See table 2)

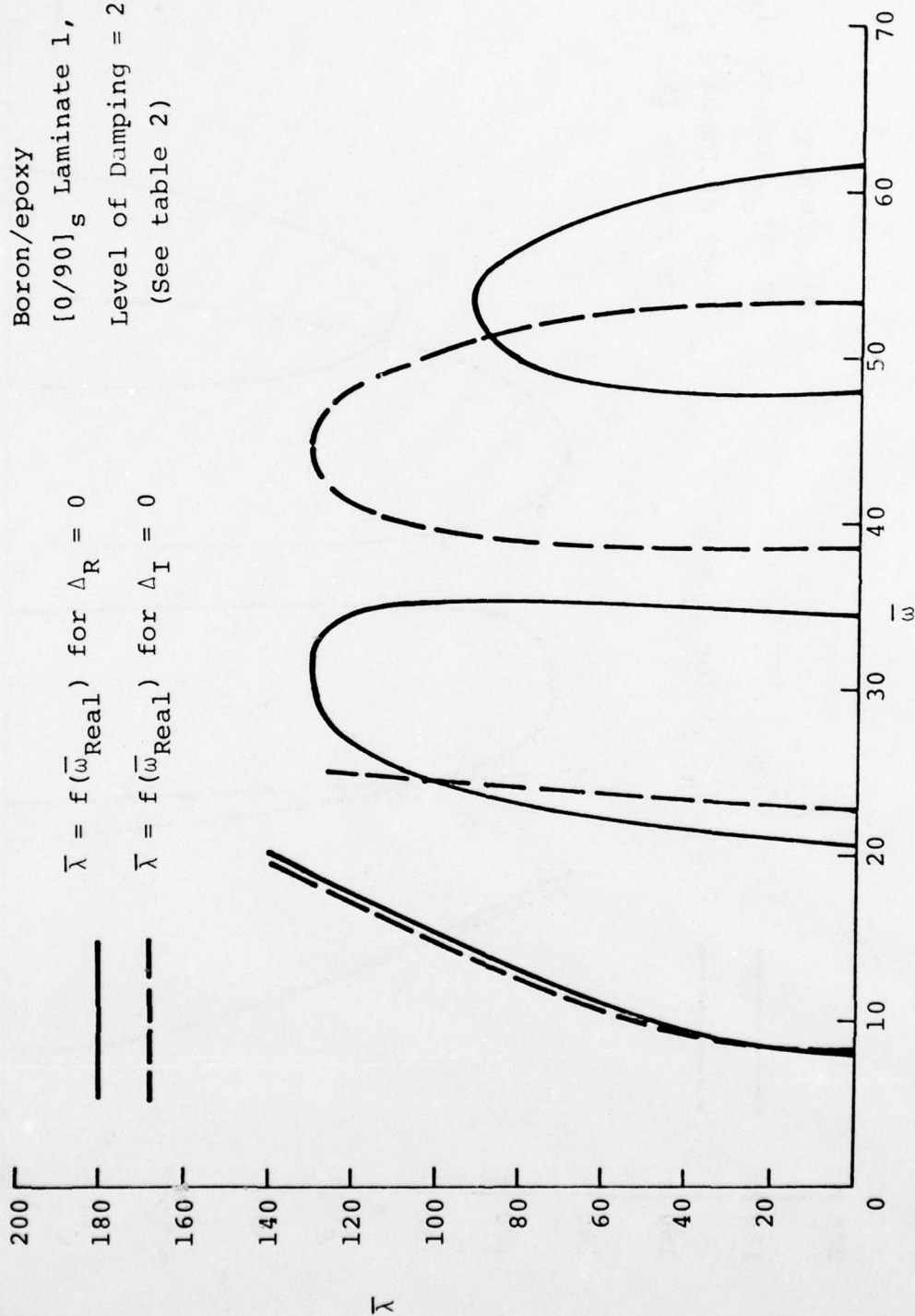


Figure 31. Flutter Parameter - Frequency Plot

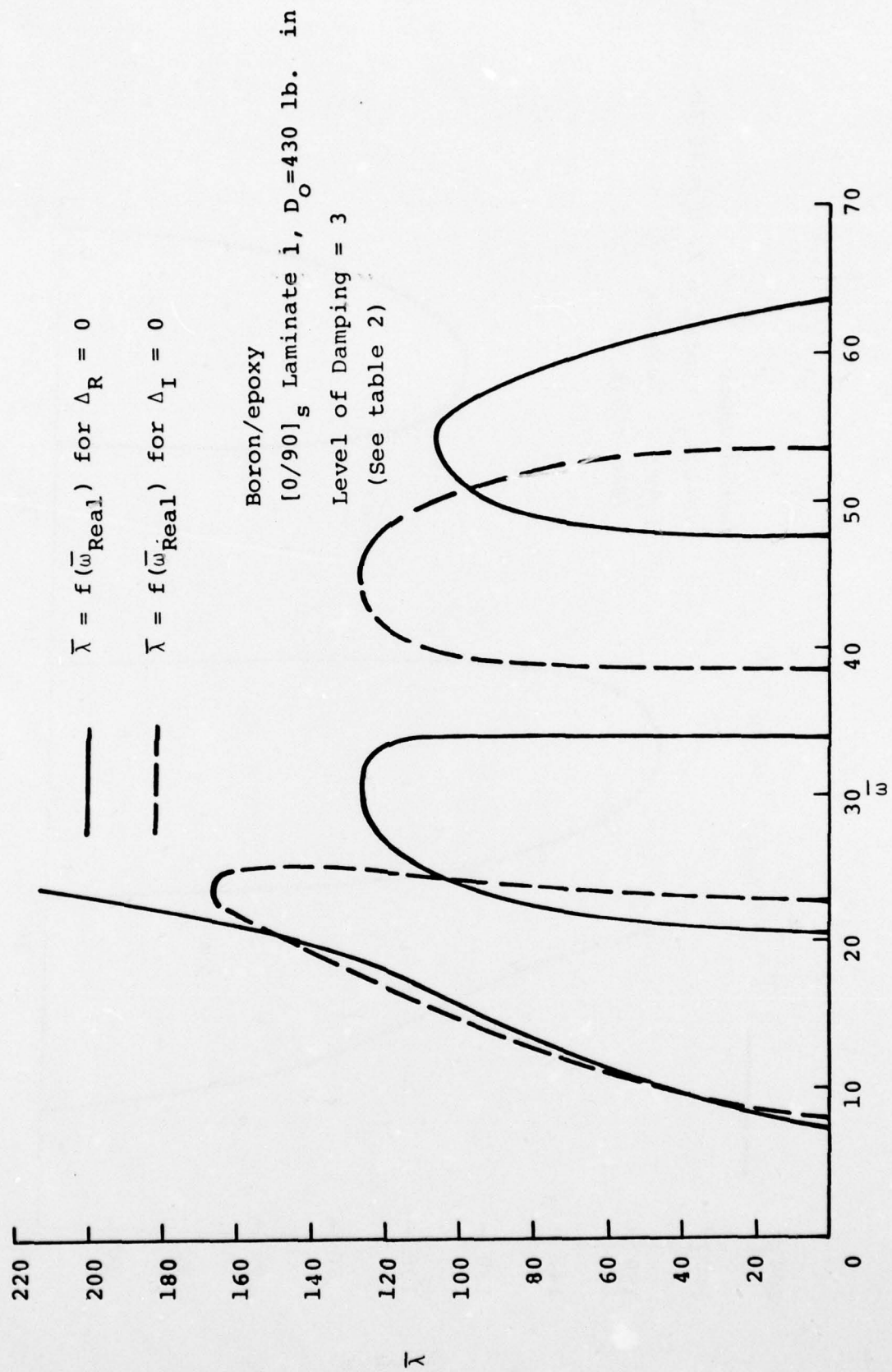


Figure 32. Flutter Parameter - Frequency Plot

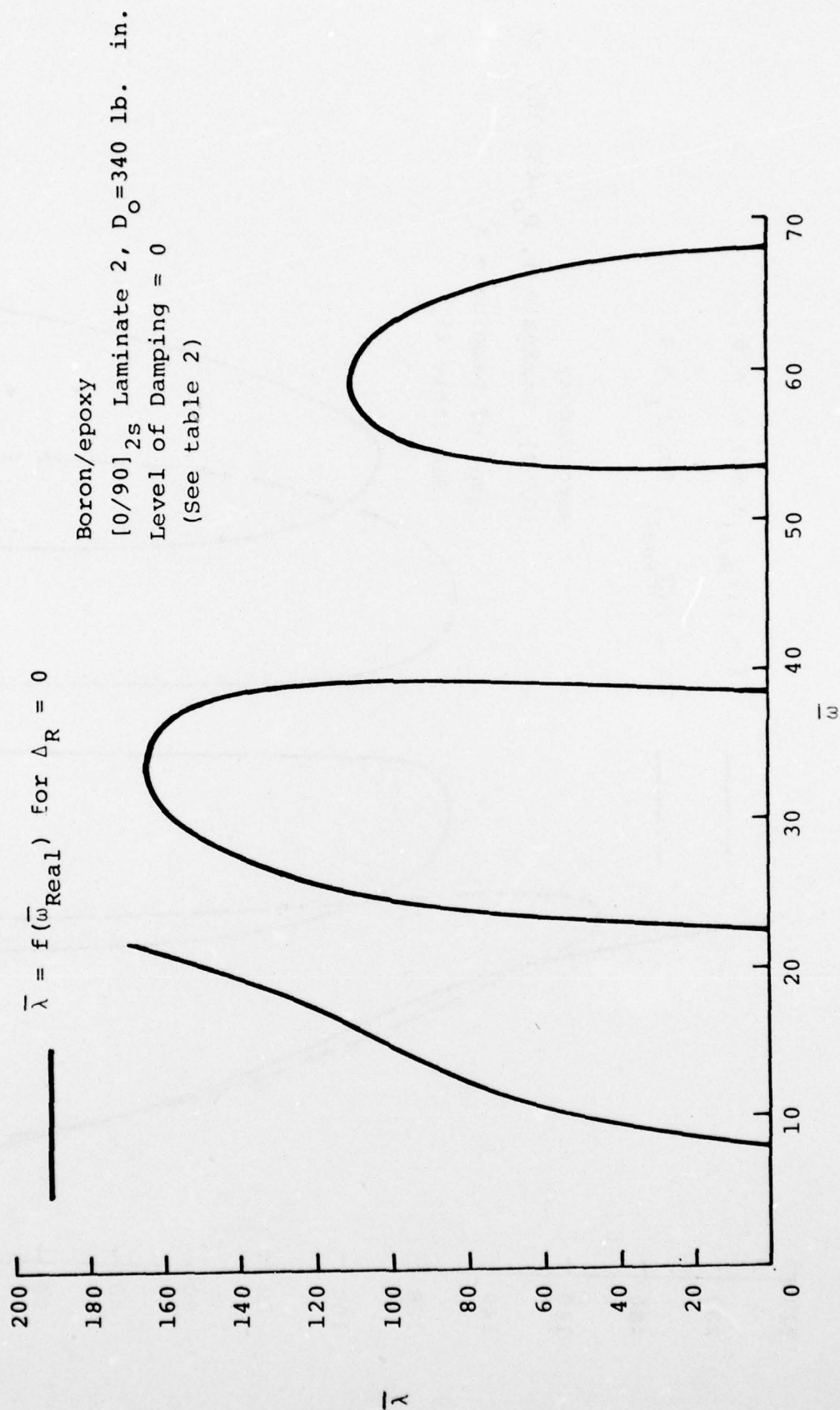


Figure 33. Flutter Parameter - Frequency Plot



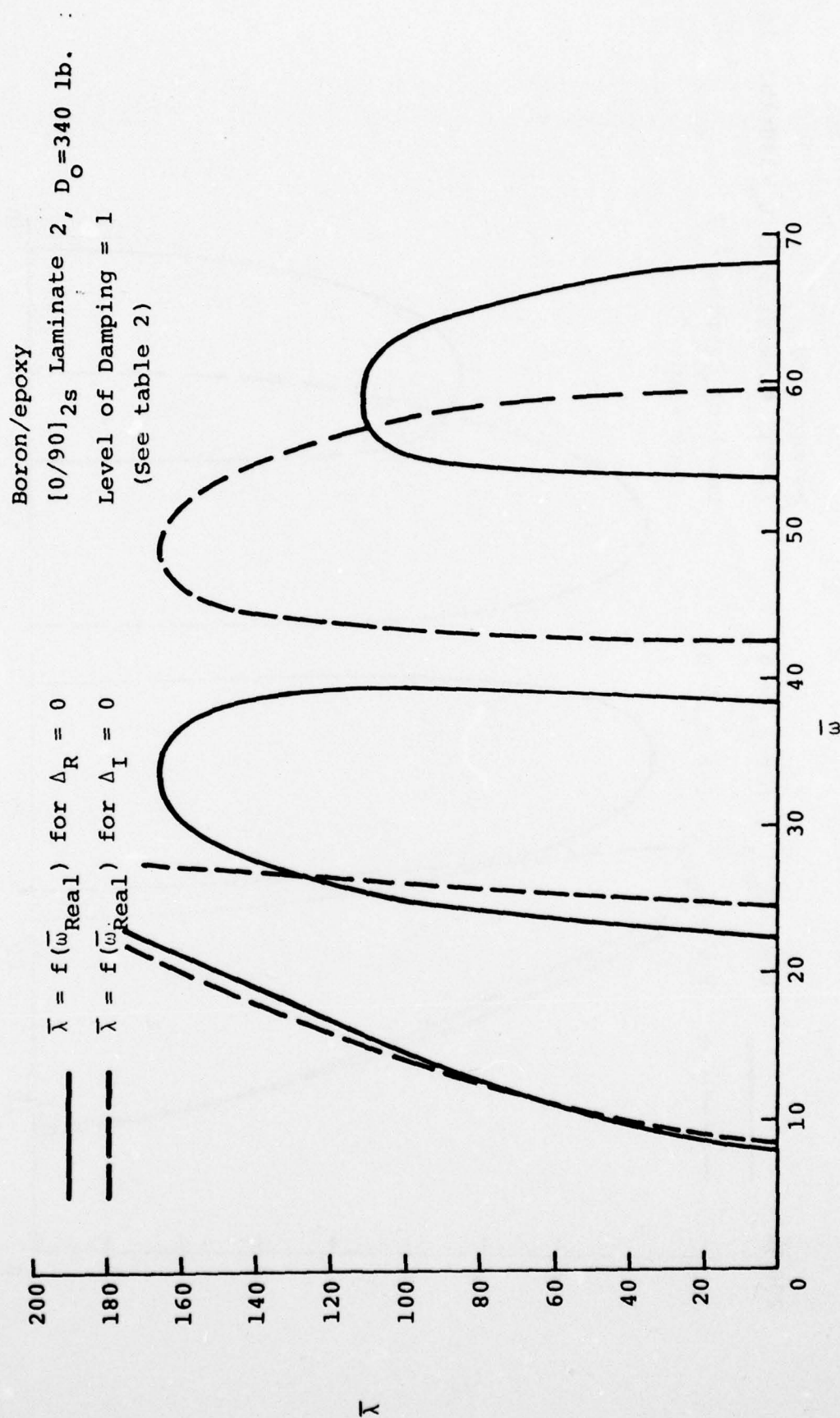


Figure 34. Flutter Parameter - Frequency Plot

Boron/epoxy  
 $[0/90]_S$  Laminate 2.  $D_0 = 340$  lb. in.  
 Level of Damping = 2  
 (See table 2)

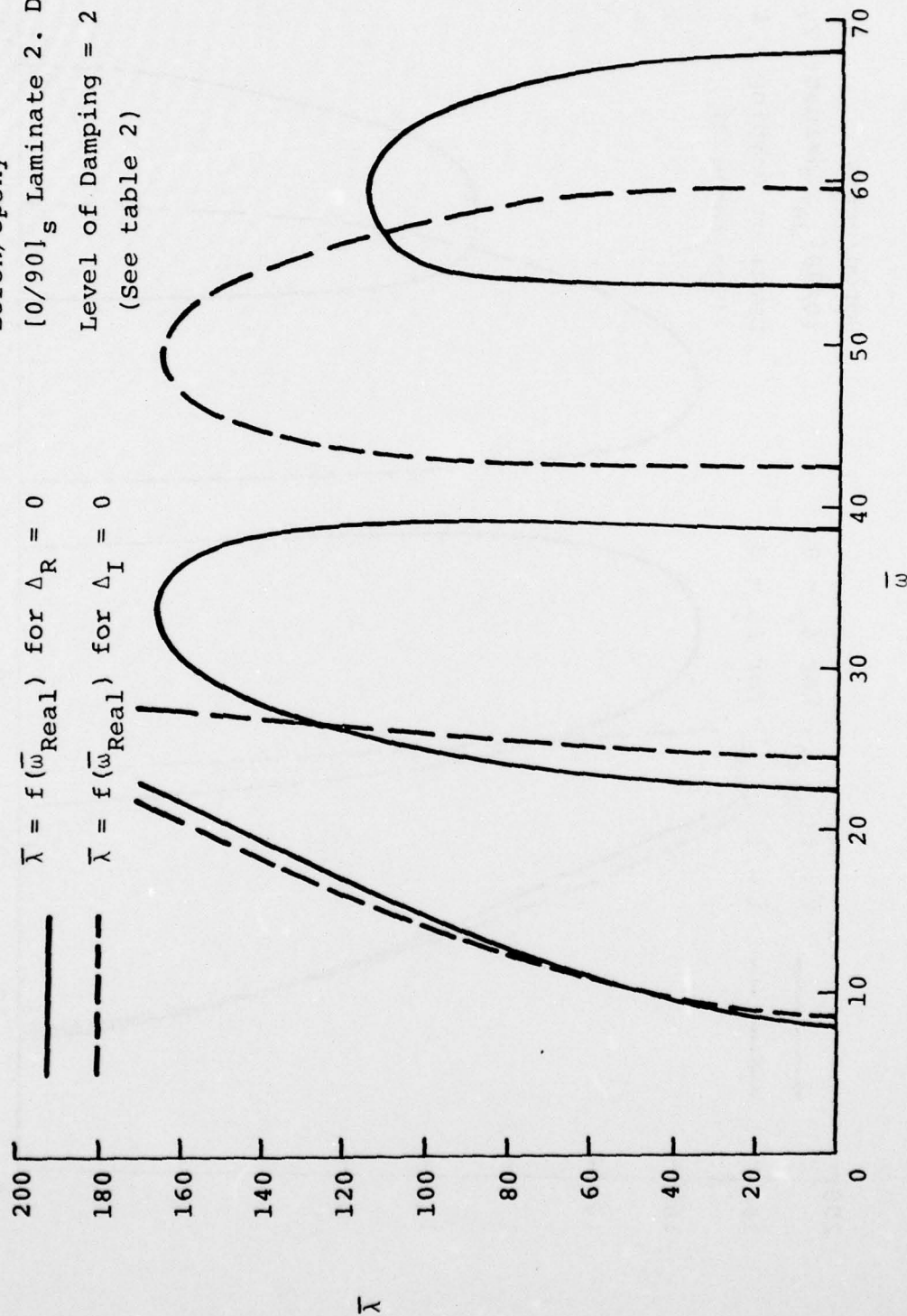


Figure 35. Flutter Parameter - Frequency Plot

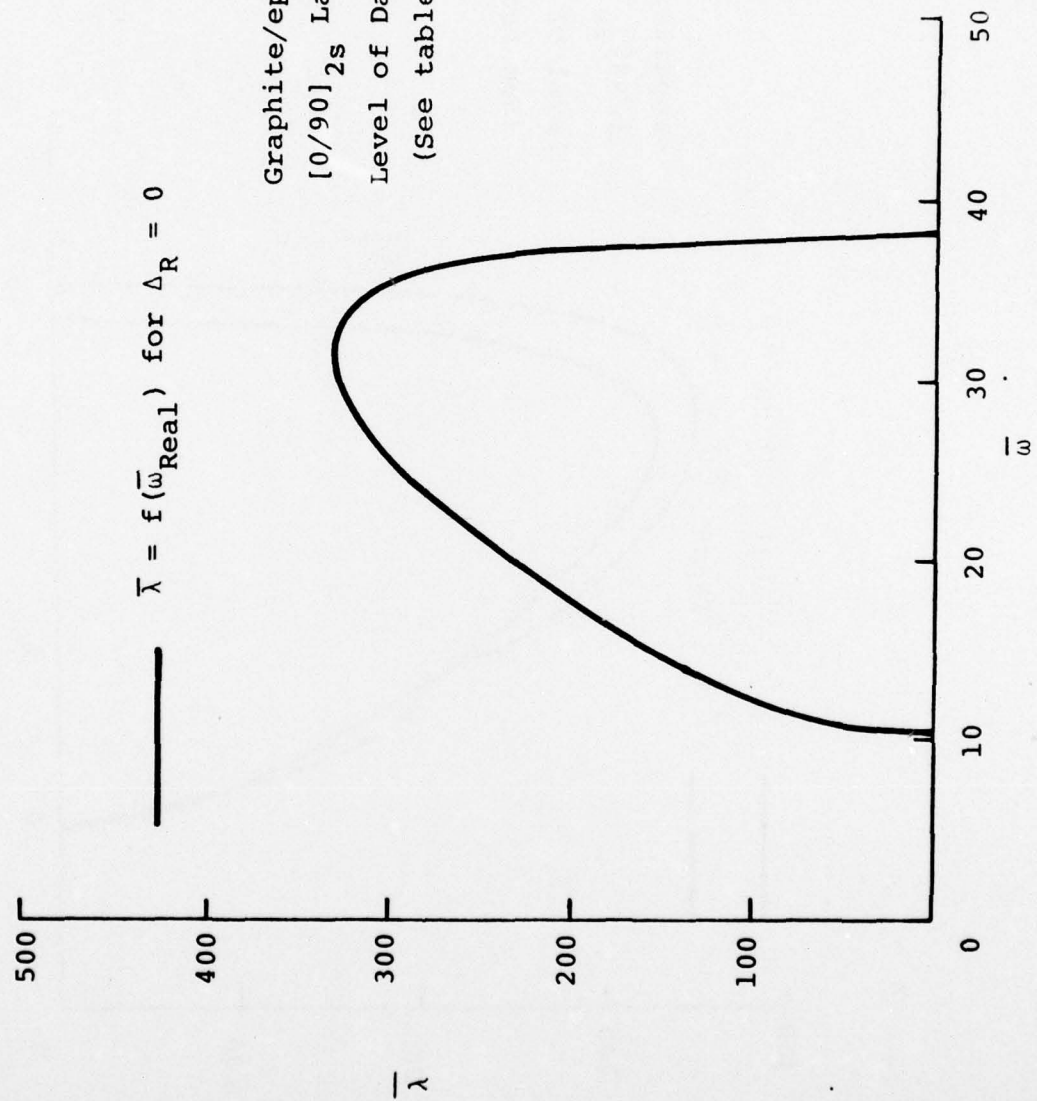
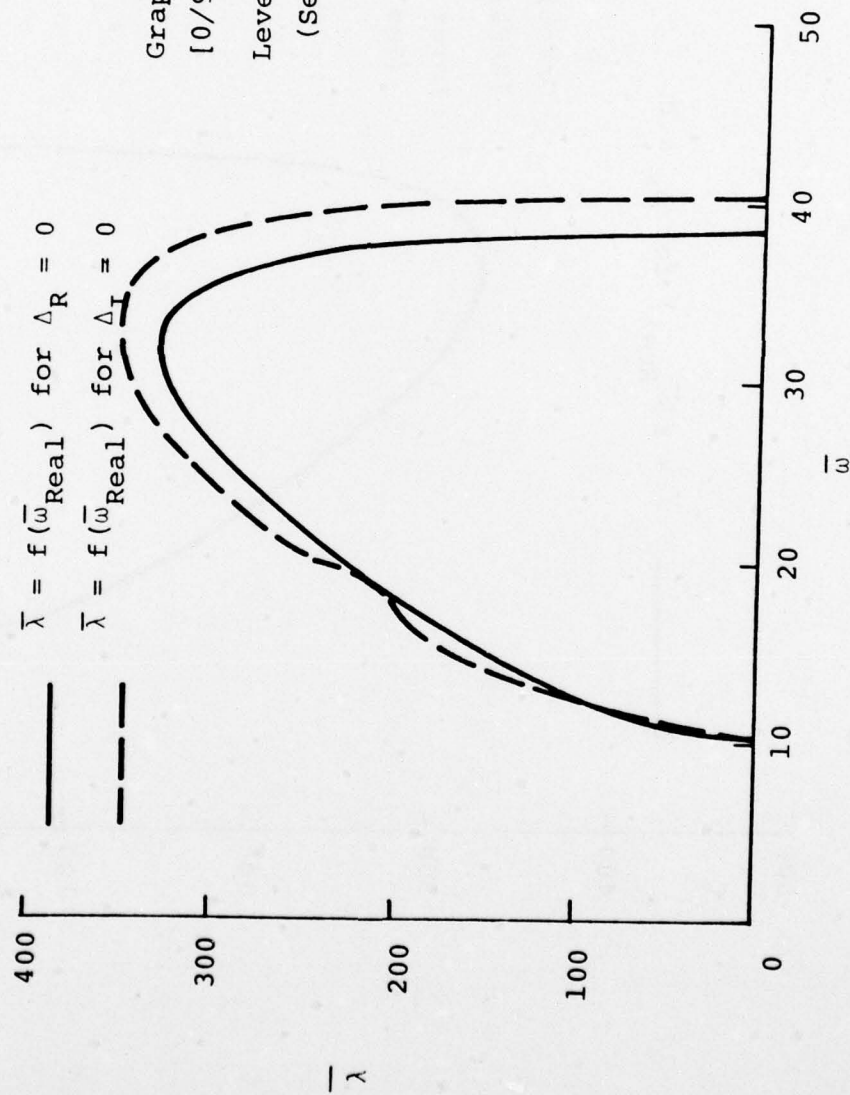


Figure 36. Flutter Parameter - Frequency Plot





Graphite/epoxy  
 $[0/90]_{2s}$  Laminates 3,  $D_0 = 220 \text{ lb.in.}$   
 Level of Damping = 1, 2, 3  
 (See table 2)

Figure 37. Flutter Parameter - Frequency Plot

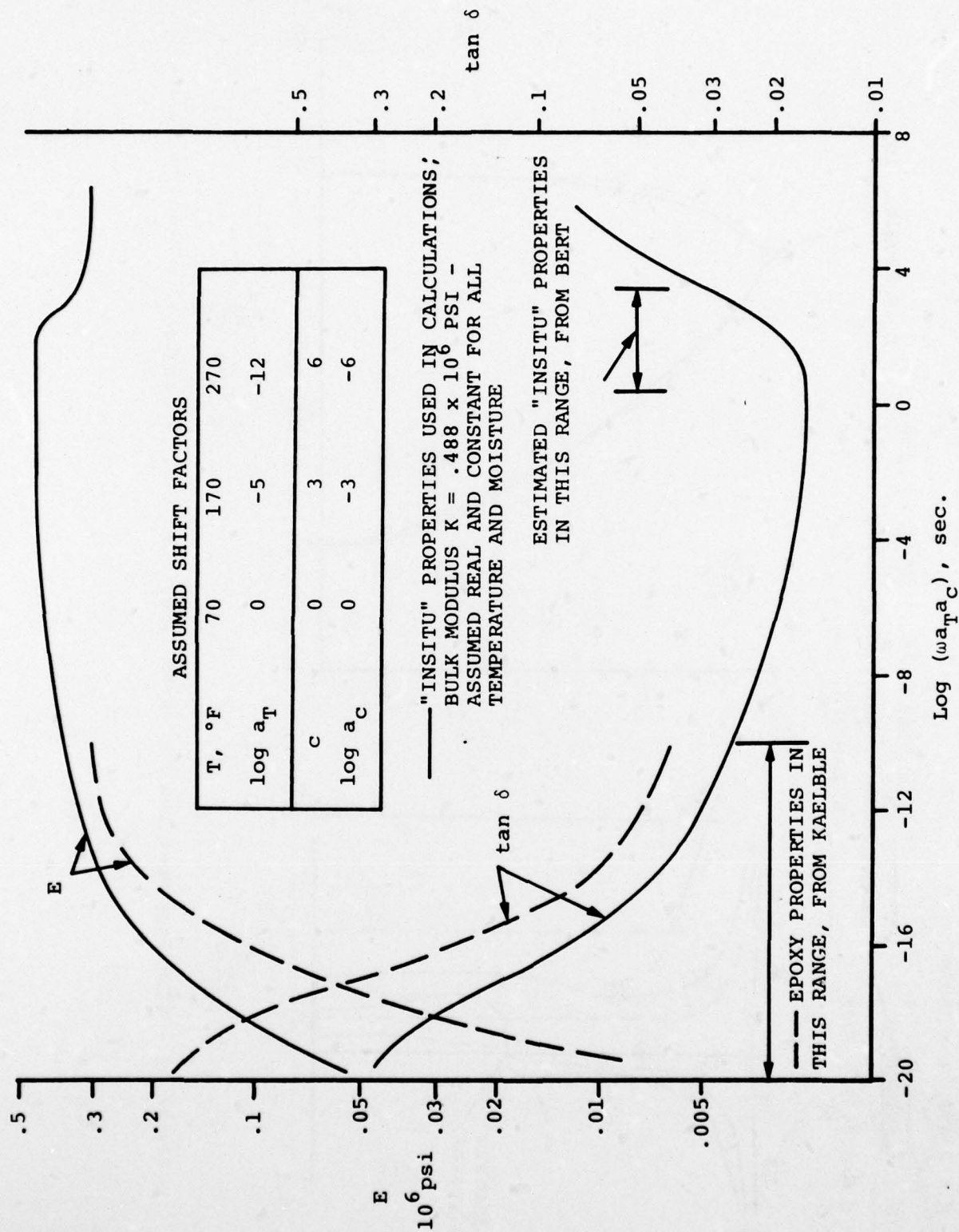


Figure 38. Master Curve for Dynamic Properties of Epoxy - Reference Temperature = 70°F

$C = 2.57\%$ ,  $T = 250^\circ\text{F}$   
 { LAMINATE }  
 $C = 0.0$ ,  $T = 70^\circ\text{F}$   
 ROOM TEMP., NO MOISTURE  
 TEMP., MOISTURE GRADIENT  
 NO DAMPING,  $\tan \delta = 0$

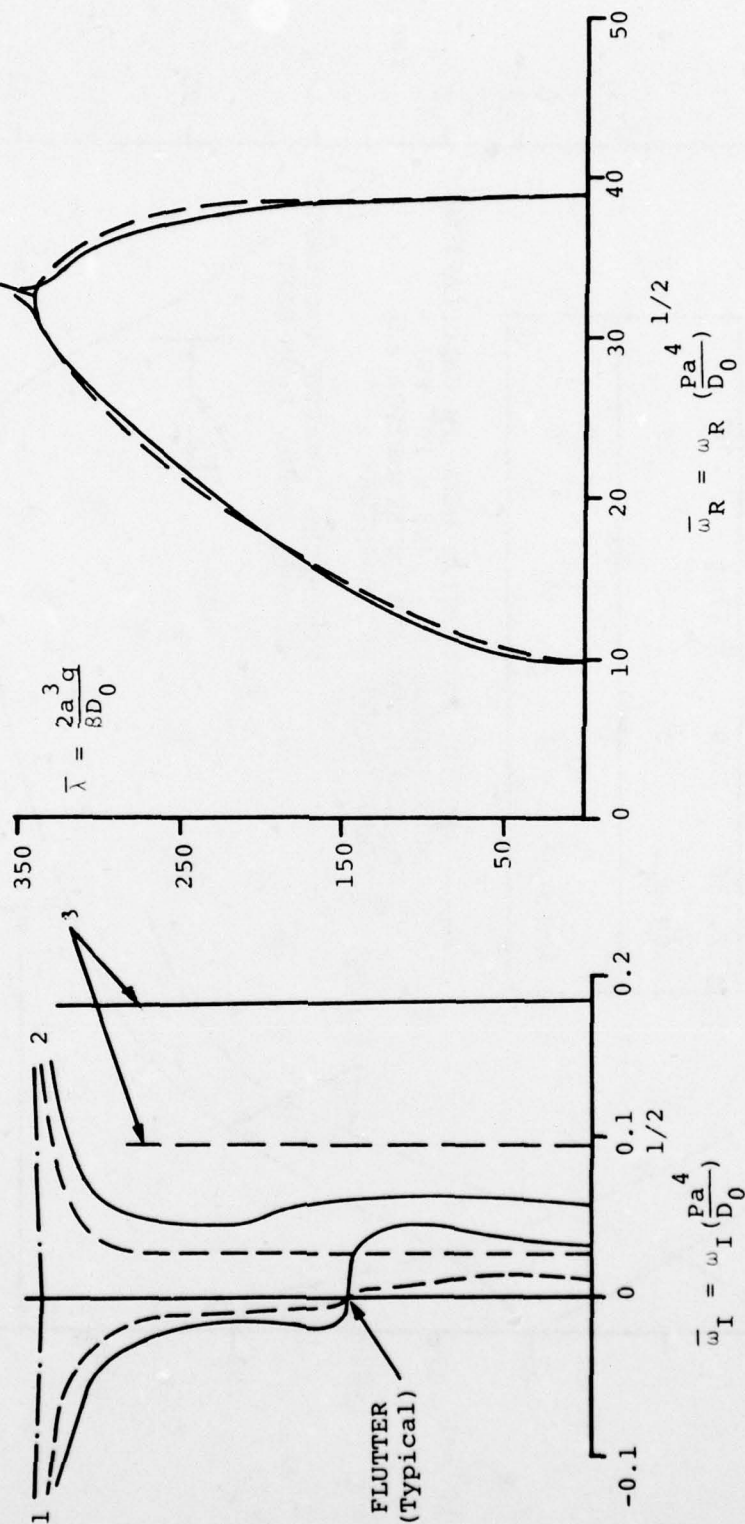


Figure 39. Frequency Spectrum for  $[0/90/0/90]_s$  Cross-Ply Laminate 4,  $a/h=60$ ,  $h=.06 \text{ in.}$



$\bar{\lambda}_{cr1}$	$\bar{\lambda}_{cr2}$	$\bar{\lambda}_{cr3}$
141	152	48
158	169	51

$D_0 = 220 \text{ lb. in.}$

— ROOM TEMP., NO MOISTURE

--- TEMP., MOISTURE GRADIENT

Very High Transverse Shear Stiffness  
(Negligible Shear Deformation)

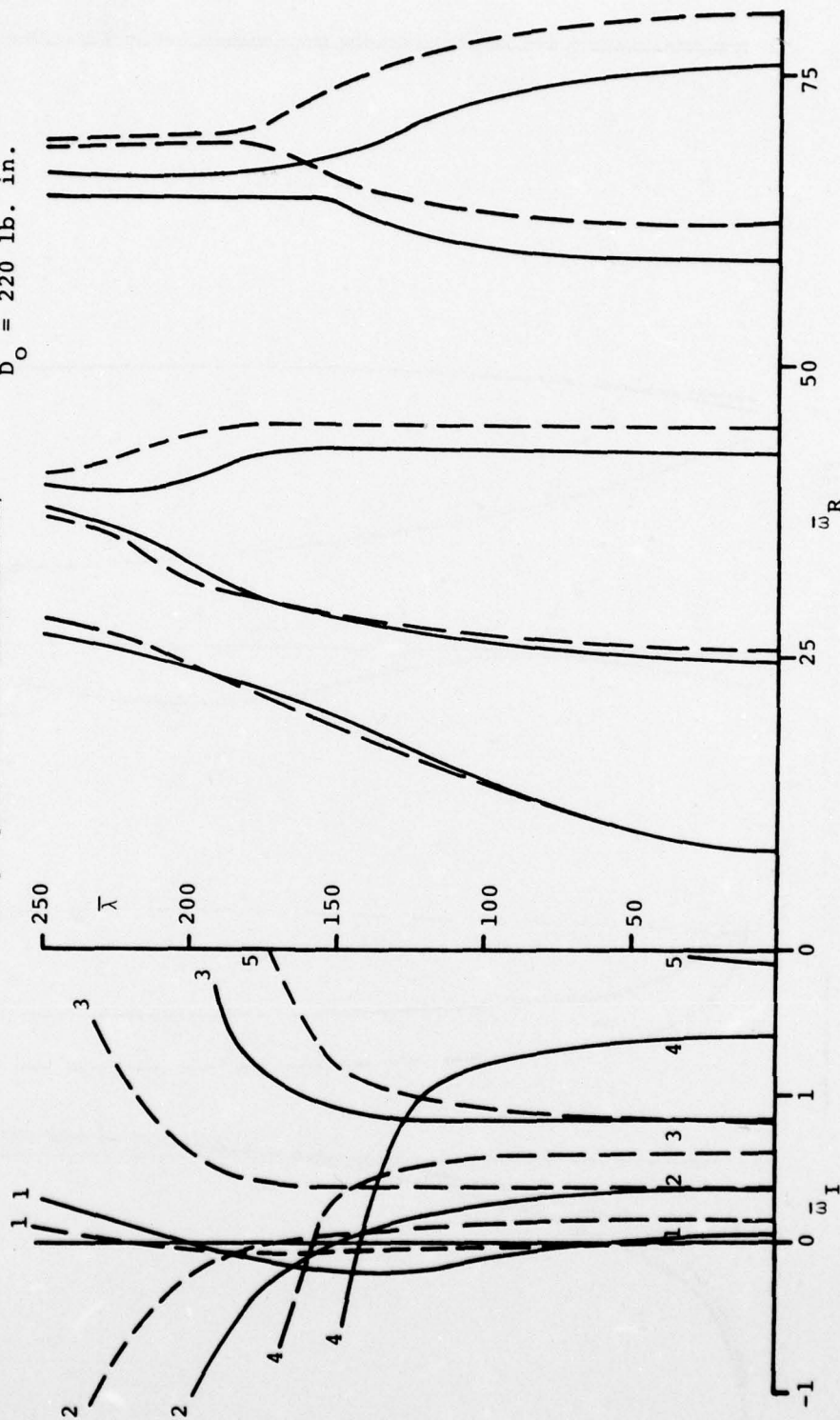


Figure 40. Frequency Spectrum for  $[0/90/0/90]_s$  Cross Ply Laminate 5,  $a/h = 10$ ,  $h = 0.06 \text{ in.}$

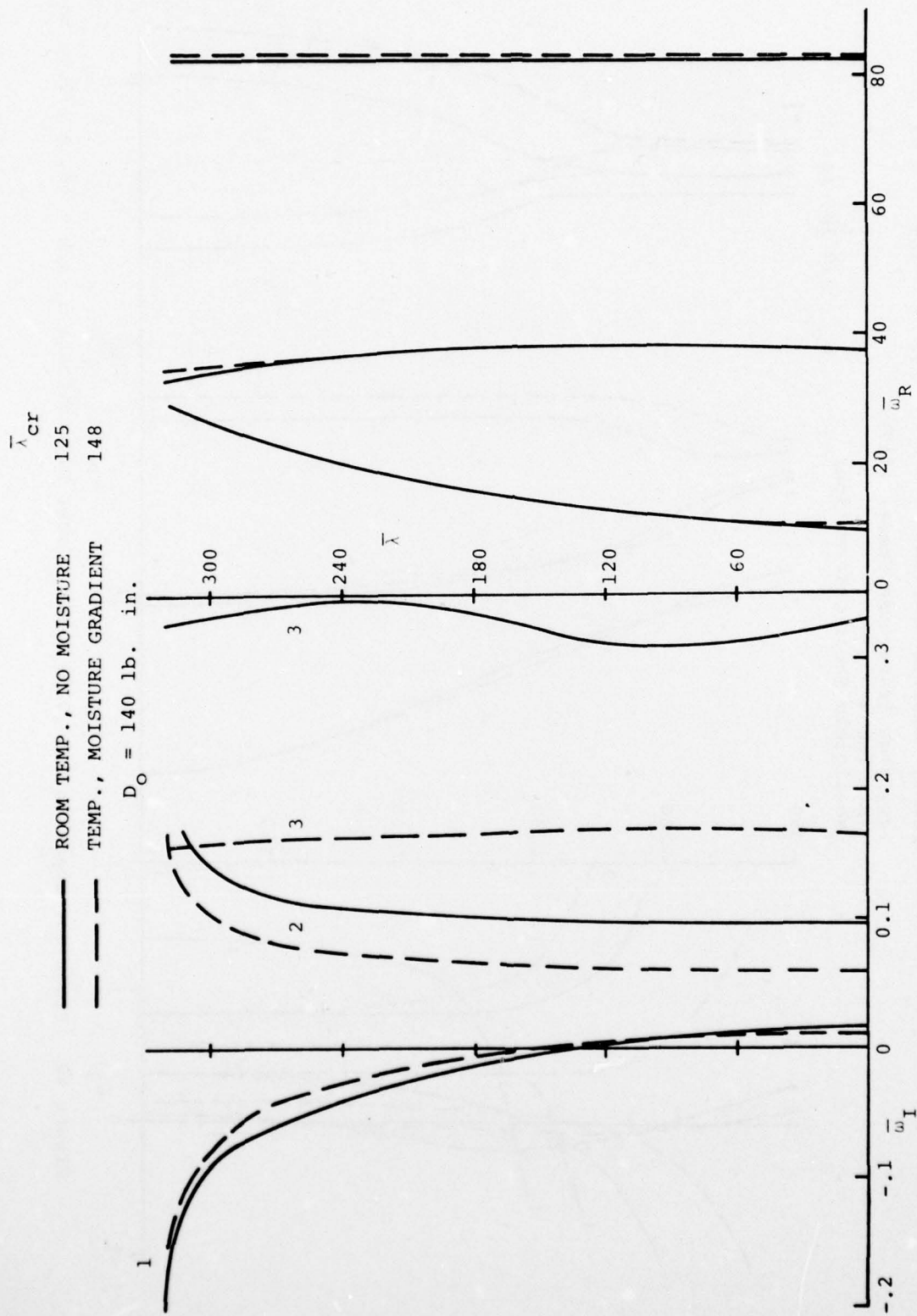


Figure 41. Frequency Spectrum for  $[45/0_2/90]_s$  Laminate 6,  $a/h = 40$ ,  $h = .06 \text{ in.}$

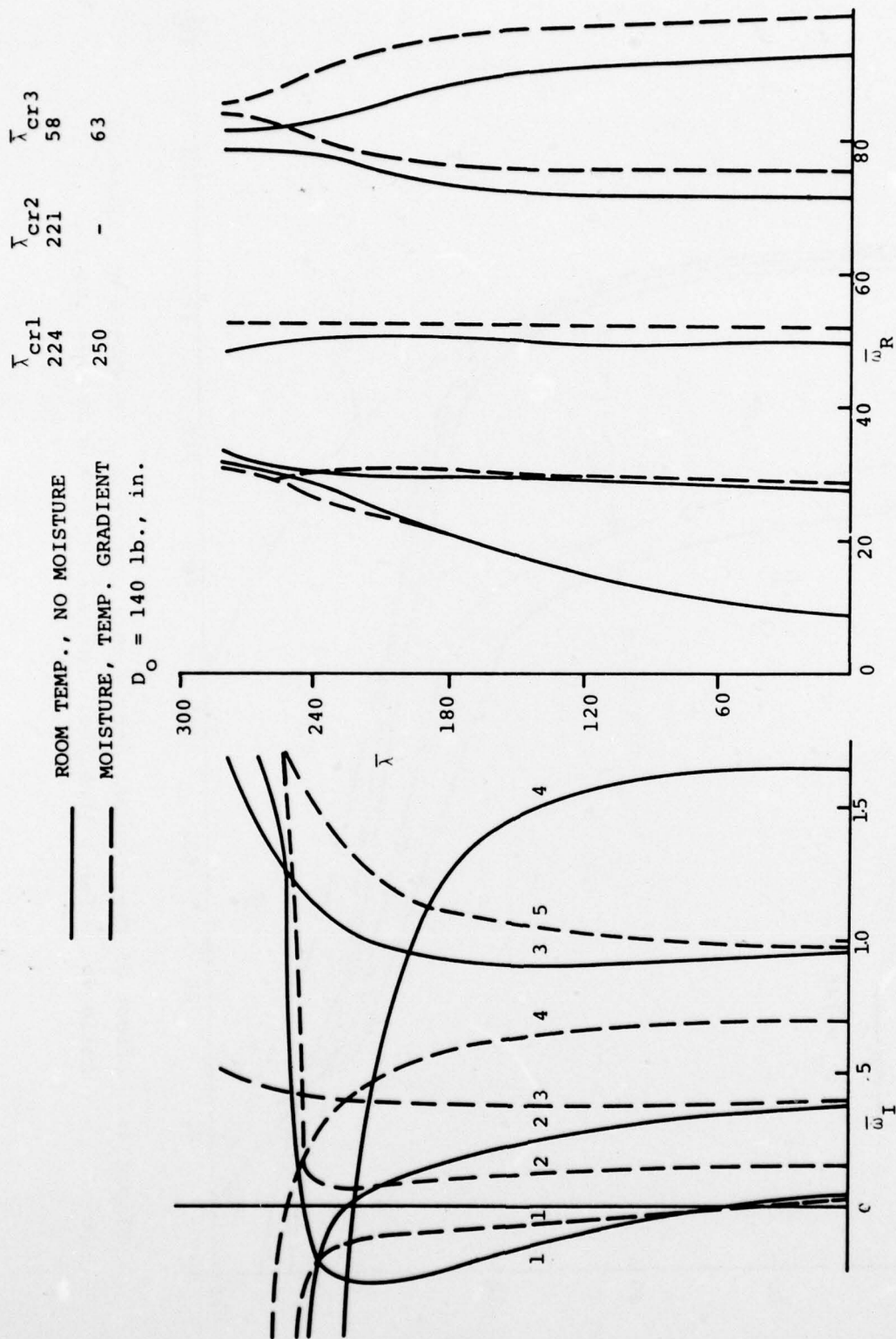


Figure 42. Frequency Spectrum for  $[+45/-45/0_2/90]_s$  Laminates  $7, a/h = 10, h = .06 \text{ in.}$



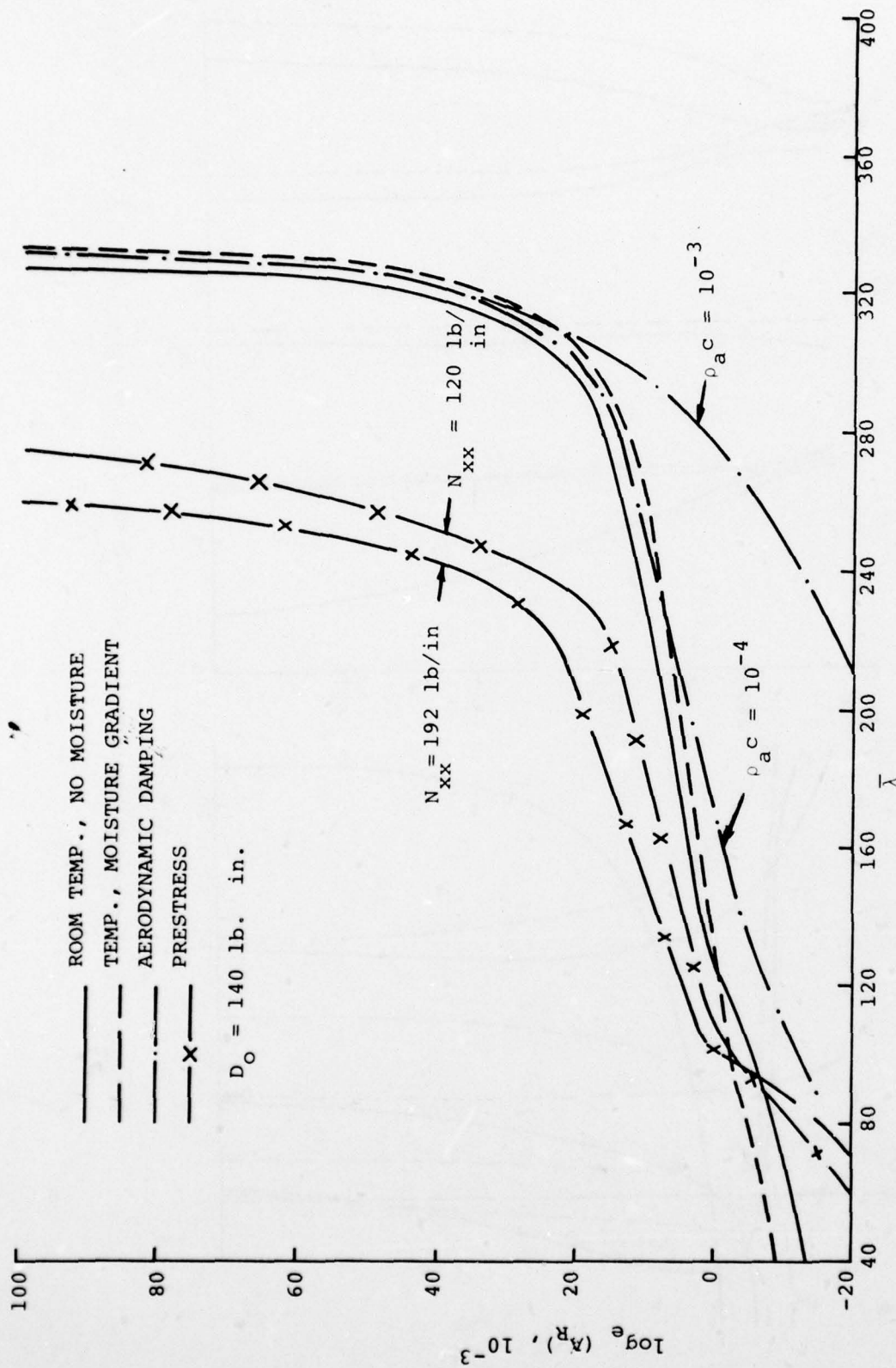


Figure 43. Effect of Environment, Aerodynamic Damping and Prestress on Amplitude Ratio vs.  $\bar{\lambda}$  for  $[\pm 45/0_2/90]_s$  Laminate 6,  $a/h = 40$ ,  $h = .06 \text{ in.}$